



## **Codes And Methods Improvements for VVER comprehensive safety assessment**

Grant Agreement Number: 945081

Start date: 01/09/2020 - Duration: 36 Months

---

### **WP4 - Task 4.2**

## **D4.4 – Results of the verification phases on PWR and VVER geometry configurations**

---

Marco TIBERGA, Pierre LAURENT, Adrien WILLIEN, Nathalie GULER (EDF), Barbara VEZZONI, Alberto BRIGHENTI (FRAMATOME), Gianfranco HUACCHO ZAVALA (KIT)

---

Version 1.0 – 31/08/2023



This project has received funding from the Euratom research and training programme 2019-2020 under grant agreement No 945081.

Document title	Results of the verification phases on PWR and VVER geometry configurations
Author(s)	Marco TIBERGA, Pierre LAURENT, Adrien WILLIEN, Nathalie GULER, Barbara VEZZONI, Alberto BRIGHENTI, Gianfranco HUACCHO ZAVALA
Document type	Deliverable
Work Package	WP4
Document number	D4.4 - version 1.0
Issued by	EDF
Date of completion	31/08/2023
Dissemination level	Public

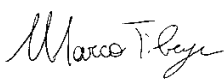
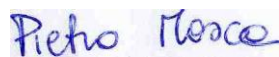

### Summary

The H2020 CAMIVVER project aims to develop and improve codes and methods for VVER comprehensive safety assessment.

In the Work Package 4 (WP4), Task 4.1 is intended to the creation of a multi-parametric neutron data library generator prototype based on APOLLO3<sup>®</sup>. Task 4.2, for its part, is dedicated to the verification of the consistency of the prototype generator based on APOLLO3<sup>®</sup>. The activity carried out within Task 4.2 is organised in two parts: first one is the definition and selection of test cases (VVER and PWR) to be used and the parameters to be compared and second one is the result comparison on the basis of the selected configurations. The present document fits in the second part of Task 4.2 and corresponds to Deliverable 4.4 (*Results of the verification phases on PWR and VVER geometry configurations*) of the CAMIVVER project.

This document presents the automatic comparison tool DICE and summarizes the main outcomes of the first V&V activity performed on the NEMESI platform.

### Approval

Version	First Author	WP leader	Project Coordinator
1.0	M. Tiberga (EDF) 30/08/2023	P. Mosca (CEA) 31/08/2023	D. Verrier (Framatome) 31/08/2023
	Signature 	Signature 	Signature 

EDF R&D

PERFORMANCE AND INDUSTRIAL RISKS PREVENTION USING STUDIES AND SIMULATION

NEUTRONIC CORE SIMULATION

7 boulevard Gaspard Monge 91120 PALAISEAU - +33 (1) 78 19 32 00

08/31/2023

CAMIVVER - D4.4 - Results of the verification phases on PWR and VVER geometry configurations

Marco TIBERGA	EDF R&D - PERICLES
Pierre LAURENT	EDF R&D - PERICLES
Adrien WILLIEN	EDF R&D - PERICLES
Nathalie GULER	EDF R&D - PERICLES
VEZZONI Barbara	FRAMATOME
HUACCHO ZAVALA Gianfranco	KIT

6125-1108-2023-02020-EN	1.0		
Information type : Technical note			
<p>Within the H2020 CAMIVVER Project, the Work Package 4 (WP4) aims at making a step forward in the framework of multi-parameter neutron data libraries generation for Gen II and Gen III LWR (in particular for VVER) using the new-generation deterministic code APOLLO3<sup>®</sup>. A lattice calculation platform prototype, named NEMESI, has been developed in the framework of Task 4.1 following system engineering practices and is presented in detail in Deliverable 4.2. Task 4.2 aims instead at verifying and benchmarking NEMESI against other deterministic and Monte Carlo codes. To this purpose, in the first phase a series of assembly test cases (on both VVER and PWR geometries) have been selected and the representative output parameters to be compared have been defined. They are described in detail in Deliverable 4.3. In the second phase, a selection of test cases was calculated with NEMESI, and the results compared to those obtained with APOLLO2, TRIPOLI-4<sup>®</sup> and SERPENT-2, by exploiting an automatic post processing tool named DICE. This document presents the automatic comparison tool DICE and summarizes the main outcomes of the first V&amp;V activities performed on the NEMESI platform. This document corresponds to the Deliverable 4.4 of the CAMIVVER project. The results obtained for all configurations at nominal state (with or without control rods) and during depletion show in general very good agreement between NEMESI and the Monte Carlo codes and/or APOLLO2. DICE has helped with the identifications of several sources of discrepancies (input file errors, differences in compositions, geometry, etc.), thus considerably speeding up the iterations among partners. Nevertheless, some remaining issues were identified especially when comparing 2D reaction rates distributions, and they will be addressed in future versions of NEMESI. The prototype development as well as its V&amp;V with the help of DICE will in fact continue during the follow-up of the CAMIVVER project.</p>			

EDF R&D	CAMIVVER - D4.4 - Results of the verification phases on PWR and VVER geometry configurations	6125-1108-2023-02020-EN Version 1.0
---------	--	--

### Circuit de validation

<b>Auteur</b>	Marco TIBERGA	31/08/2023	
<b>Vérificateur</b>	Pierre LAURENT	31/08/2023	
<b>Approbateur</b>	Adrien WILLIEN	31/08/2023	

<b>Code affaire</b>	P11IS
---------------------	-------

EDF R&D	CAMIVVER - D4.4 - Results of the verification phases on PWR and VVER geometry configurations	6125-1108-2023-02020-EN Version 1.0
---------	--	--

## Liste de diffusion

<b>Groupe destinataire</b>
1108-SNC

Pré-diff	Diff	Destinataire	Structure	E-mail
	X	BERGE Ludovic	EDF R&D - FC	ludovic.berge@edf.fr
X	X	BRIGHENTI Alberto	FRAMATOME	alberto.brighenti@framatome.com
X	X	GULER Nathalie	EDF R&D - PERICLES	nathalie.guler@edf.fr
X	X	HUACCHO ZAVALA Gianfranco	KIT	gianfranco.zavala@kit.edu
X	X	LAURENT Pierre	EDF R&D - PERICLES	pierre.laurent@edf.fr
X	X	MOSCA Pietro	CEA	pietro.mosca@cea.fr
	X	RUPA Nathalie	EDF R&D - PERICLES	nathalie.rupa@edf.fr
	X	TEXERAUD Jerome	EDF R&D - PERICLES	jerome.texeraud@edf.fr
	X	THIEBAUT Virginie	EDF R&D - PERICLES	virginie.thiebaut@edf.fr
X	X	TIBERGA Marco	EDF R&D - PERICLES	marco.tiberga@edf.fr
X	X	VERRIER Denis	FRAMATOME	denis.verrier@framatome.com
X	X	VEZZONI Barbara	FRAMATOME	barbara.vezzoni@framatome.com
X	X	WILLIEN Adrien	EDF R&D - PERICLES	adrien.willien@edf.fr

## AVERTISSEMENT / CAUTION

L'accès à ce document, ainsi que son utilisation, sont strictement limités aux personnes expressément habilitées par EDF.

EDF ne pourra être tenu responsable, au titre d'une action en responsabilité contractuelle, en responsabilité délictuelle ou de toute autre action, de tout dommage direct ou indirect, ou de quelque nature qu'il soit, ou de tout préjudice, notamment, de nature financière ou commerciale, résultant de l'utilisation d'une quelconque information contenue dans ce document.

Les données et informations contenues dans ce document sont fournies "en l'état" sans aucune garantie expresse ou tacite de quelque nature que ce soit.

Toute modification, reproduction, extraction d'éléments, réutilisation de tout ou partie de ce document sans autorisation préalable écrite d'EDF ainsi que toute diffusion externe à EDF du présent document ou des informations qu'il contient est strictement interdite sous peine de sanctions.

-----

The access to this document and its use are strictly limited to the persons expressly authorized to do so by EDF.

EDF shall not be deemed liable as a consequence of any action, for any direct or indirect damage, including, among others, commercial or financial loss arising from the use of any information contained in this document.

This document and the information contained therein are provided "as are" without any warranty of any kind, either expressed or implied.

Any total or partial modification, reproduction, new use, distribution or extraction of elements of this document or its content, without the express and prior written consent of EDF is strictly forbidden. Failure to comply to the above provisions will expose to sanctions.

EDF R&D	CAMIVVER - D4.4 - Results of the verification phases on PWR and VVER geometry configurations	6125-1108-2023-02020-EN Version 1.0, CURRENT
---------	--	---

## Summary

Within the H2020 CAMIVVER Project, the Work Package 4 (WP4) aims at making a step forward in the framework of multi-parameter neutron data libraries generation for Gen II and Gen III LWR (in particular for VVER) using the new-generation deterministic code APOLLO3®.

A lattice calculation platform prototype, named NEMESI, has been developed in the framework of Task 4.1 following system engineering practices and is presented in detail in Deliverable 4.2 - *Description of the architectural choices and implementation of the multi-parametric libraries generator prototype and future perspectives*.

Task 4.2 aims instead at verifying and benchmarking NEMESI against other deterministic and Monte Carlo codes. To this purpose, in the first phase a series of assembly test cases (on both VVER and PWR geometries) have been selected and the representative output parameters to be compared have been defined. They are described in detail in Deliverable 4.3 - *Definitions of tests cases for the verification phases of the multi-parametric library generator*. In the second phase, a selection of test cases was calculated with NEMESI, and the results compared to those obtained with APOLLO2, TRIPOLI-4® and SERPENT-2, by exploiting an automatic post processing tool named DICE (*"Data comparison driver for the benchmark, validation, and verification of NEMESI"*).

This document presents the automatic comparison tool DICE and summarizes the main outcomes of the first V&V activities performed on the NEMESI platform. It is the result of a collaboration among EDF, Framatome, CEA, and KIT. This document corresponds to the Deliverable 4.4 - *Results of the verification phases on PWR and VVER geometry configurations* of the CAMIVVER project.

The results obtained for all configurations at nominal state (with or without control rods) and during depletion show in general very good agreement between NEMESI and the Monte Carlo codes and/or APOLLO2. DICE has helped with the identifications of several sources of discrepancies (input file errors, differences in compositions, geometry, etc.), thus considerably speeding up the iterations among partners. Nevertheless, some remaining issues were identified especially when comparing 2D reaction rates distributions, and they will be addressed in future versions of NEMESI. The prototype development as well as its V&V with the help of DICE will in fact continue during the follow-up of the CAMIVVER project.

## Table of Contents

<b>AVERTISSEMENT / CAUTION</b> .....	<b>1</b>
<b>SUMMARY</b> .....	<b>2</b>
<b>TABLE OF CONTENTS</b> .....	<b>3</b>
<b>1. INTRODUCTION</b> .....	<b>4</b>
<b>2. BENCHMARKS DEFINITION</b> .....	<b>5</b>
2.1. THE DICE TEST MATRIX.....	5
2.2. DATA MODIFICATIONS WITH RESPECT TO D4.3 .....	6
2.2.1. Moderator isotopic composition for KHM2 assemblies.....	6
2.2.2. Dysprosium isotopic composition .....	6
2.2.3. Specific power .....	6
<b>3. CODE PLATFORMS INVOLVED IN THE V&amp;V ACTIVITY</b> .....	<b>7</b>
3.1. NEMESI .....	7
3.2. APOLLO2.....	9
3.3. TRIPOLI-4®.....	9
3.4. SERPENT-2.....	10
3.5. SUMMARY OF THE CHOSEN CALCULATION OPTIONS.....	11
<b>4. AUTOMATIC POST-PROCESSING TOOL</b> .....	<b>12</b>
4.1. DESCRIPTION OF THE VALJEAN FRAMEWORK .....	12
4.1.1. eponine module.....	12
4.1.2. eponine.dataset class.....	13
4.2. DESCRIPTION OF DICE.....	14
4.2.1. DataManager module.....	14
<b>5. RESULTS OF THE FIRST V&amp;V CAMPAIGN ON NEMESI</b> .....	<b>15</b>
5.1. NOMINAL STATE .....	15
5.1.1. VVER configurations.....	15
5.1.2. PWR configurations.....	21
5.2. CONTROL RODS FULLY INSERTED .....	25
5.3. DEPLETED STATE .....	28
<b>6. CONCLUSIONS AND PERSPECTIVES</b> .....	<b>32</b>
<b>7. APPENDIX A – ASSEMBLY CONFIGURATIONS</b> .....	<b>33</b>
7.1. APPENDIX A1 – VVER ASSEMBLY CONFIGURATIONS .....	33
7.2. APPENDIX A2 – PWR ASSEMBLY CONFIGURATIONS.....	38
<b>8. APPENDIX B – OVERVIEW OF NEMESI INPUT DATA FOR T4.2</b> .....	<b>43</b>
<b>9. APPENDIX C – DETAILED RESULTS</b> .....	<b>50</b>
<b>10. APPENDIX D – TRIPOLI-4® AND SERPENT-2 ANALYSIS</b> .....	<b>66</b>
10.1. APPENDIX D.1 – A SIMPLIFIED BENCHMARK .....	66
10.2. APPENDIX D.2 – RESULTS COMPARISON WITH DIFFERENT NDLS .....	67
<b>REFERENCES</b> .....	<b>70</b>



# 1. Introduction

The H2020 CAMIVVER project [1] aims at developing and improving codes and methods for VVER comprehensive safety assessment.

One of the main goals of the CAMIVVER Work Package 4 (WP4) is to set up the framework for the development of an industrial calculation platform performing neutronics lattice analyses and generating multi-parameter data libraries for core calculations of Gen II and Gen III LWR (in particular for VVER), using APOLLO3® [2], the new generation deterministic code developed by the Commissariat à l'Énergie Atomique et aux Énergies Alternatives (CEA) with support of Framatome and Électricité de France (EDF).

The lattice calculation platform prototype, named NEMESI, has been developed in the framework of Task 4.1 following system engineering practices and is presented in detail in Deliverable 4.2 [3]. Task 4.2, for its part, is dedicated to the verification of NEMESI's consistency and its benchmark against other deterministic and stochastic solvers. To this purpose, first a series of test cases (on both VVER and PWR geometries) has been selected and the interesting output parameters to be compared have been defined. They are described in detail in Deliverable 4.3 [4].

The present document, which corresponds to Deliverable 4.4 of the CAMIVVER project ("*Results of the verification phases on PWR and VVER geometry configurations*"), summarizes the main outcomes of the second half of Task 4.2, that is, the first verification and validation (V&V) activities carried out on the NEMESI platform (collaboration among EDF, Framatome, CEA, and KIT). As such, this document is of great importance as it represents the first validation elements of NEMESI (albeit far from being comprehensive).

In fact, V&V, as defined by IAEA [5], aims at providing confidence in a code's ability to predict, realistically or conservatively, the values of the safety parameter or parameters of interest. Being NEMESI a prototype for a future industrial code involved in safety analysis, the demonstration of its validation is therefore paramount (and mandatory). This explains the will to start the V&V process as soon as possible, in parallel with NEMESI's development, in order to reduce the transfer delay from lab to industry.

The document is structured as follows. In Section 2, we list the selected benchmarks from Deliverable 4.3 and recall their main characteristics. In Section 3, we briefly describe the computational tools used to establish the reference results and the main calculation options used by each code. For the sake of maintainability of NEMESI's validation and to ensure the robustness and the non-regression of the results at each development step (before and after NEMESI's industrial deployment), an automatic test matrix has been led off in the context of this task. Hence, in Section 4 we describe the main parts of this automatic comparison tool, named DICE ("*Data comparison driver for the benchmark, validation, and verification of NEMESI*"). In Section 5, we compare the results obtained with the last version of NEMESI (v0.2) to the reference calculations and analyze the discrepancies, in order to validate the NEMESI's capability to produce neutronic libraries for industrial safety analysis. In particular, we focus on results at nominal conditions (Section 5.1), during depletion (Section 5.3) and with inserted control rods (Section 5.2). Finally, in Section 6 we conclude by providing a synthesis of the work carried out in Task 4.2 regarding NEMESI's validation and the future work required to its industrial deployment.

## 2. Benchmarks definition

### 2.1. The DICE test matrix

The starting point of the validation process of any industrial code is the definition of the test cases considered, which must be representative of the code's usage scope. For this reason, at the beginning of the CAMIVVER project (T0+6), Deliverable 4.3 ("*Definitions of tests cases for the verification phases of the multi-parametric library generator*") [4] was redacted to feed the construction of a test matrix dedicated to NEMESI's validation.

The chosen test cases cover VVER-1000 hexagonal assembly technology from the OECD NEA benchmark Kozloduy-6 (KZL6) and the AER Symposium benchmark Khmel'nitsky-2 (KHM2) [6][7] as well as PWR square assembly technology taken from public numerical benchmarks: the well-known KAIST benchmark [8][9], and a 32-assembly minicore described in [10][11] and based on [12]. Moreover, D4.3 covers a wide range of existing and hypothetic fuel technology: uranium dioxide (UOX), mixed oxides (MOX), UOX and MOX with gadolinium burnable absorber pins (UGD) or with pin concentration heterogeneities. In total, twenty different types of assemblies have been selected. Finally, dysprosium-titanate ( $Dy_2TiO_5$  – concisely indicated with Dy in the reminder), boron carbide ( $B_4C$ ), and silver-indium-cadmium (AIC) control rod configurations were also considered. We refer to D4.3 for a detailed description of all chosen assembly configurations [4].

A set of eleven assembly configurations were selected for the first validation activity on NEMESI described in this document, ensuring nevertheless the coverage of the entire technology and fuel spectrum. The first version of the NEMESI test matrix, as implemented in the automatic comparison tool DICE (see Section 4) is summarized in Table 1. We considered (in brackets the assembly's name used in DICE):

- from the KZL6 benchmark, two hexagonal assemblies with UOX fuel and uniform enrichment (FA4\_4\_F) or with zoning (FA3\_3\_G, with and without  $B_4C$  control rods inserted);
- from the KHM2 benchmark, three hexagonal assemblies with stiffeners at the corners with UOX fuel and uniform enrichment (13AU) or with Gd pins and double (390GO) or triple UOX zoning (30AV5) (with and without Dy control rods inserted);
- from the minicore benchmark, a square assembly with UOX fuel and uniform enrichment (A37, with and without AIC control rods inserted); and
- from the KAIST benchmark, two square assemblies with UOX fuel and uniform enrichment (UOX2 and UOX33), one with UOX-Gd fuel pins (UGD), and two with MOX fuel and zoning with (MOX\_GD) or without Gd (MOX).

The main characteristics of each assembly are described in Appendix A – Assembly configurations. Note that no VVER assembly with MOX fuel was considered in the CAMIVVER project. Some complementary configurations will be added in the project follow-up.

**Table 1 - First version of DICE test matrix.**

		Assembly type		
		Hexagonal	Hexagonal + stiffener	Square
Fuel type	UOX	FA4_4_F	13AU	UOX2
				UOX33
				A37 (with or without AIC rods)
	UOX heterogeneous	FA3_3_G (with or without $B_4C$ rods)		
	UGD		390GO (with or without Dy rods)	UGD
			30AV5	
MOX			MOX_GD	
MOX heterogeneous			MOX	

## 2.2. Data modifications with respect to D4.3

While performing the required calculations, three inconsistencies in the available data listed in D4.3 were pointed out:

- the isotopic composition of the moderator material for the Khmel'nitsky-2's assemblies and the reported 800 ppm boron concentration are actually not coherent;
- two natural isotopes of dysprosium are actually missing from the JEFF-3.1.1 nuclear data library [13] used for calculations;
- the specific power to be imposed for each benchmark configuration.

We detail the chosen solutions in the reminder of the section.

### 2.2.1. Moderator isotopic composition for KHM2 assemblies

In [4] – Table 1, the reported nominal boron concentration for the Khmel'nitsky-2 assemblies, which is used during depletion calculations, is 600 ppm. However, Table 17 of [4] is wrong: the caption indicates 600 ppm of boron while the composition included in the table corresponds to 800 ppm. Also, Table 17 of D4.3 reports a moderator density of 0.7526 g/cm<sup>3</sup>, which corresponds to the one indicated in Table 1 for Khmel'nitsky-2 but not for Kozloduy-6. The water isotopic composition for Kozloduy-6 (0.725 g/cm<sup>3</sup>) is not provided in [4].

This inconsistency was resolved by using a boron concentration of 600 ppm for the VVER assembly calculations of Task 4.2 and by ignoring the compositions reported in Table 17 of [4]. The isotopic compositions actually considered for calculations are reported in Table 2.

### 2.2.2. Dysprosium isotopic composition

In [4] – Table 29, the dysprosium natural isotopic composition includes <sup>156</sup>Dy and <sup>158</sup>Dy. However, these isotopes are absent in the JEFF3.1.1 nuclear data library that was used for calculations. It was then decided to fuse <sup>156</sup>Dy and <sup>158</sup>Dy with <sup>160</sup>Dy. In fact, their concentration is small with respect to the concentration of <sup>160</sup>Dy (<sup>156</sup>Dy and <sup>158</sup>Dy are respectively almost 40 and 25 times less abundant), which in turn is 10 times less abundant than the other Dy isotopes. Moreover, the cross sections as well as the resonance integral of <sup>156</sup>Dy and <sup>158</sup>Dy are of the same order of magnitude as those of <sup>160</sup>Dy. For these reasons, this modification was judged to have a negligible impact on the results. The concentration of <sup>160</sup>Dy considered for calculation then becomes 3.28108E20 at/cm<sup>3</sup>.

**Table 2 - Moderator isotopic composition for VVER test cases (replacing Table 17 of [4]).**

Reactor	KHM2	KZL6
Density (g/cm <sup>3</sup> )	0.7526	0.7250
Elements	Atomic density (10 <sup>24</sup> at/cm <sup>3</sup> )	
H2O	2.51494E-02	2.42271E-02
B-10	4.97996E-06	4.79733E-06
B-11	2.01713E-05	1.94316E-05

### 2.2.3. Specific power

In [4], an error was made in the calculation of the specific power for each benchmark configuration reported in Table 1, Table 36, and Table 49. The values reported there must be therefore replaced by those reported in Table 3, which were used for the calculations reported in this document.

**Table 3 – Specific power used for each benchmark case (replacing values reported in Table 1, Table 36, and Table 49 of [4]).**

Reactor	Specific power (MW/MTHM)
Kozloduy6 and Khmel'nitsky2	42.5
Minicore	19.4
KAIST	37.7

### 3. Code platforms involved in the V&V activity

In this section, we briefly introduce NEMESI and the other codes involved in its first validation and benchmarking campaign – the deterministic code APOLLO2 and the Monte Carlo codes TRIPOLI-4® and SERPENT-2 – summarizing the main calculation options adopted by each of them.

#### 3.1. NEMESI

NEMESI is a prototype of a multi-parameter neutron data library generator for LWR applications that is based on the deterministic code APOLLO3® [2] and uses the GUI ALAMOS [14] for mesh generation of VVER cases. Figure 1 schematically shows the structure of NEMESI.

NEMESI was conceived to make the final user's set-up of industrial lattice calculations as easy as possible. To achieve this, the user is given the possibility to modify the input parameters and options. The provided input is used to load predefined calculation sequences or create objects necessary to the simulation. The predefined directives, specialized to reactor type (VVER, PWR), are used in all simulation types (e.g., standalone, depletion, or branch calculations), like isotope definitions, self-shielding options, output homogenization directives, etc. Other objects, like the depletion iterator or the Archive object (to store some specific results), are created depending on the chosen simulation type and provided input.

The first version of NEMESI was issued at T0+24 (“MS2 - First version of prototype based on APOLLO3®”). Since then, several improvements were included and finally made available in NEMESI v0.2, released at the end of the CAMIVVER project. It is the version used to perform the calculations analyzed in this document.

With respect to v0.1, NEMESI v0.2 implements some basic parameters and options, but they nevertheless allow performing lattice depletion and branch calculations for lattice simulations and preparing PWR and VVER assembly multi-parameter library (MPO) for core calculations.

To perform only parallel branch calculations, it is first mandatory to complete a simulation to generate the Archive HDF file containing the isotopic concentrations, then let the branch calculations restart from that Archive. The strategy of performing the depletion calculation separately, followed by the execution of branch calculations, allows generating a shared Archive HDF file that can be in parallel read by all processes of the branch calculations allowing a reduction of the computational time. Other advantages are that if a branch calculation fails, it does not stop the overall execution, and it is possible to add additional branch points “a posteriori” by simply defining the new state point values and running the simulation for that branch.

In version 0.2, the final user has access to a restricted number of parameters for setting up the calculations (either a standalone simulation, a depletion calculation, or a depletion with branches calculation), a choice done in view of a future industrialization of the tool.

The entry points of NEMESI are a Python script called `compute.py`, and a JSON file, called `inputMain.json` (an example of which is shown in Figure 2). The user modifies the JSON file according to the kind of simulation to perform. Then, the Python script is launched providing the name of the JSON file as an input parameter. An interactive mode is also available as described in [3].

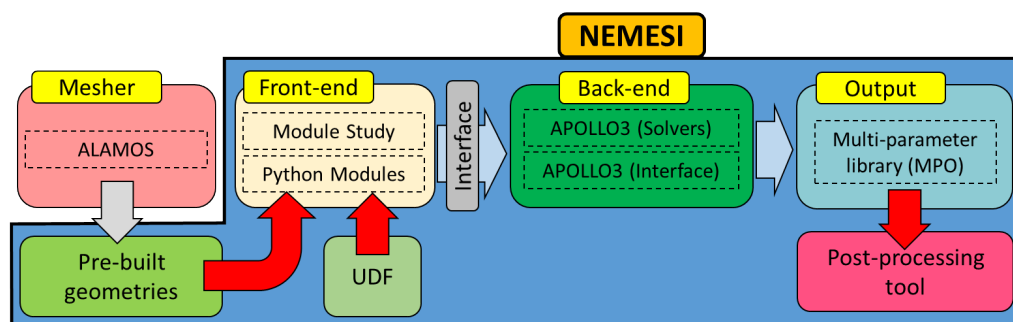


Figure 1 - Schematic representation of NEMESI (from [3]).

```

1  {
2      "reactor": "PWR32",
3      "assembly": "A37",
4      "configurations": ["ARO", "AIC"],
5      "geometry_type": "EXTERNAL",
6      "calculation_scheme": "SHEMOC",
7      "boundary_conditions": "SPECULAR",
8      "leakage_model": "B2ZERO",
9      "out_number_of_groups": 2,
10     "output_settings": [8, "HOM"],
11     "mpo_configurations": ["ARO", "AIC"],
12     "usage": "standalone",
13     "flux_normalization": [36.8577, "PowerDensity", ""],
14     "generate_output": false,
15     "generate_mpo": true,
16     "generate_archive": true,
17     "generate_tripoli": false,
18     "depleting_configuration": "ARO",
19     "generate_branches": true,
20     "burnup_steps": [0.0, 10.0],
21     "boron_concentration": [600.0, 2800.0],
22     "fuel_temperature": [700.0, 1200.0],
23     "coolant_density": [0.4, 0.6],
24     "points_per_branch": 4,
25     "launch_branches_once_finished": false,
26     "launch_branches_sequential": false,
27     "branch_number": null,
28     "dump_input": true
29 }

```

**Figure 2 - Example of inputMain.json file for NEMESI (from [3]).**

NEMESI is written in Python, following PEP 8 guidelines, and it is based on a hybrid approach: a set of Python modules embedding the Python and UDF interface of APOLLO3® starting from release v2.2 [15] but integrating then v2.3 [16] and later development versions<sup>1</sup>. For v0.2, the prerequisites of NEMESI in addition to the ones on APOLLO3® are the `iapws` Python package for computing water properties and, implicitly, its dependencies.

The interested reader can find a detailed description of NEMESI in Deliverable 4.2 “Description of the architectural choices and implementation of the multi-parameter library generator prototype and future perspectives” [3] as well as in a paper recently presented at the M&C2023 conference [17].

For the V&V activities reported in this document, we used NEMESI v0.2 to generate MPO files (HDF format) for each assembly configuration in the test matrix (Table 1). The MPOs, used as outputs to be passed to DICE, were generated with the following main options:

- adoption of the method of characteristics (MOC) for flux calculations (notably, the step-constant scheme, SC);
- adoption of the fine structure (FS) method for self-shielding calculations, without any geometry simplifications (exact  $P_{ij}$  method). Choice of the Livolant-Jeanpierre method to treat resonant mixtures;
- adoption of the SHEM-281 multi-group neutron data library [18] (without upscattering), based on JEFF 3.1.1;
- no Debye correction to determine the fuel effective temperature;
- anisotropy level: P3 for VVER calculations and P0c (i.e., using transport corrected P0 moments of the scattering cross section) for PWR calculations;

<sup>1</sup> Several development versions were considered for carrying out V&V activities in support to NEMESI development. The calculations reported here are the last ones produced with APOLLO3® 2.3dev (last calculations run with version from commit 6bf50bbe)

EDF R&D	CAMIVVER - D4.4 - Results of the verification phases on PWR and VVER geometry configurations	6125-1108-2023-02020-EN Version 1.0, CURRENT
---------	--	---

- depletion modeled up 70 GWd/t, with a burnup mesh with more than 60 calculation points as indicated in D4.3 [4], imposing constant power conditions;
- nominal conditions for temperatures, boron concentration, and water density as reported in [4];
- pin-by-pin output homogenization;
- leakage treatment:  $B^2 = 0$ .

The detailed NEMESI JSON input files used for each test case are reported in Appendix B – Overview of NEMESI Input Data for T4.2.

### 3.2. APOLLO2

APOLLO2 [19] is a deterministic spectral transport code maintained by CEA with the support of EDF and Framatome. It is widely used for cross section generation and for reference direct transport calculations, with a range of applications spanning from reactor physics to criticality safety studies and to fuel cycle analysis. All the French nuclear actors (CEA, EDF, Framatome, IRSN) have been using APOLLO2 for years for both R&D and industrial calculations. In fact, it was integrated in Framatome's and EDF's neutronics code packages SCIENCE and CASSIOPEE as well as in the new platform under development [20]. As such, APOLLO2 can count on decades of employment and validation efforts. For this reason, it constitutes a qualified benchmark for NEMESI.

For the V&V activities reported in this document, we used the industrial multi-parameter neutron data library generator based on APOLLO2.8-A (the latest APOLLO2 version available). Results were output in the APEX format and directly passed to DICE for their postprocessing. We chose the same main calculation options adopted with NEMESI, except for self-shielding as NEMESI requires an exact-Pij solver, while APOLLO2 requires a multicell-Pij solver. Moreover, the P0\* anisotropy order was chosen (as customary in industrial schemes), which corresponds to a P0c expansion for all isotopes except fission products, for whom a pure P0 expansion is chosen. Only the PWR cases were simulated with APOLLO2. In fact, its industrialized version used in CAMIVVER is not equipped with the necessary functionalities to deal with VVER geometries.

### 3.3. TRIPOLI-4®

TRIPOLI-4® [21] is a three-dimensional, continuous energy code for particle transport based on the Monte Carlo method. It can simulate the transport of neutrons, photons, electrons, and positrons, and it is designed for both reactor physics and radiation shielding applications. The code is being developed, since its first version in the late sixties, at CEA with the support of EDF, and it is extensively used by all French nuclear actors for the validation of their respective deterministic code platforms.

For the calculations reported in this document, we used version 4.12, which is the most recent version available, adopting the following main simulation options:

- 15000 neutrons per cycle;
- 40000 active criticality cycles;
- 100 discarded cycles;
- neutron data taken from the JEFF-3.1.1 library and interpolated according to the square root of the temperature;
- NJOY, to use pointwise cross-sections evaluated with NJOY 99;
- default epithermal broadening model, that is, the Sampling of the Velocity of the Target nucleus (SVT).

TRIPOLI-4® is coupled to ROOT, an object-oriented software package used to process and analyze data developed at CERN [22]. We exploited this feature by using a Python PyROOT script to generate the geometry of each test case and to associate the correct material properties to each volume, thus greatly simplifying the calculations setup phase.

### 3.4. SERPENT-2

SERPENT-2 is a continuous energy Monte Carlo code developed by the Finnish VTT Technical Research Centre [23]. It is used for a wide range of reactor physics applications, and it is capable of burnup and multi-physics calculations.

For the calculations in Task 4.2, geometries and material compositions for each test case were set up using the native input file options. The following main simulation options were adopted:

- 1E6 neutrons per cycle in nominal state-points (1E5 for burnup cases);
- 300 active criticality cycles in nominal state-points (500 for burnup cases);
- 100 discarded cycles;
- no Xenon equilibrium calculation;
- Processed neutron data library (NDL) based on the JEFF-3.1.1 provided with the SERPENT-2 code was used at first. A second processed NDL from IRSN [25] was also tested for comparison;
- Default Doppler-broadening pre-processor TMP;
- Interpolation between two neighbor temperature-dependent thermal scattering cross sections is used;
- no sampling of probability tables in the unresolved resonance range;
- 2 energy group constants are generated with a leakage-corrected critical spectrum (new B1 mode with default intermediate multi-group structure). Infinite spectrum is used for burnup calculations;
- LELI time integration mode for burnup calculations. Suggested burnup points in D4.3 are used;
- For depletion zones in burnup calculation, each pin is treated independently and divided into ten radial subregions;
- Fixed power density according to the fuel assembly case is considered for normalization; and
- Default energy deposition model is used for burnup calculation (constant energy deposition per fission) (the reader is referred to the SERPENT-2 manual [24] for more details).

### 3.5. Summary of the chosen calculation options

Table 4 summarizes the main neutronics scheme options adopted for calculations with NEMESI and APOLLO2, while Table 5 those chosen for calculations performed with the Monte Carlo codes TRIPOLI-4® and SERPENT-2.

**Table 4 - Main calculation options adopted by each deterministic code.**

	NEMESI		APOLLO2
Solver	MOC		MOC
Energy mesh	SHEM-281		SHEM-281
Anisotropy	PWR	VVER	P0* (only PWR treated)
	P0c	P3	
SSH methods	Fine Structure (exact Pij)		Fine Structure (multicell Pij)
Upscattering	No		No
Debye Correction	-		No
Leakage	No leakage ( $B^2 = 0$ )		No leakage ( $B^2 = 0$ )
Nuclear Data	JEFF-3.1.1		JEFF-3.1.1

**Table 5 - Main calculation options adopted by each Monte Carlo code.**

	TRIPOLI-4®	SERPENT-2	
Number batches	40000 (+100 discarded)	NOMINAL STATE-POINT	BURNUP
		300 (+100 discarded)	500 (+100 discarded)
Batches size	15000	1000000	100000
Total particle simulated	600000000	300000000	50000000
Doppler broadening method	Default (SVT)	TMP (Solbrig's kernel)	
Nuclear Data	JEFF-3.1.1	JEFF-3.1.1	
Probability tables for unresolved resonances	No	No	
Temperature interpolation	Sqrt(T)	Only for thermal scattering cross sections	



## 4. Automatic post-processing tool

The necessity for an automatic test matrix and post-processing tool is driven by the following objectives:

1. During the development phase: to ensure and facilitate the comparison between NEMESI's results and the references. This, in addition to unit tests, helps developers correcting possible bugs and increases confidence in each feature newly developed;
2. During the industrialization: to informatically ensure the comparison between NEMESI's results and each reference, and to automatically generate the comparison report analyzed in the validation report;
3. During the industrial use: to ensure that the results obtained with each NEMESI's version are still in agreement with the validation report by proving robustness and non-regression or, conversely, by showing discrepancies that must be acceptable, explainable, and kept under control.

For these reasons, in the context of Task 4.2 of the CAMIVVER project we developed a Python module, named DICE<sup>2</sup> (*"Data comparison driver for the benchmark, validation, and verification of NEMESI"*), that we used to benchmark the results of NEMESI v0.2 presented in Section 5. DICE is largely based on the exploitation of the `valjean` framework [26] developed by CEA and mainly used as a tool for the V&V of the TRIPOLI-4<sup>®</sup> Monte-Carlo code. The following subsections describe first the functionalities used and developed in `valjean` and then those in DICE before giving an example of NEMESI's V&V suite capabilities.

DICE plays an essential role in automatizing the future test matrix of NEMESI, and thus it will hold an important role in reducing the delays in transferring the APOLLO3<sup>®</sup> lab solution to industry. Moreover, DICE's API can provide a valuable assistance in building a non-regression test suite, which is a mandatory step to prove that any code modification has no unexpected impact on the results or that the validation report can be reproduced on different computational platforms.

### 4.1. Description of the valjean framework

`valjean` is a framework for building test suites for scientific computing [26]. It can help with the automation of most of the steps of a typical test suite, including checkout and compilation of the source code, execution of calculations, post-processing of calculations results, hypothesis testing and generation of test reports. Only the post-processing, testing, and report generation features were exploited in this work, but other capabilities like compilation of the source code followed by execution of calculations are features of great interest that will likely be integrated in DICE in the future.

`valjean` sources are organized in packages API as follows:

- **cambronne**: logs manager;
- **cosette**: Python Task creator, executor, and manager;
- **gavroche**: testing module;
- **javert**: test report administrator;
- **eponine**: results reader, dataset creator and interface.

In the following, we report the main features of each module.

#### 4.1.1. eponine module

In the `eponine` module lie all the functionalities relative to the results reading and their logical ordering.

Submodules composing `eponine` are logically divided in two parts: one `dataset` module dedicated to the definition of the `valjean` dataset object structure (that will be manipulated by all the other modules, especially `gavroche` and `javert`) and modules for data parsing/reading that provide methods for

---

<sup>2</sup> To be pronounced "dike"

building `valjean` dataset objects containing parsed/read data. The reader/parser modules are specific to each neutronic code and so they bear the name of the code they were developed for.

The `eponine` submodules are:

- **dataset**: common module to structure data in the same way for all codes;
- **tripoli4**: TRIPOLI-4® parser module;
- **apollo3**: APOLLO3® reader module. This module was enriched during the CAMIVVER project to handle the MPO (multi parametric output) format of the APOLLO3® results. It calls the parser `MPOlib` [27], developed by CEA, to easily access the MPO content;
- **apollo2**: APOLLO2 reader module. This module was entirely developed during the CAMIVVER project to handle the APEX (Apollo2 Portable data EXchange) format of the APOLLO2 results;
- **serpent2**: SERPENT-2 parser module. This module was fully developed during the CAMIVVER project to handle SERPENT-2 results data files. It calls the module `serpentTools` to easily access the results;

#### 4.1.2. `eponine.dataset` class

The first difficulty when comparing results from different codes is the large range of possibilities offered to represent each physical quantity:

- it can be stored in many different file formats (e.g., txt, hdf, etc.);
- it can be expressed in many different units;
- it can be expressed in many different bins and order in many ways;
- finally, it can be normalized or manipulated at will.

Before comparing two quantities from different codes, one needs to make sure the manipulated objects are comparable and thus must fully understand the logic used by each code to express its own quantity. The more codes involved, the harder it is to identify all these specifications. The `eponine` module addresses this problem, leaving the file format problem to dedicated submodules in order to produce a unified and shared data object: the `dataset valjean`.

The `dataset` object is correctly ordered at initialization and holds bins information, thus ensuring that compared dataset share the same bins and are physically comparable.

A `dataset valjean` consists of five elements:

- **value**: a `numpy.ndarray` or a `numpy.generic` (scalar from `numpy`) for storing data values;
- **error**: an object of same type as `value` for storing data errors (relevant especially for Monte Carlo codes);
- **bins**: a `collection.OrderedDict` which explicitly defines the value dimensions<sup>3</sup>;
- **name**: name of the dataset (optional);
- **what**: text information of the dataset (optional).

Moreover, a `dataset valjean` provides standard operations (e.g., +, -, \*, /, indexing, and slicing).

<sup>3</sup> For a scalar value (e.g., a mono-group absorption rate in an homogeneous assembly), bins is an empty `OrderDict()`. For a multi-dimensional value (e.g., a multi-group absorption rate at cell/pin level), bins' attributes have information about spatial and energy discretization (number of groups x number of regions) and values scheduling, for example:

```
OrderDict({'x', array([ 1,  2,  3,  4,  5,  6,  7,  8,  9, 10, 11, 12, 13, 14, 15, 16, 17, 18, 19, 20, 21])), ('y', array([ 1,  2,  3,  4,  5,  6,  7,  8,  9, 10, 11, 12, 13, 14, 15, 16, 17, 18, 19, 20, 21])), ('energy', array([2.00e+01, 6.25e-07, 1.00e-11]))
```

## 4.2. Description of DICE

DICE is a Python collection of modules built to make the final user's set-up of comparison scripts as easy as possible. In the V&V process, code results on chosen cases, defined by an object (e.g., an assembly in the case of NEMESI's V&V in CAMIVVER) in specific conditions – also called “state point conditions” in library generation context – are compared to reference results according to a test method.

DICE's sources are organized in order to separate the V&V steps presented below. The following modules compose this Python API for V&V:

- **DataManager**: a collection of Python classes dedicated to data reading/parsing and to building each Quantity of Interest (QoI) in `valjean dataset` format;
- **StateManager**: a Python class `state.state` that at initialization sets up the nominal conditions for a given reactor. Then, `state elements`<sup>4</sup> can be manipulated using simple and automatic class methods: `set`, `set_to_nominal` and `set_rods`;
- **TestManager**: a Python class to manage comparison tests;
- **tests**: the unitary and functional tests of DICE;
- **tutorials**: Python scripts to launch comparisons, hexagonal plot generation and report generation.

### 4.2.1. DataManager module

The `DataManager` module is a collection of the following submodules:

- **phyType**: QoI naming manager;
- **assembly**: Parent class defining QoI attributes and providing common methods for data manipulation: `_homogenize_XS_`, `_homogenize_flux_`, `force_set_energy_mesh`, etc;
- **apollo2\_apex**: Child class inheriting from `assembly` that works as a collection of `valjean dataset` for each QoI available in a given APEX format result file. It is initiated with a result file's path and a `state` object set-up on the expected state point;
- **apollo2**: Child class inheriting from `assembly` that works as a collection of `valjean dataset` for each QoI available in a given DKLib format result file. It is initiated with a result file's path and a `state` object set-up on the expected state point;
- **apollo3**: Child class inheriting from `assembly` that works as a collection of `valjean dataset` for each QoI available in a given MPO format result file. It is initiated with a result file's path, a `state` object set-up on the expected state point, and information about reactor technology (VVER or PWR) for hexagonal or square assembly geometry identification;
- **serpent**: Child class inheriting from `assembly` that works as a collection of `valjean dataset` for each QoI available in a given SERPENT-2's result file. It is initiated with a result file's path, a `state` object set-up on the expected state point, and information about reactor technology (VVER or PWR) for hexagonal or square assembly geometry identification;
- **tripoli4**: Child class inheriting from `assembly` that works as a collection of `valjean dataset` for each QoI available in a given TRIPOLI-4<sup>®</sup> result file. It is initiated with a result file's path<sup>5</sup> and information about reactor technology (VVER or PWR) for hexagonal or square assembly geometry identification.

<sup>4</sup> The number of descriptive attributes for a state point condition is flexible. Classical parameters are burnup, fuel temperature, moderator density, moderator temperature (optional), boron concentration, xenon level and rods configuration.

<sup>5</sup> In NEMESI's V&V, TRIPOLI-4<sup>®</sup> was used only for simulations at burnup zero. Then, state conditions are fixed and can be directly linked to the result's file name, which is obviously part of the result file's path.

## 5. Results of the first V&V campaign on NEMESI

In this section, we report and analyze the results obtained during the first V&V campaign of NEMESI carried out in Task 4.2 of the CAMIVVER project.

For each of the test cases described in Section 2, we compared the following Qol<sup>6</sup>:

- infinite multiplication factor ( $k_{\infty}$ );
- normalized mono-group fission rate at pin-by-pin level; and
- normalized mono-group absorption rate at pin-by-pin level.

Each of these Qol was compared at nominal state, during depletion, and – when relevant – with control rods fully inserted. For the sake of clarity, in the remainder of the section we analyze only the main results obtained. The complete set of results generated by DICE are reported in Appendix C – Detailed results.

All NEMESI output files are available via the CAMIVVER Tuleap portal (<https://codev-tuleap.cea.fr/plugins/document/apollo3-camivver/folder/14228>), as well as the TRIPOLI-4<sup>®</sup> and SERPENT-2 input and output files and the full V&V report generated by DICE. They will be uploaded to an open access platform according to CAMIVVER's dissemination plan.

Depletion Monte Carlo simulations are extremely expensive, and nowadays they are in practice unfeasible with the TRIPOLI-4<sup>®</sup> code. Hence, calculations were carried out only with SERPENT-2<sup>7</sup>.

### 5.1. Nominal state

#### 5.1.1. VVER configurations

Table 6 displays the  $k_{\infty}$  obtained with NEMESI for the selected VVER assembly configurations, alongside the deviations with respect to the other code packages chosen for NEMESI's benchmarking. Deviations between two results are given in terms of reactivity:

$$\Delta k_{\infty} = \frac{1}{k_{\infty,ref}} - \frac{1}{k_{\infty,NEMESI}}$$

The level of agreement between NEMESI and both TRIPOLI-4<sup>®</sup> and SERPENT-2 is very good, with most discrepancies staying below 100 pcm, except for the Khmelnitsky 30AV5 case where the discrepancy with TRIPOLI-4<sup>®</sup> reaches 120 pcm. Reactivity in TRIPOLI-4<sup>®</sup> is also systematically higher than in NEMESI. Also, notice a very good agreement between TRIPOLI-4<sup>®</sup> and SERPENT-2, with results differing by almost 30 pcm at maximum. These are the latest set of results by SERPENT-2 and were obtained with the JEFF3.1.1 IRSN NDL. The original results with the JEFF3.1.1 VTT NDL were characterized by a discrepancy between 50 and 100 pcm with respect to TRIPOLI-4<sup>®</sup>. An effort to investigate and reduce the discrepancies between the two Monte Carlo codes was in fact carried out.

<sup>6</sup> These are the Qol considered for validation purposes, that is, when comparing NEMESI's results with those obtained with Monte Carlo codes. The complete set of Qol for verification and non-regression purposes consists of 32 Qol, which, among others, include:

- the 3 validation Qol;
- 2-groups flux ratio at assembly level;
- geometrical buckling ( $B^2$ );
- assembly flux discontinuity factors on external surfaces and external corners of the whole fuel assembly;
- multi-group absorption assembly-homogenized macroscopic cross sections;
- multi-group scattering assembly-homogenized macroscopic cross sections;
- multi-group total assembly-homogenized macroscopic cross sections;
- multi-group fission assembly-homogenized macroscopic cross sections;
- multi-group (n,2n) assembly-homogenized macroscopic cross sections;
- kinetic data;
- <sup>235</sup>U, <sup>238</sup>U and <sup>239</sup>Pu concentration;
- 2D distribution of fuel pin burnup; etc.

<sup>7</sup> Using the following BU mesh: [0.01, 0.02, 0.03, 0.04, 0.05, 0.075, 0.1, 0.15, 0.2, 0.25, 0.3, 0.35, 0.4, 0.45, 0.5, 0.75, 1, 1.5, 2, 2.5, 3, 3.5, 4, 4.5, 5, 6, 7, 8, 9, 10, 11, 12, 13, 14, 15, 16, 17, 18, 19, 20, 21, 22, 23, 24, 25, 26, 27, 28, 29, 30, 32, 34, 36, 38, 40, 42, 44, 46, 48, 50, 52, 54, 56, 58, 60, 62, 64, 66, 68, 70] GWd/t.

Details of the investigation are presented in Appendix D – TRIPOLI-4® and SERPENT-2 analysis.

Table 7 (resp. Table 8) shows the minimum, maximum, and standard deviation errors on the normalized absorption (resp. fission) cell rates for each VVER assembly configuration, evaluated according to

$$\Delta\tau\% = (\tau_{ref} - \tau_{NEMESI}) \times 100.$$

The maximum deviation for the two Kozloduy cases was higher than 1% for both normalized absorption and fission rates, and with respect to both TRIPOLI-4® and SERPENT-2. Looking at the rates 2D distributions within the FA\_3\_3\_G assembly, we noticed that the cells with maximum discrepancies were always located at the border of the assembly. After some investigation, we discovered that this issue was due to a geometry/mesh incoherence between NEMESI and Monte-Carlo calculations. In fact, in the APOLLO3® geometry, the water blade at the edge of the assembly shrank the external cells as shown in Figure 3. It led to inconsistent results on the external row that thus were not comparable to Monte-Carlo simulations. The corner's cell, shrunk on two sides by the water blade, were holding the maximum discrepancies only because it was the cell whose volume was the most inconsistent with respect to the corresponding cell in the Monte Carlo mesh. Anyhow, APOLLO3® output geometry was eventually corrected, and the comparison carried out on the most recent results shows very good agreement between NEMESI and Monte-Carlo on Kozloduy cases for un-rodged configurations (see Figure 4).

**Table 6 –Comparison of  $k_{\infty}$  between NEMESI, TRIPOLI-4®, and SERPENT-2 for VVER benchmark assemblies.**

	NEMESI $k_{\infty}$	TRIPOLI-4® $k_{\infty}$	$\Delta$ TRIPOLI-4® (pcm)	SERPENT-2 $k_{\infty}$	$\Delta$ SERPENT-2 (pcm)
KZL6 FA_3_3_G	1.24060	1.24164	67	1.24160	65
KZL6 FA_4_4_F	1.31633	1.31760	73	1.31726	54
KHM2 13AU	0.96872	0.96943	75	0.96951	85
KHM2 390GO	1.24749	1.24895	94	1.24907	101
KHM2 30AV5	1.13810	1.13966	120	1.13929	91

**Table 7 – Error statistics on normalized absorption rate between NEMESI, TRIPOLI-4®, and SERPENT-2 for VVER benchmark assemblies.**

	$\Delta$ TRIPOLI-4® (%)			$\Delta$ SERPENT-2 (%)		
	Min	Max	Std	Min	Max	Std
KZL6 FA_3_3_G	-0.26	0.22	0.10	-0.54	0.73	0.19
KZL6 FA_4_4_F	-0.28	0.23	0.10	-0.22	0.28	0.09
KHM2 13AU	-0.52	0.23	0.11	-0.22	0.25	0.08
KHM2 390GO	-0.39	1.06	0.17	-0.64	1.29	0.23
KHM2 30AV5	-0.97	2.04	0.38	-1.18	2.04	0.37

**Table 8 – Error statistics on normalized fission rate between NEMESI, TRIPOLI-4®, and SERPENT-2 for VVER benchmark assemblies.**

	$\Delta$ TRIPOLI-4® (%)			$\Delta$ SERPENT-2 (%)		
	Min	Max	Std	Min	Max	Std
KZL6 FA_3_3_G	-0.30	0.26	0.10	-0.75	0.97	0.24
KZL6 FA_4_4_F	-0.38	0.29	0.11	-0.30	0.34	0.11
KHM2 13AU	-0.39	0.39	0.11	-0.24	0.25	0.09
KHM2 390GO	-0.43	0.32	0.12	-0.74	0.70	0.25
KHM2 30AV5	-1.27	0.82	0.34	-1.40	1.12	0.42

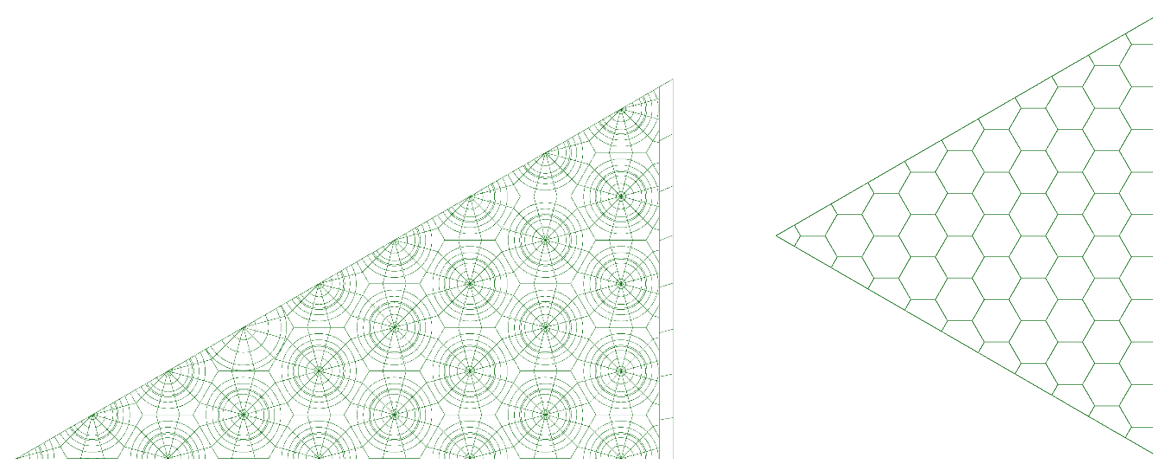


**Figure 3 – KZL6 FA3\_3\_G test case: old flux mesh (on the left) and output mesh (on the right) used in NEMESI calculations. Contrary to Monte Carlo calculations, boundary cells were truncated by the water blade. This issue was eventually fixed.**

The maximum deviation is higher than 1% for the two Khmel'nitsky UGD assembly cases (even higher than 2% on the absorption rate for the Khmel'nitsky 30AV5 assembly). Looking at the error distributions in Figure 5 and Figure 6, it can be noticed that these cells always correspond to gadolinium pins. However, the fact that some gadolinium pins from 30AV5 do not display differences with respect to TRIPOLI-4® suggests that this issue probably arises from a difference in the definition of some gadolinium pins between the computations. The fact that gadolinium pins on symmetry axis shows good agreement with Monte-Carlo suggest that APOLLO3®'s rotation should be investigated. The difference between NEMESI and Monte-Carlo test cases on normalized fission rates is also slightly higher for 30AV5 than for the other VVER assemblies.

Finally, as shown in Figure 7, also for the Khmel'nitsky assemblies the MOC mesh used in APOLLO3® calculations is characterized by an external row of cells row truncated by the water blade and the stiffener. The output mesh however is coherent with the one used for Monte Carlo calculations. Anyhow, once more the agreement with Monte Carlo calculations is on average extremely satisfactory, as the standard deviation error on both reaction rates is around 0.1% for the 13AU and the 390GO configurations and around 0.4% for the 30AV5 one.

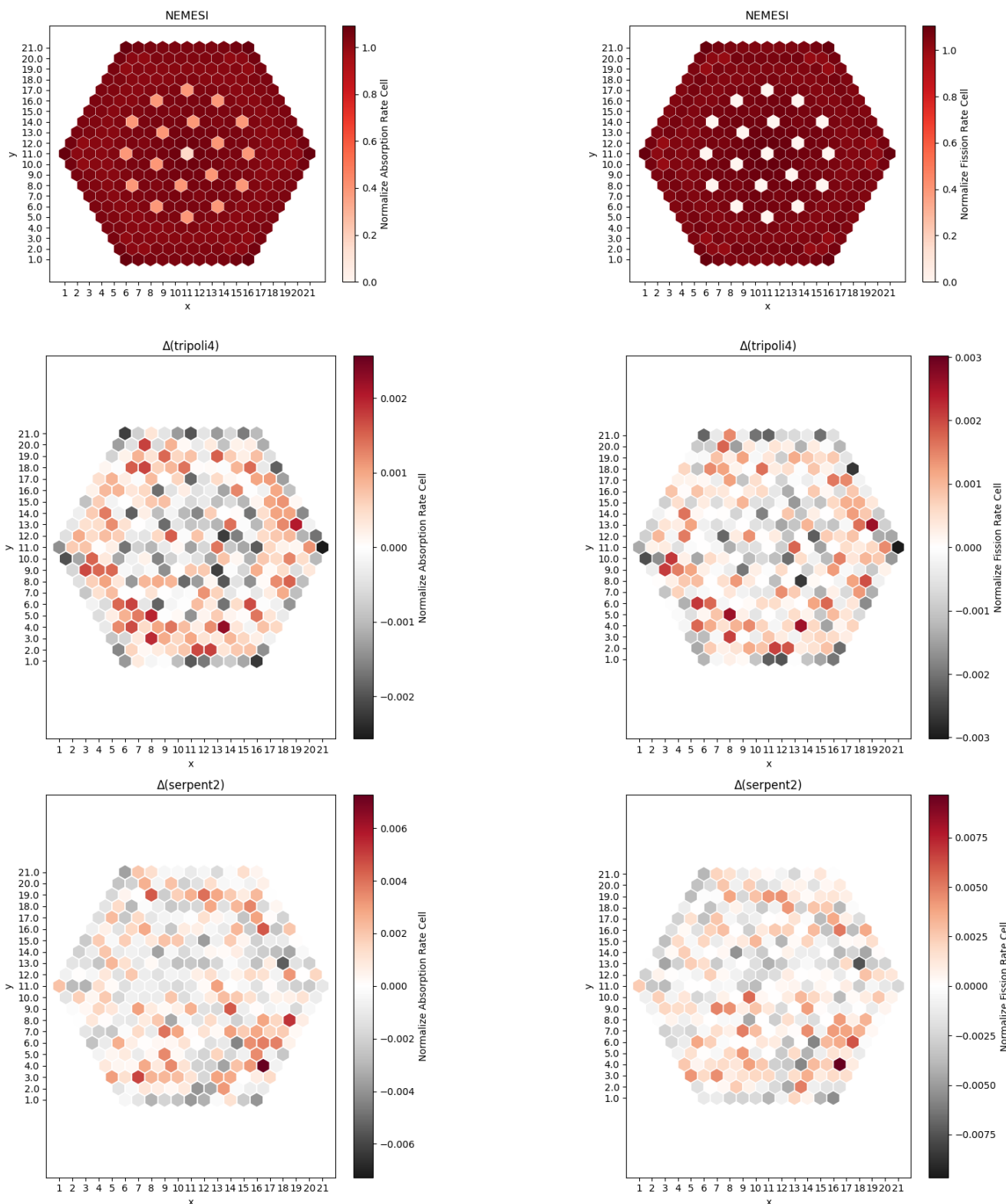


Figure 4 – Normalized absorption and fission rates for KZL6 – FA3\_3\_G obtained with NEMESI and comparisons with TRIPOLI-4® and SERPENT-2.

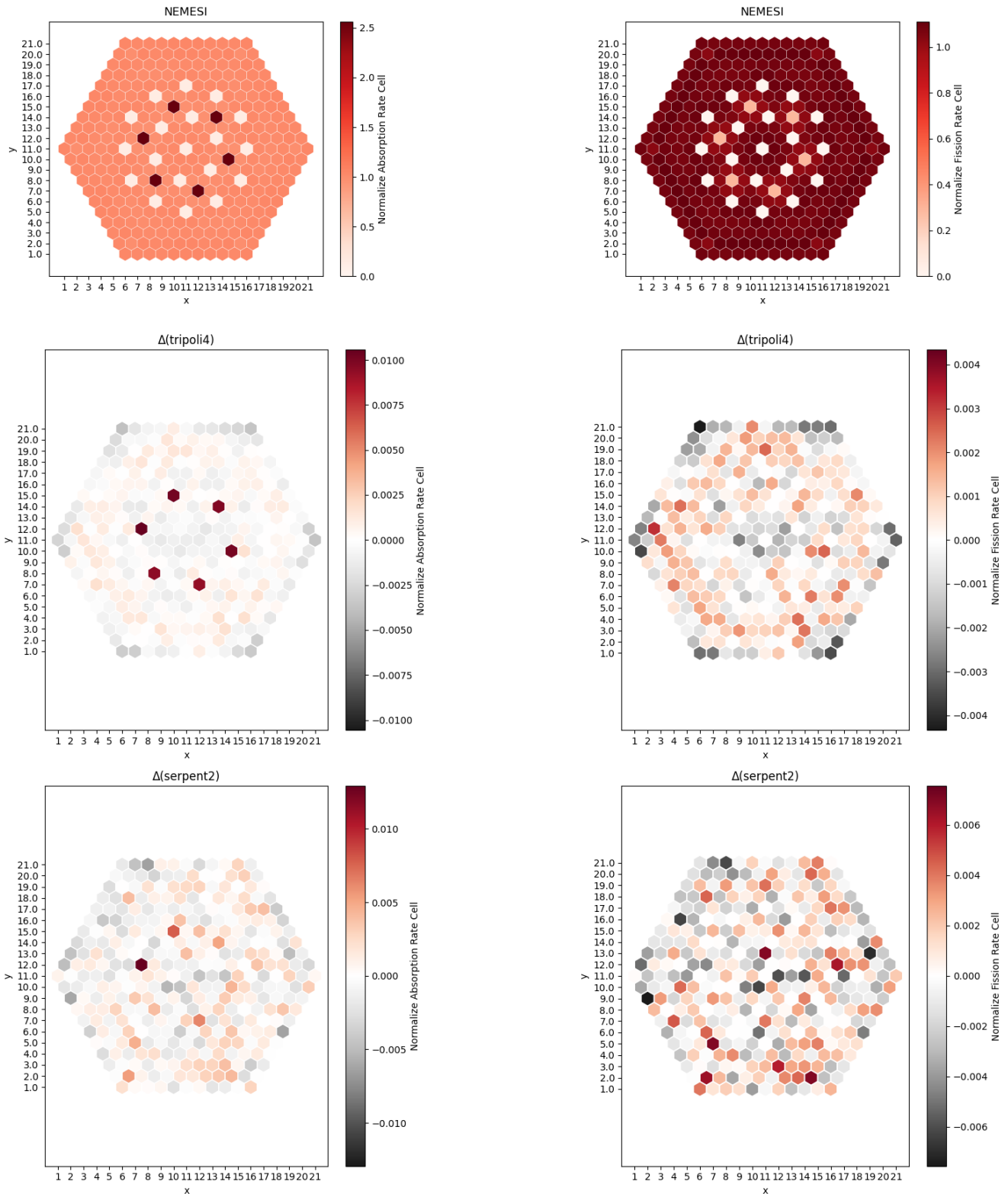
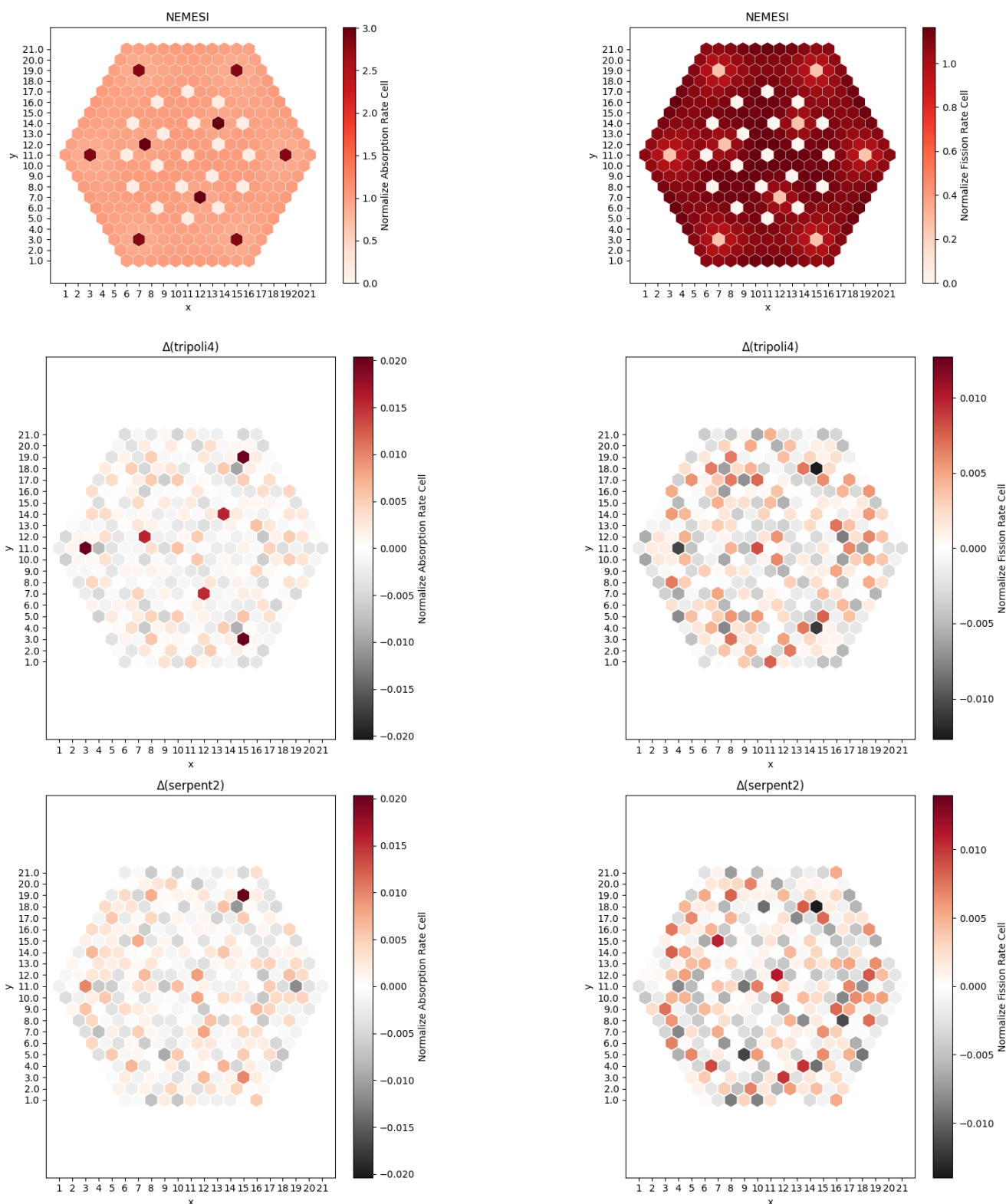
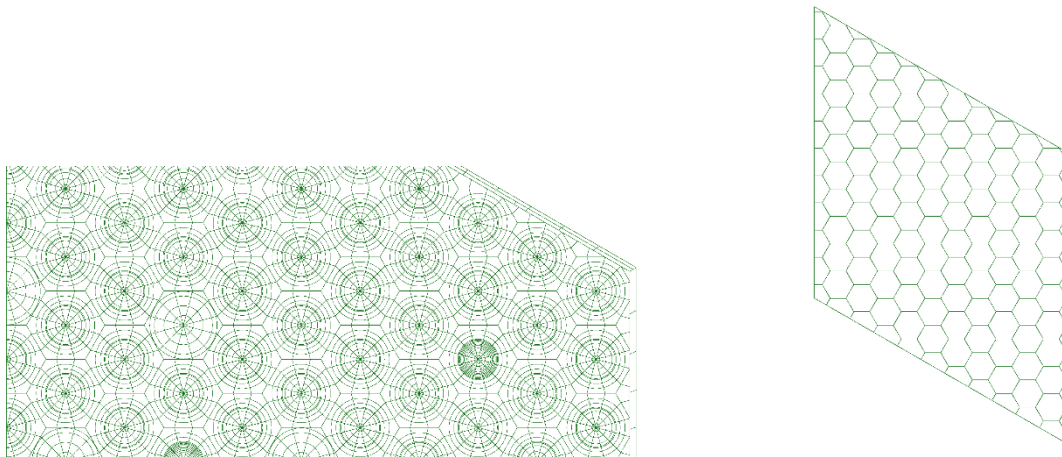


Figure 5 – Normalized absorption and fission rates for KHM2 – 390GO obtained with NEMESI and comparisons with TRIPOLI-4® and SERPENT-2.





**Figure 6 – Normalized absorption and fission rates for KHM2 – 30AV5 obtained with NEMESI and comparisons with TRIPOLI-4® and SERPENT-2.**



**Figure 7 – KHM2 30AV5 test case: flux mesh (on the left) and output mesh (on the right) used in NEMESI calculations.**

### 5.1.2. PWR configurations

The  $k_{\infty}$  results for the PWR assembly configurations are reported in Table 9. As for the VVER cases, the agreement between NEMESI and the Monte Carlo codes is very good. With the JEFF3.1.1 IRSN NDL, SERPENT-2 results very close to TRIPOLI-4<sup>®</sup> are obtained, except on the KAIST MOX\_GD case, where we notice a discrepancy of 70 pcm. This might be due also to the absence of <sup>152</sup>Gd in the JEFF3.1.1 IRSN NDL. The matter is discussed more in detail in Appendix D – TRIPOLI-4<sup>®</sup> and SERPENT-2 analysis. An approximate 60-70 pcm discrepancy can be noticed between NEMESI and APOLLO2, probably mainly correlated to the different model used for self-shielding calculations (exact or multicell Pij) and to the different anisotropy order adopted for the fission products (P0c or P0) (see Table 4). Thanks to recent developments in APOLLO3<sup>®</sup>, we plan to carry out further analyses to quantify the impact of these choices in the future follow-up project.

Table 10 (resp. Table 11) shows the minimum, maximum, and standard deviation errors on the normalized absorption (resp. fission) cell rates for each PWR assembly configuration. Similarly to what was observed for the Khmel'nitsky UGD assemblies, the maximum deviation with respect to NEMESI is close to 2% for the normalized absorption rate in the KAIST MOX\_GD configuration with respect to both TRIPOLI-4<sup>®</sup> and SERPENT-2, and the corresponding cells are again gadolinium pins (see Figure 8). However, we notice that the KAIST UGD configuration is not affected by this problem, suggesting that the issue in APOLLO3<sup>®</sup> symmetry previously pointed out only affects rotation symmetry.

On average, NEMESI results are once more very satisfactory, being the standard deviation error on both reaction rates around 0.2% for all test cases (except for the KAIST MOX\_GD where it remains nevertheless around 0.4%).

**Table 9 – Comparison of  $k_{\infty}$  between NEMESI, TRIPOLI-4<sup>®</sup>, SERPENT-2, and APOLLO2 for PWR benchmark assemblies.**

	NEMESI $k_{\infty}$	TRIPOLI-4 <sup>®</sup> $k_{\infty}$	$\Delta$ TRIPOLI-4 <sup>®</sup> (pcm)	SERPENT-2 $k_{\infty}$	$\Delta$ SERPENT-2 (pcm)	APOLLO2 $k_{\infty}$	$\Delta$ APOLLO2 (pcm)
KAIST UOX2	1.10486	1.10444	34	1.10443	35		
KAIST UOX33	1.25388	1.25350	-24	1.25352	-23		
KAIST UGD	1.04796	1.04750	-42	1.04722	-68	1.04730	-60
KAIST MOX_GD	1.12628	1.12547	-63	1.12462	-131		
KAIST MOX	1.16483	1.16349	-99	1.16350	-98	1.16393	-66
Minicore A37	1.30568	1.30554	-9	1.30456	-65	1.30459	-64

**Table 10 – Error statistics on normalized absorption rate between NEMESI, TRIPOLI-4®, and SERPENT-2 for PWR benchmark assemblies.**

	$\Delta$ TRIPOLI-4® (%)			$\Delta$ SERPENT-2 (%)			$\Delta$ APOLLO2 (%)		
	Min	Max	Std	Min	Max	Std	Min	Max	Std
KAIST UOX2	-0.34	0.26	0.12	-0.36	0.29	0.12			
KAIST UOX33	-0.35	0.30	0.13	-0.47	0.41	0.14			
KAIST UGD	-0.43	0.34	0.17	-1.01	0.56	0.26	-0.22	0.85	0.21
KAIST MOX_GD	-0.77	1.84	0.39	-1.00	2.07	0.42			
KAIST MOX	-0.50	0.61	0.24	-0.63	0.58	0.25	-0.23	0.28	0.10
Minicore A37	-0.48	0.39	0.23	-0.79	0.88	0.28	-0.36	0.31	0.17

**Table 11 – Error statistics on normalized fission rate between NEMESI, TRIPOLI-4®, and SERPENT-2 for PWR benchmark assemblies.**

	$\Delta$ TRIPOLI-4® (%)			$\Delta$ SERPENT-2 (%)			$\Delta$ APOLLO2 (%)		
	Min	Max	Std	Min	Max	Std	Min	Max	Std
KAIST UOX2	-0.37	0.32	0.12	-0.35	0.29	0.12			
KAIST UOX33	-0.35	0.29	0.12	-0.46	0.42	0.14			
KAIST UGD	-0.57	0.52	0.20	-0.85	0.82	0.31	-0.28	0.36	0.13
KAIST MOX_GD	-0.80	0.71	0.25	-1.03	1.19	0.34			
KAIST MOX	-0.50	0.60	0.21	-0.67	0.58	0.23	-0.15	0.19	0.07
Minicore A37	-0.54	0.54	0.24	-0.92	0.89	0.32	-0.50	0.37	0.20

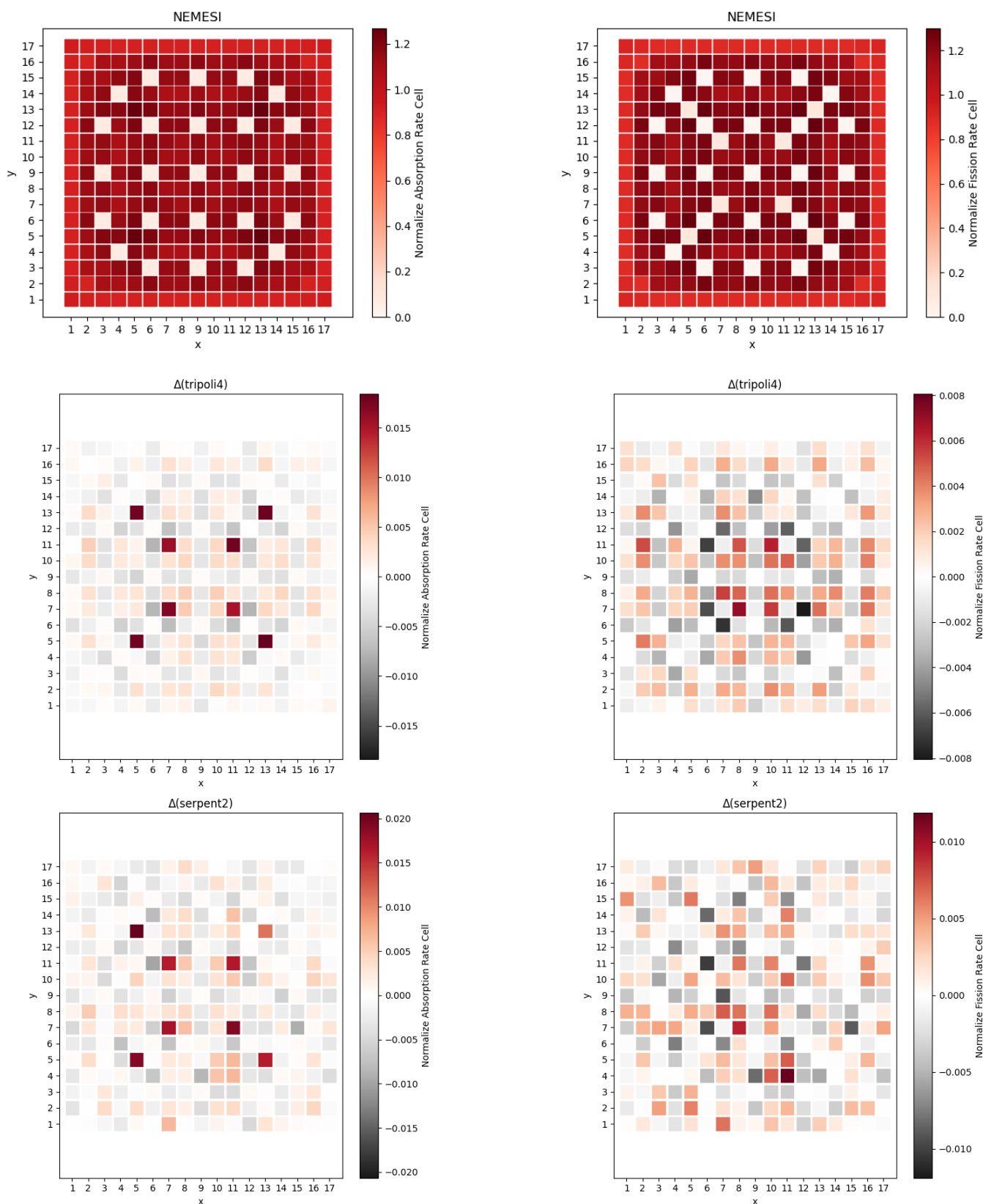


**Figure 8 – Normalized absorption and fission rates for KAIST – MOX\_GD obtained with NEMESI and comparisons with TRIPOLI-4® and SERPENT-2.**

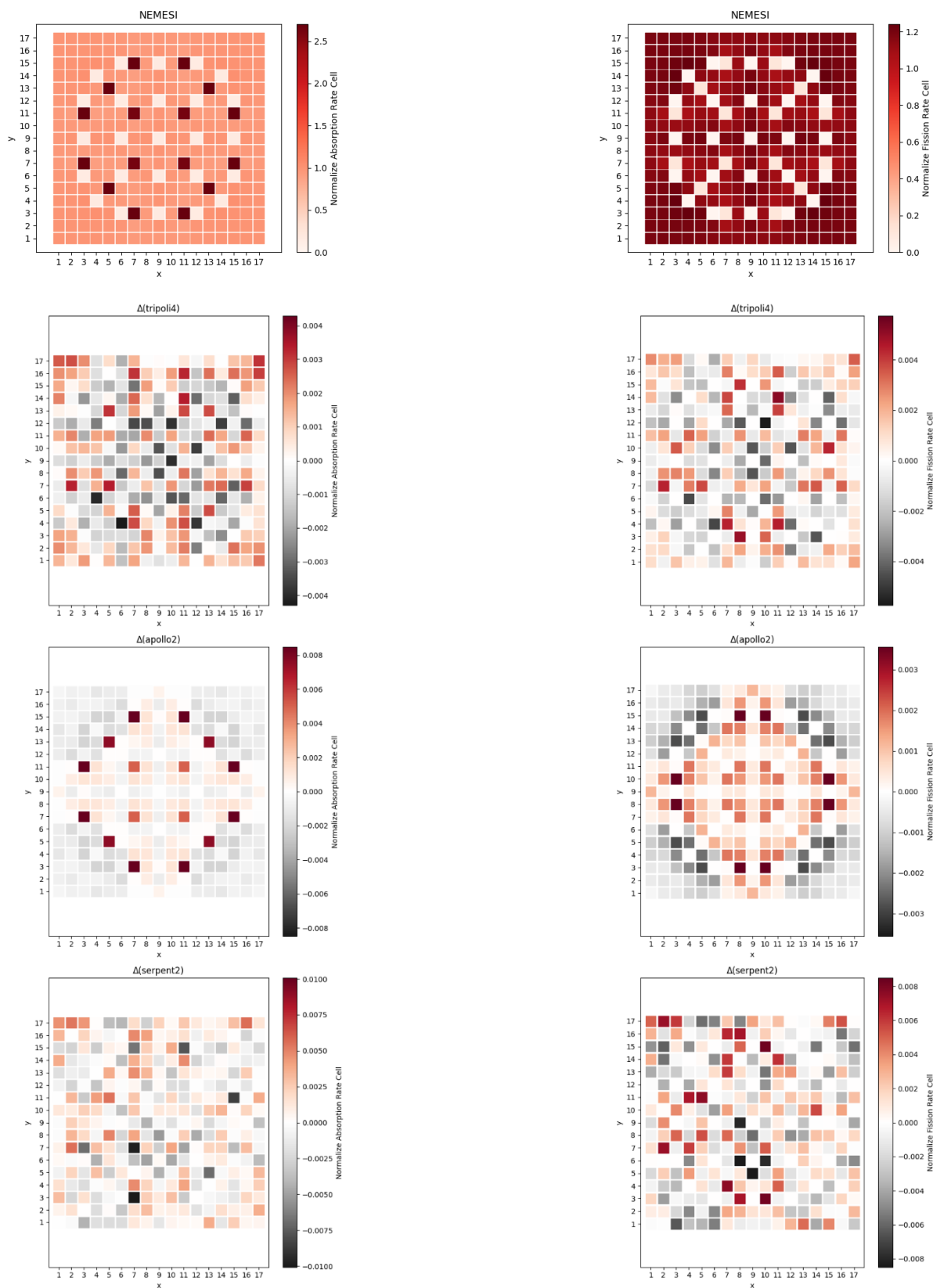


Figure 9 – Normalized absorption and fission rates for KAIST – UGD obtained with NEMESI and comparisons with TRIPOLI-4®, APOLLO2, and SERPENT-2.

## 5.2. Control rods fully inserted

The results in terms of  $k_{\infty}$  for the assembly configurations with inserted control rods are displayed in Table 12. The agreement between NEMESI, the Monte Carlo codes, and APOLLO2 is very good for the KZL6 FA\_3\_3\_G and the Minicore A37 configurations. For the KHM2 390GO, the error with respect to TRIPOLI-4<sup>®</sup> increases to almost 250 pcm. However, since the acceptance criterion on  $k_{\infty}$  is normally set to 300 pcm in the industrial V&V activities on APOLLO2, the result obtained remains satisfactory. Note that SERPENT-2 results were only obtained with the default VTT nuclear data library, due to lack of time.

Table 13 (resp. Table 14) shows the minimum, maximum, and standard deviation errors on the normalized absorption (resp. fission) cell rate for each assembly configuration with inserted rods. The strongest differences appear with the insertion of dysprosium rods for the Khmelnitsky 390GO and AIC rods for the Minicore A37 test cases. For Khmelnitsky 390GO, the absorption rates are significantly higher in the rodded cells when compared to TRIPOLI-4<sup>®</sup> (up to 2%). For the Minicore A37 some further investigations are required to use higher anisotropy orders in NEMESI calculations (i.e., P3 instead of P0c), to better model the strong local flux anisotropy due to the rods' presence.

Anyhow, on average results are very good, as standard deviation errors on both normalized reaction rates remain below 0.6% for all configurations.

**Table 12 – Comparison of  $k_{\infty}$  between NEMESI, TRIPOLI-4<sup>®</sup>, SERPENT-2, and APOLLO2 for benchmark assemblies with rods inserted.**

	NEMESI $k_{\infty}$	TRIPOLI-4 <sup>®</sup> $k_{\infty}$	$\Delta$ TRIPOLI-4 <sup>®</sup> (pcm)	SERPENT-2 $k_{\infty}$	$\Delta$ SERPENT-2 (pcm)	APOLLO2 $k_{\infty}$	$\Delta$ APOLLO2 (pcm)
KZL6 FA_3_3_G	0.96311	0.96399	94	0.96256	60		
KHM2 390GO	1.05495	1.05768	244				
Minicore A37	0.88665	0.88687	27			0.88760	120

**Table 13 – Error statistics on normalized absorption rate between NEMESI, TRIPOLI-4<sup>®</sup>, SERPENT-2, and APOLLO2 for benchmark assemblies with rods inserted.**

	$\Delta$ TRIPOLI-4 <sup>®</sup> (%)			$\Delta$ SERPENT-2 (%)			$\Delta$ APOLLO2 (%)		
	Min	Max	Std	Min	Max	Std	Min	Max	Std
KZL6 FA_3_3_G	-0.66	0.25	0.14	-0.75	0.26	0.14			
KHM2 390GO	-0.55	1.83	0.38						
Minicore A37	-0.73	1.35	0.39				-0.80	1.72	0.53

**Table 14 – Error statistics on normalized fission rate between NEMESI, TRIPOLI-4<sup>®</sup>, SERPENT-2, and APOLLO2 for benchmark assemblies with rods inserted.**

	$\Delta$ TRIPOLI-4 <sup>®</sup> (%)			$\Delta$ SERPENT-2 (%)			$\Delta$ APOLLO2 (%)		
	Min	Max	Std	Min	Max	Std	Min	Max	Std
KZL6 FA_3_3_G	-0.48	0.33	0.14	-0.42	0.26	0.12			
KHM2 390GO	-0.49	0.38	0.15						
Minicore A37	-1.16	1.10	0.54				-1.19	0.94	0.56

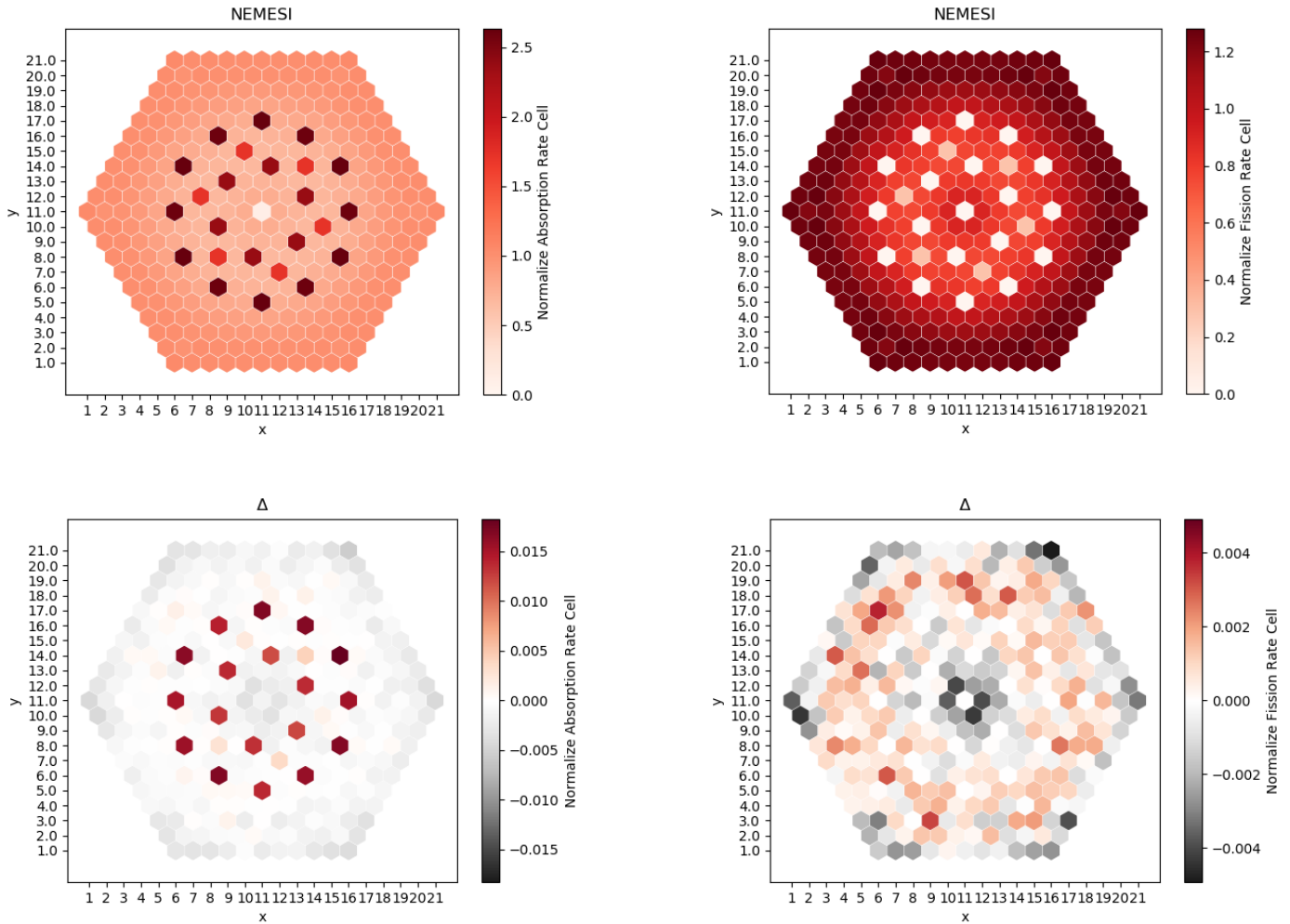


Figure 10 – Normalized absorption and fission rates for KHM2 – 390GO, with Dysprosium rods inserted, obtained with NEMESI and comparisons with TRIPOLI-4®.

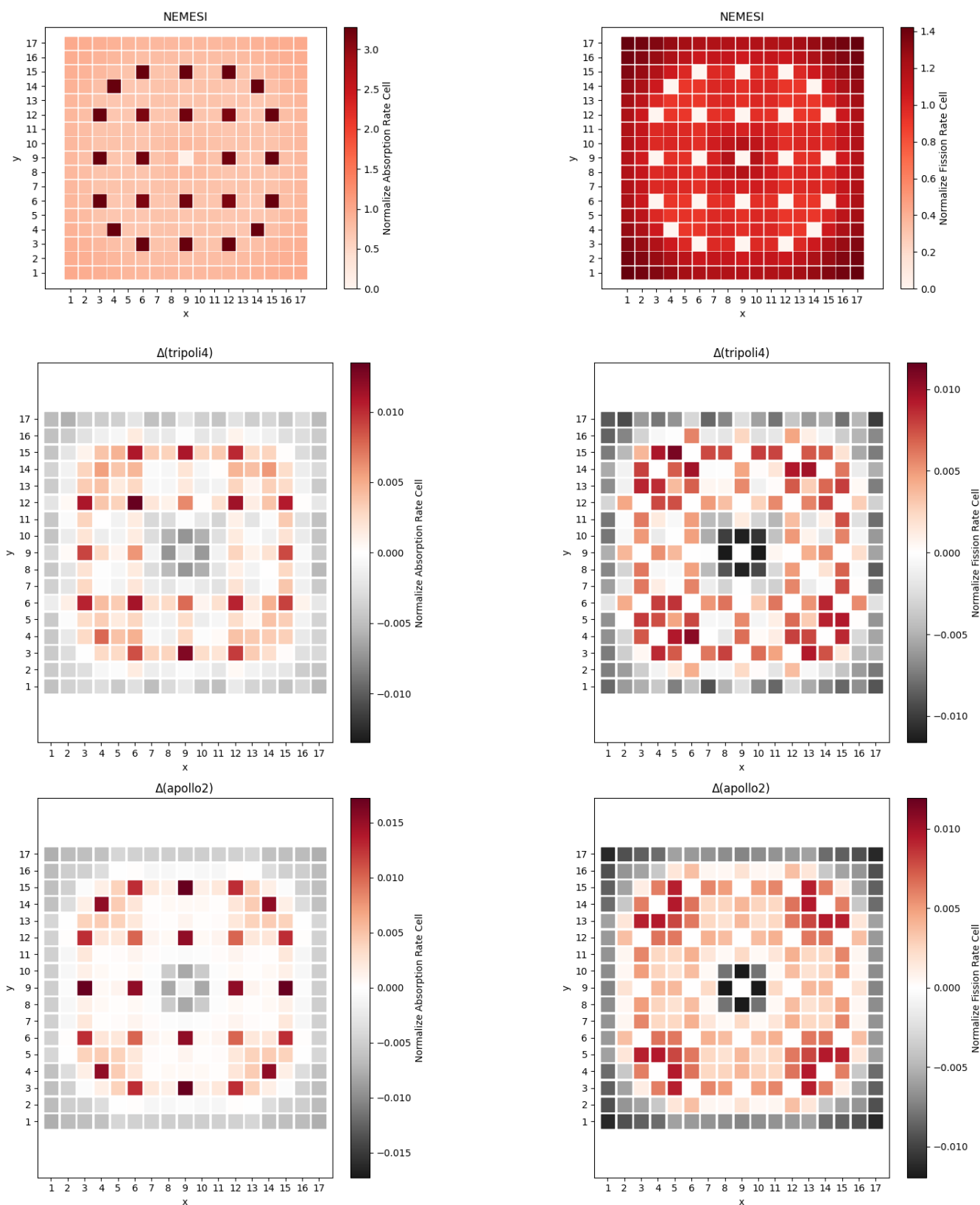


Figure 11 – Normalized absorption and fission rates for Minicore – A37, with AIC rods inserted, obtained with NEMESI and comparisons with TRIPOLI-4® and APOLLO2.



### 5.3. Depleted state

Figure 12 shows the  $k_{\infty}$  obtained from NEMESI during the depletion of the Kozloduy FA3\_3\_G, Khmel'nitsky 390GO and 30AV5 test cases, and the difference in terms of reactivity with respect to SERPENT-2. Results are similar for the three cases, with a good agreement at the beginning of the depletion but stronger discrepancies for higher burnup values, with a peak around 30 GWd/t (up to 600 pcm for the KHM 390GO) then reducing again towards 60 GWd/t. These results were obtained with the new JEFF3.1.1 IRSN NDL, while those with the JEFF3.1.1 VTT NDL were much closer to NEMESI (see Appendix D – TRIPOLI-4® and SERPENT-2 analysis). This suggests that, despite the improvements highlighted in the previous sections, further analyses must be carried out on the depletion test cases, concerning not only the neutron data libraries adopted by the codes, but also for example the power renormalization options. These analyses are foreseen in the project follow up.

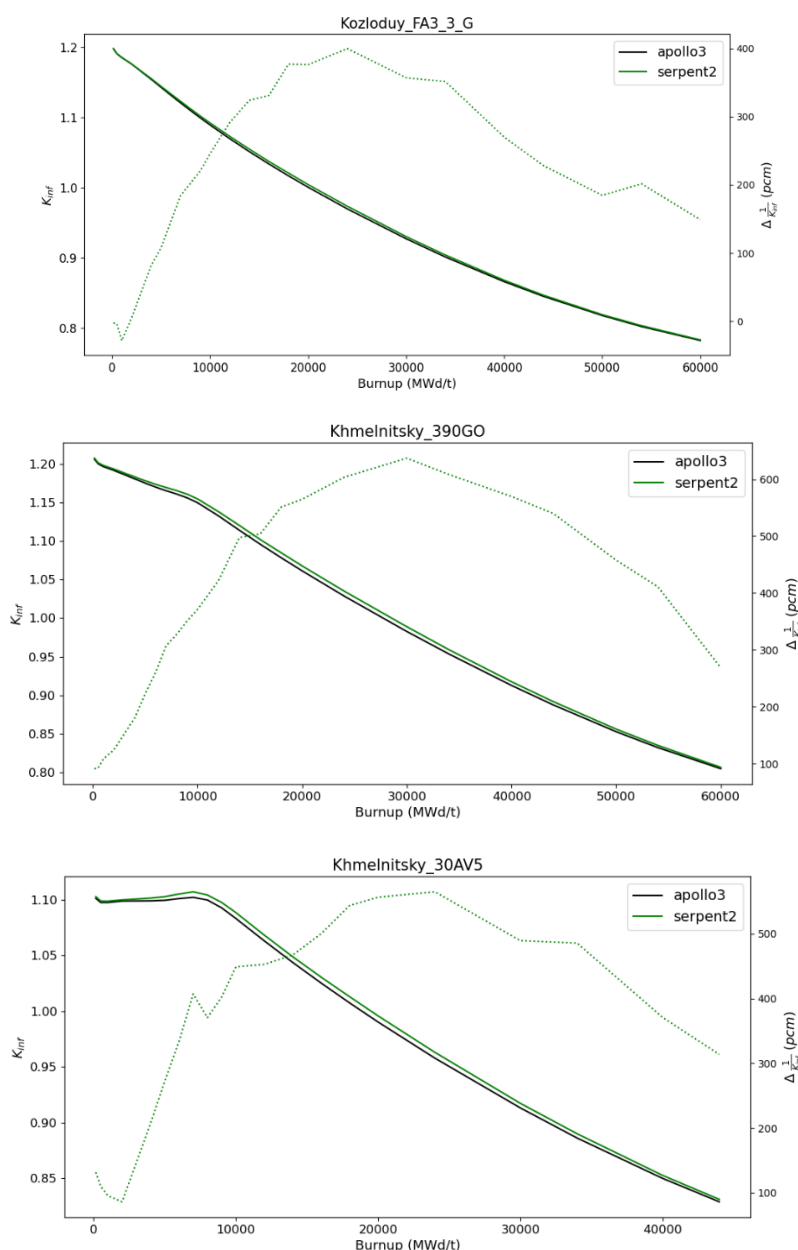
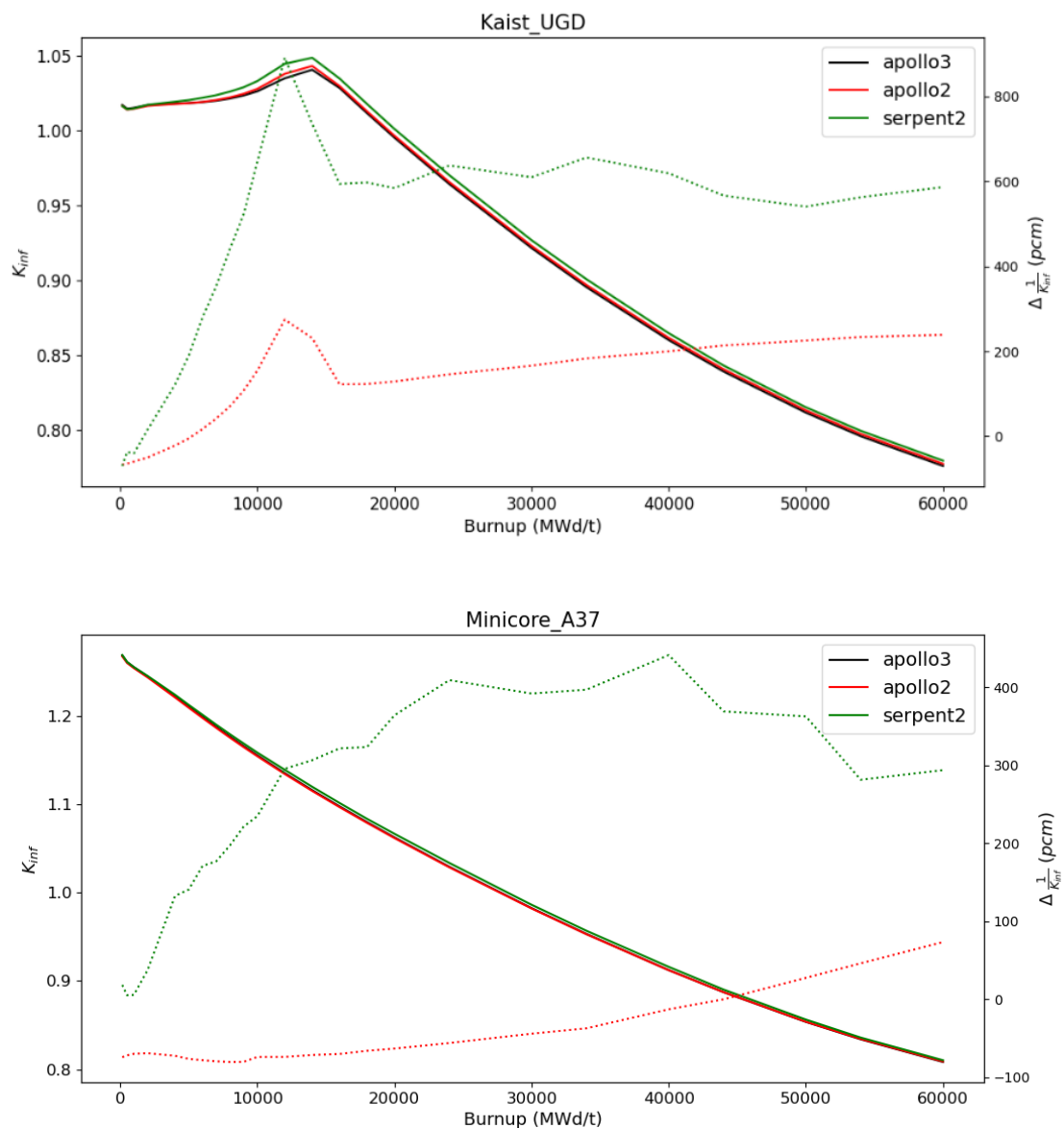


Figure 12 - Comparison of  $k_{\infty}$  between NEMESI and SERPENT-2 during depletion for VVER benchmark assemblies.

Figure 13 displays the evolution of the  $k_{\infty}$  and the reactivity discrepancies with APOLLO2 and SERPENT-2 for the KAIST UGD and Minicore A37 test cases. The agreement with SERPENT-2 is good only at low burnups. In KAIST UGD, around the gadolinium peak the reactivity rises up to more than 800 pcm, then decreases afterwards nevertheless remaining at around 600 pcm. Results with the VTT NDL were much closer to NEMESI (further analyses are required, see Appendix D – TRIPOLI-4® and SERPENT-2 analysis). In general, however, the different spatial mesh used in the two calculations might also play a role. In APOLLO3®, in fact, UOX/MOX and Gd pins are divided into 6 and 11 annuli respectively, progressively more refined towards the boundary to capture the skin effect. In SERPENT-2 calculations, instead, all fuel pins are divided into 10 annuli of equal surface.

Anyhow, it can be noticed that the agreement between NEMESI and APOLLO2 – the industrial reference – is good, especially for the Minicore A37 case with a discrepancy drift from -70 pcm at 0 GWd/t to 70 pcm at 60GWd/t. For KAIST UGD, NEMESI seems to underestimate the gadolinium peak compared to APOLLO2.



**Figure 13 - Comparison of  $k_{\infty}$  between NEMESI, SERPENT-2 and APOLLO2 during depletion for PWR benchmark assemblies.**

Finally, Figure 14 and Figure 15 show the evolution of the minimum, maximum, and standard deviation error on the normalized absorption and fission cell rates during depletion. For VVER test cases, all quantities are nearly constant during the depletion. For PWR test case, the maximum discrepancy (corresponding to gadolinium pins) raises when approaching the gadolinium peak, and then it stabilizes for both SERPENT-2 and APOLLO2.

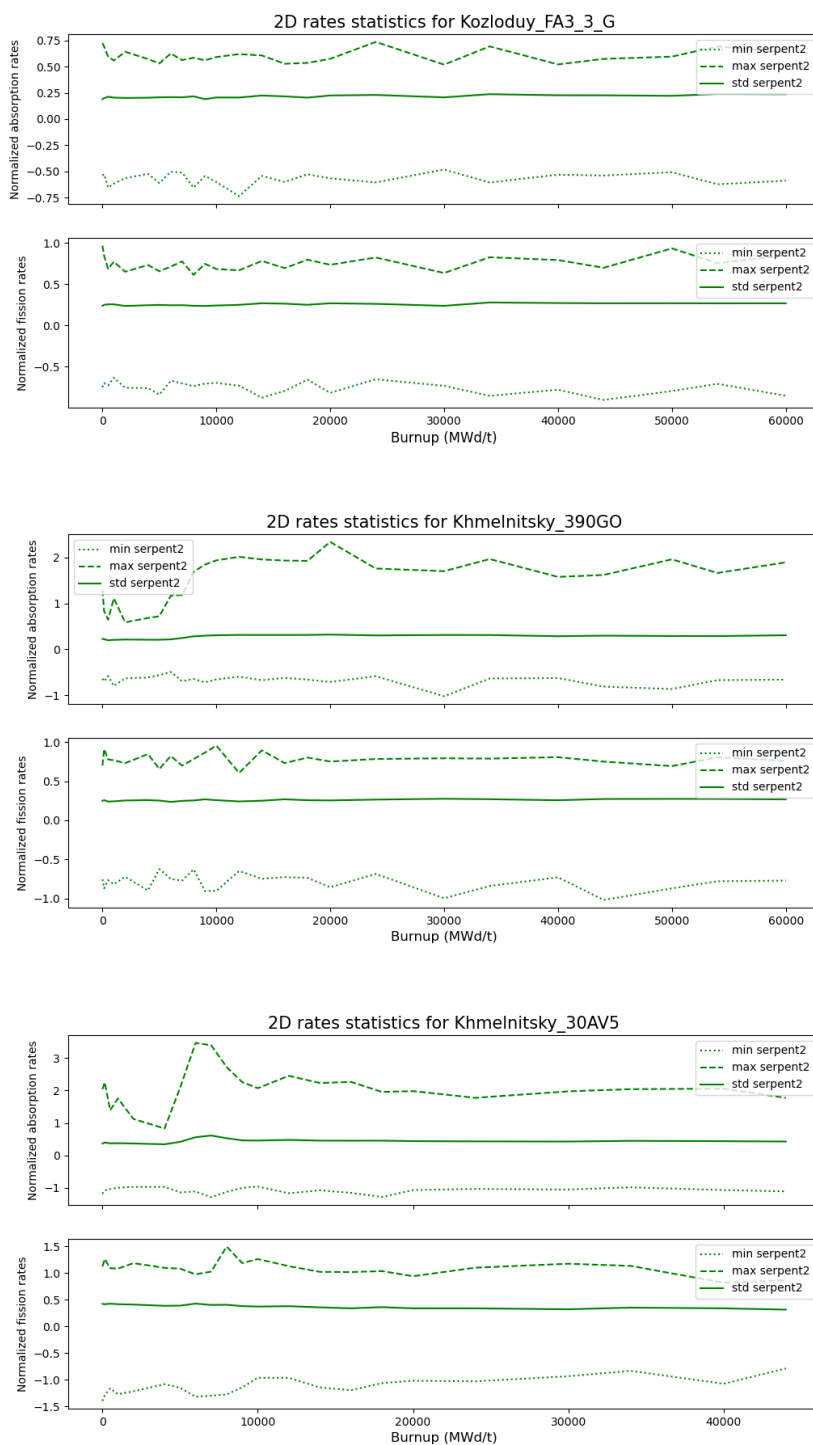


**Figure 14 - Comparison of absorption and fission rates statistics between NEMESI and SERPENT-2 during depletion for VVER benchmark assemblies.**

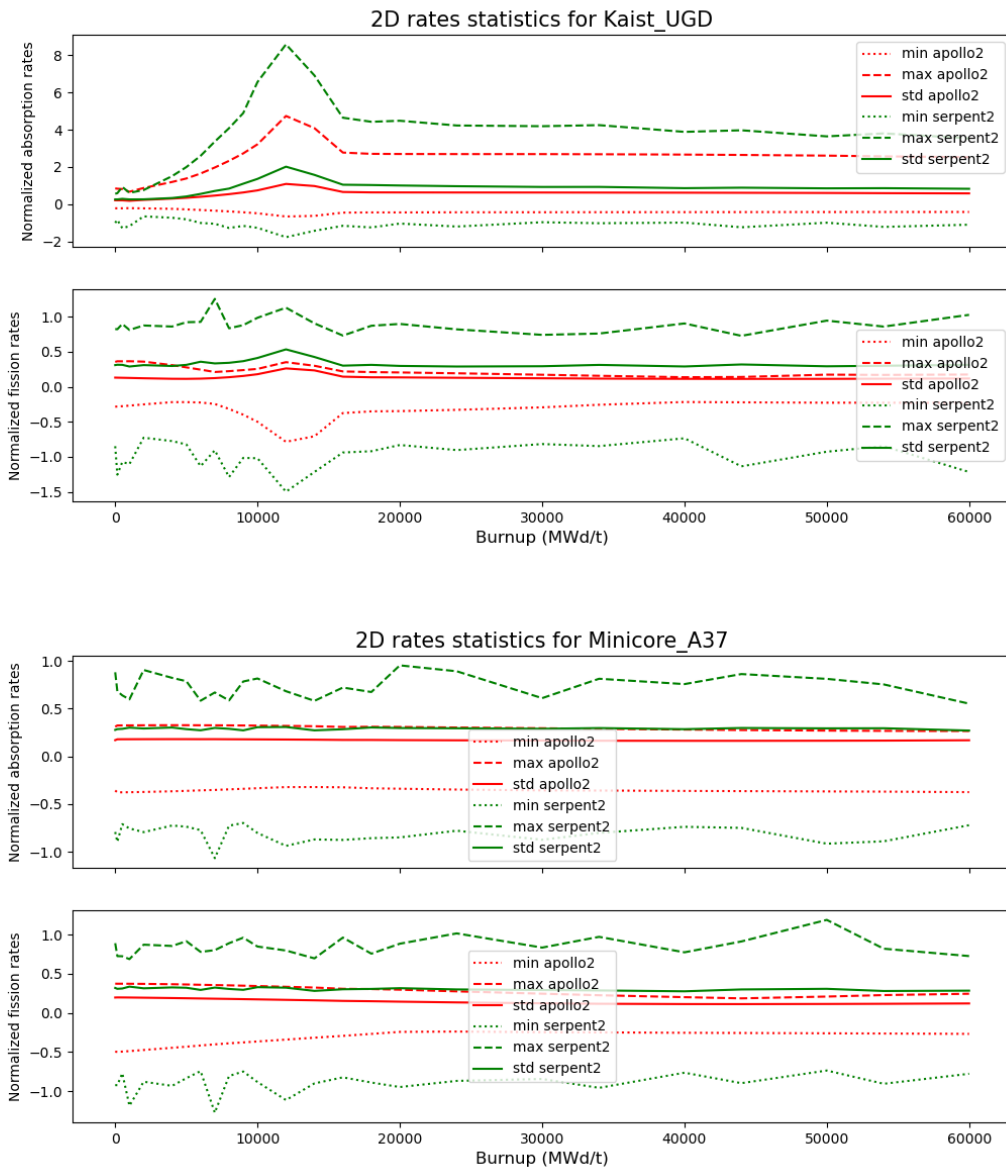


**Figure 15 - Comparison of absorption and fission rates statistics between NEMESI, SERPENT-2 and APOLLO2 during depletion for PWR benchmark assemblies.**

## 6. Conclusions and perspectives

In this document, which constitutes the Deliverable 4.4 of the H2020 CAMIVVER project, we have reported the main results of the first verification and validation (V&V) activities carried out on NEMESI, a new lattice calculation platform prototype based on the APOLLO3<sup>®</sup> code that aims at accelerating its transfer from lab to industry.

For this V&V activity, eleven test cases have been selected out of those described in Deliverable 4.3, ensuring nevertheless the coverage of the entire technology (i.e., hexagonal/square assemblies) and fuel spectrum (i.e., UOX/MOX, with or without zoning, with or without Gd burnable absorber pins, with or without control rods inserted).

This test matrix has been implemented in a Python automatic comparison tool, named DICE, which was developed during Task 4.2 of the CAMIVVER project and whose structure has been presented in this document. During the V&V campaign, DICE has facilitated the comparison of NEMESI's results with those obtained with the reference codes (deterministic, like APOLLO2, or stochastic, like TRIPOLI-4<sup>®</sup> and SERPENT-2). This tool has helped with the identifications of several sources of discrepancies (input file errors, differences in compositions, mesh incoherences, etc.), thus considerably speeding up the iterations among partners. The tool will be very useful in the project follow-up activities, and it may be adopted for other investigations by the partners.

The results obtained for all configurations at nominal state (with or without control rods) show in general very good agreement between NEMESI and the Monte Carlo codes and/or APOLLO2, with errors on  $k_{\infty}$  on average lower than 100 pcm and standard deviation errors on normalized fission and absorption reaction rates lower than 0.4%. When comparing the 2D distributions of reaction rates however, local error peaks (around 1% or 2%) have highlighted some remaining issues in the APOLLO3<sup>®</sup> calculations (i.e., imposition of rotational symmetry condition in VVER cases, or the need for a higher anisotropy order especially when considering rodded cases) that will be addressed in future versions of NEMESI.

Results obtained during depletion calculations are also satisfactory, with general good agreement with Monte Carlo and APOLLO2 calculation. For VVER calculations, however, the good agreement with SERPENT-2 rapidly degrades with increasing burnup, reaching a discrepancy of some hundred pcm at 60 GWd/t. The impact of the neutron data libraries (NDL) used by the code has already turned out to be relevant, but in a positive sense for calculations at burnup null. During depletion calculations however, the new improved NDL adopted seems to deliver less accurate results. Further investigations are then required, concerning also, for example, the power renormalization options adopted by the codes or, concerning SERPENT-2, considering more exact energy deposition models and considering critical spectrums for burnup calculations that could improve the results. This will be addressed in the future V&V activities.

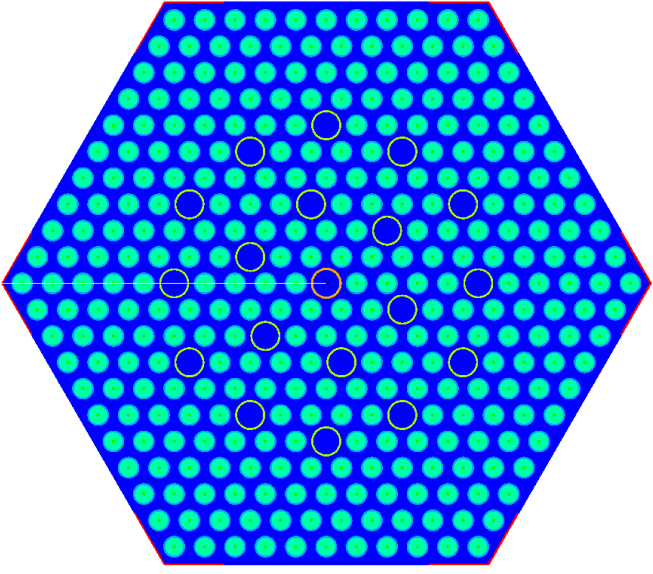
In conclusion, the DICE test matrix has proven an important tool to increase the confidence in NEMESI during the first developments carried out in the context of the CAMIVVER project. Clearly, it will continue to play a paramount role during the next development phases and the industrialization and industrial exploitation of NEMESI, helping with the maintainability of NEMESI's validation ensuring the robustness and the non-regression of the results each time a new version is released. The next V&V campaign carried out on NEMESI will in fact also include tests cases that require the adoption of industrial calculation schemes.

## 7. Appendix A – Assembly configurations

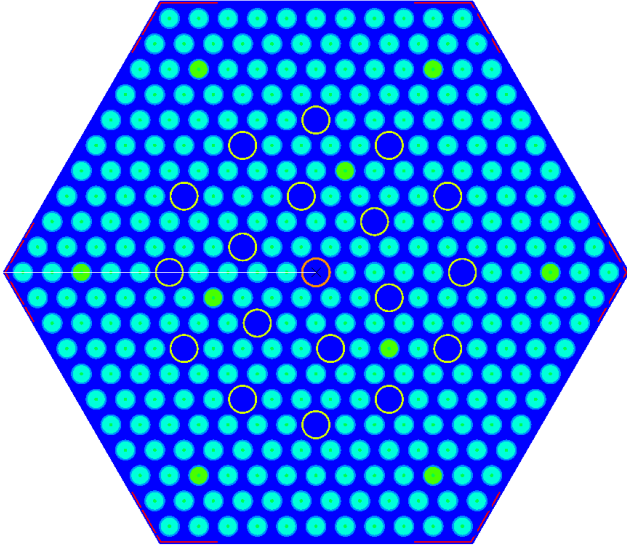
In this appendix, we report the main characteristics of the assembly configurations implemented in DICE for the first version of the NEMESI test matrix. The reader is referred to Deliverable 4.3 [4] for all missing information.

### 7.1. Appendix A1 – VVER assembly configurations

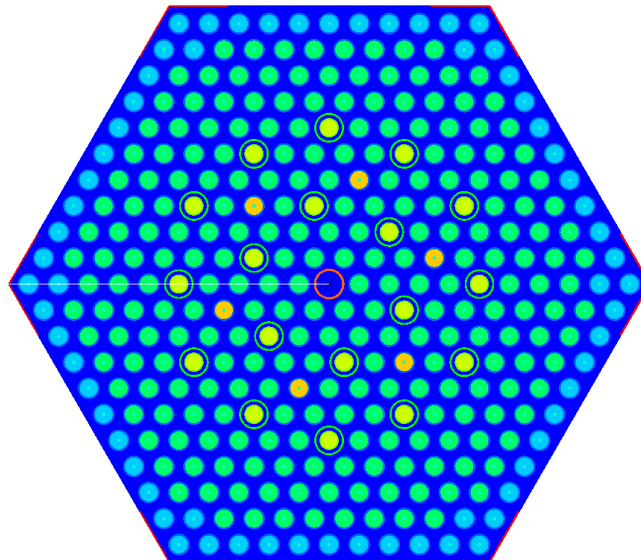
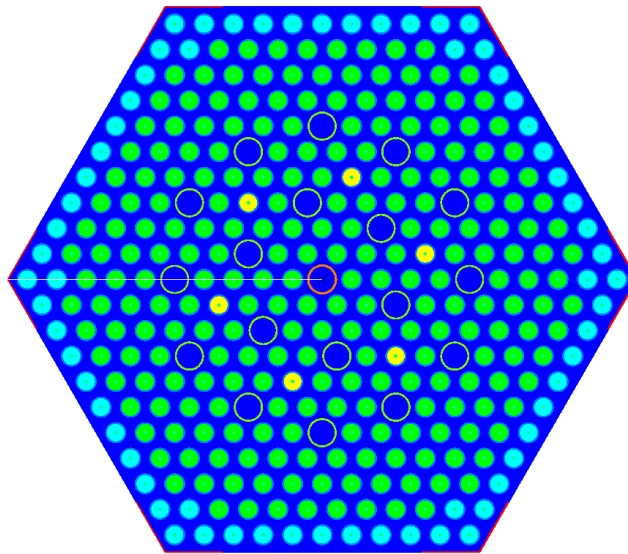
Reactor	Name	Fuel	Comments
Khmelnitsky-2	13AU	UOX 1.3% <sup>235</sup> U fuel pin	Stiffener on corners $\pi/3$ symmetry



Reactor	Name	Fuel	Comments
Khmelnitsky-2	30AV5	UGD 3.0% $^{235}\text{U}$ fuel pin (in light blue) 2.4% $^{235}\text{U}$ and 5.0% $\text{Gd}_2\text{O}_3$ burnable absorber pin (in green)	Stiffener on corners $2\pi/3$ symmetry

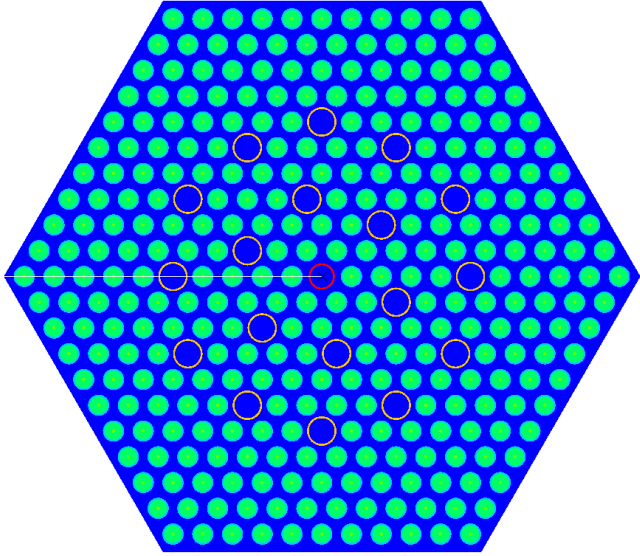


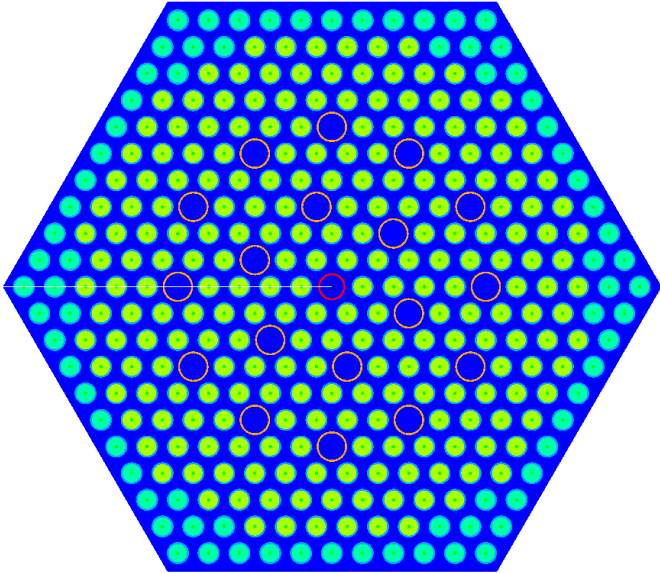
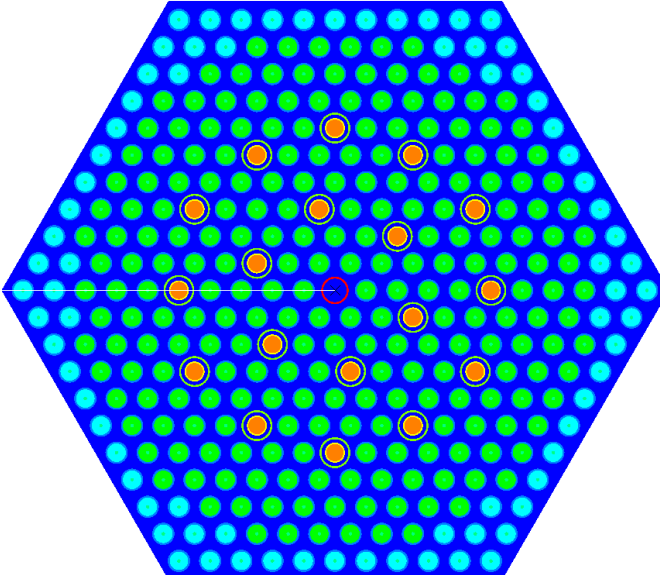
Reactor	Name	Fuel	Comments
Khmel'nitsky-2	390GO	UGD 3.6% <sup>235</sup> U fuel pin (zoning ring and corners - in light blue) 4.0% <sup>235</sup> U fuel pin (in green) 3.3% <sup>235</sup> U and 5.0% Gd <sub>2</sub> O <sub>3</sub> burnable absorber pin (in yellow and orange in the figure below)	Stiffener on corners $\pi/3$ symetry
			With dysprosium control rods (in yellow)



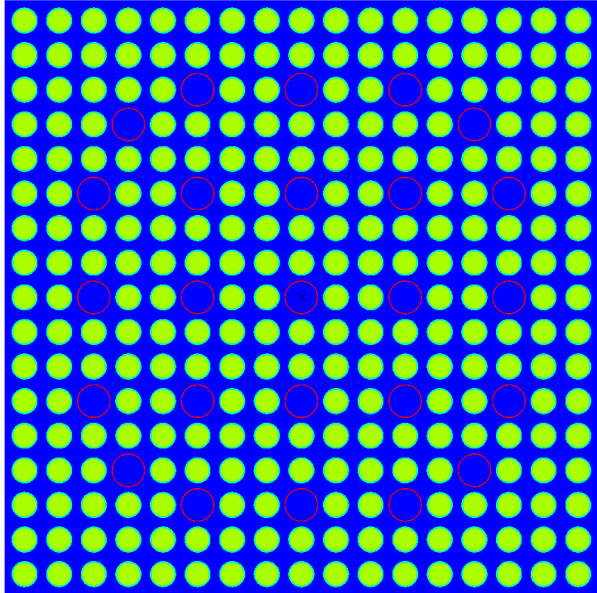


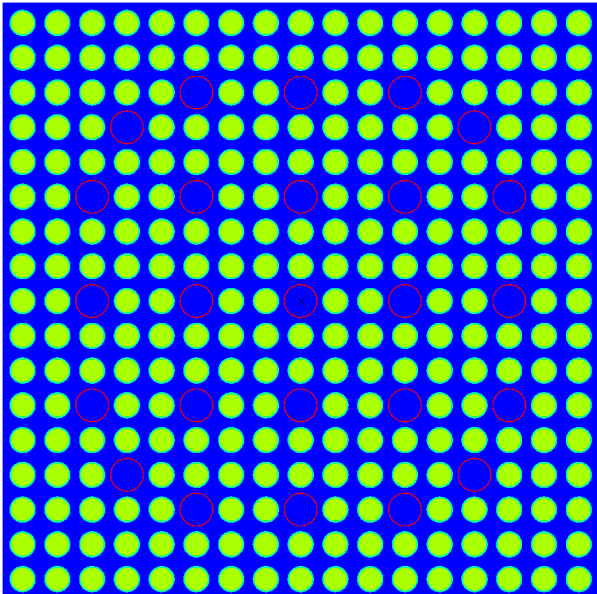
Reactor	Name	Fuel	Comments
Kozloduy-6	FA4_4_F	UOX 4.4% <sup>235</sup> U fuel pin	No stiffener $\pi/3$ symmetry



Reactor	Name	Fuel	Comments
Kozloduy-6	FA3_3_G	UOX 3.0% <sup>235</sup> U fuel pin (zoning ring and corners - in light blue)  3.3% <sup>235</sup> U fuel pin (in green)	No stiffener $\pi/3$ symetry
			
			With B <sub>4</sub> C control rods (in orange)

## 7.2. Appendix A2 – PWR assembly configurations

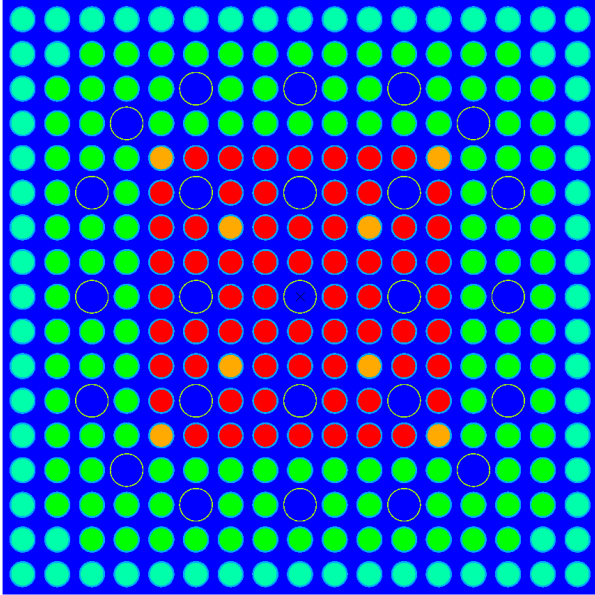
Reactor	Name	Fuel	Comments
KAIST	UOX2	UOX 2.0% <sup>235</sup> U fuel pin	No water blade 1/8 symetry
			

Reactor	Name	Fuel	Comments
KAIST	UOX33	UOX 3.3% <sup>235</sup> U fuel pin	No water blade 1/8 symetry
			

Reactor	Name	Fuel	Comments
KAIST	UGD	UGD 3.3% <sup>235</sup> U fuel pin (in green) 0.711% <sup>235</sup> U and 9.0% Gd <sub>2</sub> O <sub>3</sub> burnable absorber pin (in red)	No water blade 1/8 symetry

Reactor	Name	Fuel	Comments
KAIST	MOX	MOX 4.3 % MOX fuel pin (outer zone - in light blue) 7.0 % MOX fuel pin (intermediate zone - in green) 8.7 % MOX fuel pin (center - in red)	No water blade 1/8 symetry

Reactor	Name	Fuel	Comments
KAIST	MOX_GD	MOX 4.3% MOX fuel pin (outer zone – in light blue) 7.0% MOX fuel pin (intermediate zone - in green) 8.7% MOX fuel pin (center – in red) 0.711% <sup>235</sup> U and 9.0% Gd <sub>2</sub> O <sub>3</sub> burnable absorber pin (in orange)	No water blade 1/8 symetry



Reactor	Name	Fuel	Comments
Minicore	A37	UOX 3.7% <sup>235</sup> U fuel pin	With water blade 1/8 symetry
			With AIC control rods (in red)

## 8. Appendix B – Overview of NEMESI Input Data for T4.2

In this appendix, we report the NEMESI input files used to carry out the calculations necessary for the V&V activities within Task 4.2.

Calculations were carried out using the JSON input file of NEMESI, called `inputMain.json`, to test the flexibility for the final user. The interactive mode of NEMESI was also available as described in [3] but it was not used to provide the required results in Task 4.2. Several iterations were necessary since 2021, testing also APOLLO3® releases from V2.0.1 up to V2.3dev currently used<sup>1</sup>, as indicated in Figure 16.

The NEMESI input data used are listed in Table 15 respectively for PWR32 (A37), KAIST (UOX2, UOX33, UGD, MOX, MOX\_GD), KZL6 (FA3\_3\_G, FA4\_4\_F) and KHM2 (13AU, 390GO, 30AV5) reactor types and assemblies. For all the cases the same burnup points were considered (see `burnup_list`).

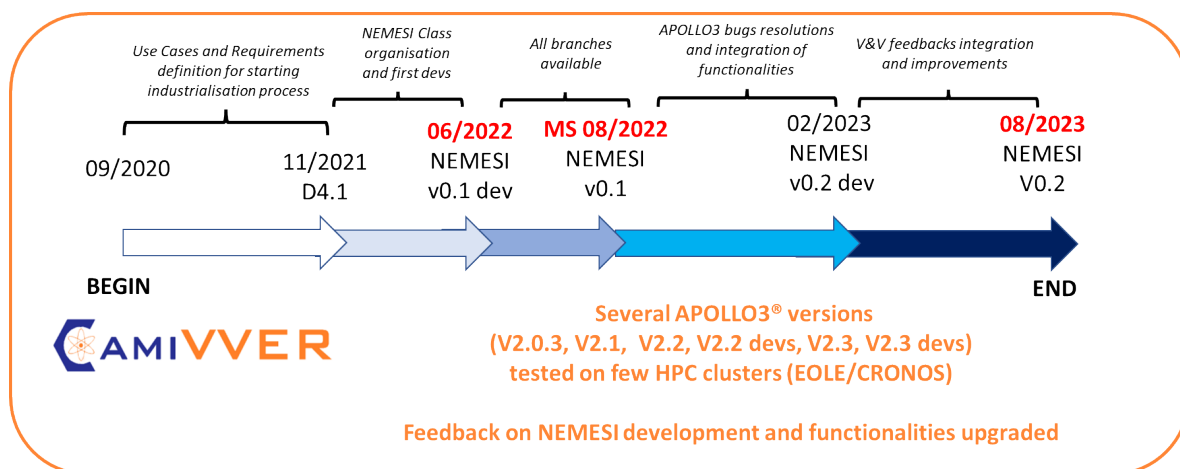


Figure 16 - NEMESI evolution and testing.

Table 15 - NEMESI input files used for calculations in Task 4.2.

inputMain.json for PWR32 case – assembly A37 – 1/8 symmetry
<pre>{   "reactor": "PWR32",   "assembly": "A37",   "configurations": ["ARO", "AIC"],   "geometry_type": "NATIVE",   "calculation_scheme": "SHEMMOC",   "boundary_conditions": "SPECULAR",   "leakage_model": "B2ZERO",   "out_number_of_groups": 2,   "output_settings": [8, "PBP"],   "mpo_configurations": ["ARO", "AIC"],   "usage": "depletion",   "flux_normalization": [19.4, "PowerDensity", ""],   "generate_output": true,   "generate_mpo": true,   "generate_archive": false,   "generate_tripoli": false,   "depleting_configuration": "ARO",   "generate_branches": false,   "burnup_steps": &lt;burnup_list&gt;,   "boron_concentration": [600.0],   "fuel_temperature": [833.15],</pre>



```
"coolant_density": [0.717],
"points_per_branch": 4,
"launch_branches_after_each_depletion": false,
"launch_branches_once_finished": false,
"launch_branches_sequential": false,
"branch_number": null,
"dump_input": true
}
```

#### inputMain.json for KAIST case – assembly UOX2 – 1/8 symmetry

```
{
  "reactor": "KAIST",
  "assembly": "UOX2",
  "configurations": ["ARO"],
  "geometry_type": "NATIVE",
  "calculation_scheme": "SHEMMOC",
  "boundary_conditions": "SPECULAR",
  "leakage_model": "B2ZERO",
  "out_number_of_groups": 2,
  "output_settings": [8, "PBP"],
  "mpo_configurations": ["ARO"],
  "usage": "depletion",
  "flux_normalization": [37.7, "PowerDensity", ""],
  "generate_output": true,
  "generate_mpo": true,
  "generate_archive": false,
  "generate_tripoli": false,
  "depleting_configuration": "ARO",
  "generate_branches": false,
  "burnup_steps": <burnup_list>,
  "boron_concentration": [800.0],
  "fuel_temperature": [900.0],
  "coolant_density": [0.7295],
  "points_per_branch": 4,
  "launch_branches_after_each_depletion": false,
  "launch_branches_once_finished": false,
  "launch_branches_sequential": false,
  "branch_number": null,
  "dump_input": true
}
```

#### inputMain.json for KAIST case – assembly UOX33 – 1/8 symmetry

```
{
  "reactor": "KAIST",
  "assembly": "UOX33",
  "configurations": ["ARO"],
  "geometry_type": "NATIVE",
  "calculation_scheme": "SHEMMOC",
  "boundary_conditions": "SPECULAR",
  "leakage_model": "B2ZERO",
  "out_number_of_groups": 2,
  "output_settings": [8, "PBP"],
  "mpo_configurations": ["ARO"],
  "usage": "depletion",
  "flux_normalization": [37.7, "PowerDensity", ""],
  "generate_output": true,
  "generate_mpo": true,
  "generate_archive": false,
  "generate_tripoli": false,
  "depleting_configuration": "ARO",
}
```

```
"generate_branches": false,
"burnup_steps": <burnup_list>,
"boron_concentration": [800.0],
"fuel_temperature": [900.0],
"coolant_density": [0.7295],
"points_per_branch": 4,
"launch_branches_after_each_depletion": false,
"launch_branches_once_finished": false,
"launch_branches_sequential": false,
"branch_number": null,
"dump_input": true
}
```

#### inputMain.json for KAIST case – assembly UGD – 1/8 symmetry

```
{
"reactor": "KAIST",
"assembly": "UGD",
"configurations": ["ARO"],
"geometry_type": "NATIVE",
"calculation_scheme": "SHEMMOC",
"boundary_conditions": "SPECULAR",
"leakage_model": "B2ZERO",
"out_number_of_groups": 2,
"output_settings": [8, "PBP"],
"mpo_configurations": ["ARO"],
"usage": "depletion",
"flux_normalization": [37.7, "PowerDensity", ""],
"generate_output": true,
"generate_mpo": true,
"generate_archive": false,
"generate_tripoli": false,
"depleting_configuration": "ARO",
"generate_branches": false,
"burnup_steps": <burnup_list>,
"boron_concentration": [800.0],
"fuel_temperature": [900.0],
"coolant_density": [0.7295],
"points_per_branch": 4,
"launch_branches_after_each_depletion": false,
"launch_branches_once_finished": false,
"launch_branches_sequential": false,
"branch_number": null,
"dump_input": true
}
```

#### inputMain.json for KAIST case – assembly MOX – 1/8 symmetry

```
{
"reactor": "KAIST",
"assembly": "MOX",
"configurations": ["ARO"],
"geometry_type": "NATIVE",
"calculation_scheme": "SHEMMOC",
"boundary_conditions": "SPECULAR",
"leakage_model": "B2ZERO",
"out_number_of_groups": 2,
"output_settings": [8, "PBP"],
"mpo_configurations": ["ARO"],
"usage": "depletion",
"flux_normalization": [37.7, "PowerDensity", ""],
"generate_output": true,
"generate_mpo": true,
}
```

```

"generate_archive": false,
"generate_tripoli": false,
"depleting_configuration": "ARO",
"generate_branches": false,
"burnup_steps": <burnup_list>,
"boron_concentration": [800.0],
"fuel_temperature": [900.0],
"coolant_density": [0.7295],
"points_per_branch": 4,
"launch_branches_after_each_depletion": false,
"launch_branches_once_finished": false,
"launch_branches_sequential": false,
"branch_number": null,
"dump_input": true
}

```

#### inputMain.json for KAIST case – assembly MOX\_GD – 1/8 symmetry

```

{
  "reactor": "KAIST",
  "assembly": "MOX_GD",
  "configurations": ["ARO"],
  "geometry_type": "NATIVE",
  "calculation_scheme": "SHEMMOC",
  "boundary_conditions": "SPECULAR",
  "leakage_model": "B2ZERO",
  "out_number_of_groups": 2,
  "output_settings": [8, "PBP"],
  "mpo_configurations": ["ARO"],
  "usage": "depletion",
  "flux_normalization": [37.7, "PowerDensity", ""],
  "generate_output": true,
  "generate_mpo": true,
  "generate_archive": false,
  "generate_tripoli": false,
  "depleting_configuration": "ARO",
  "generate_branches": false,
  "burnup_steps": <burnup_list>,
  "boron_concentration": [800.0],
  "fuel_temperature": [900.0],
  "coolant_density": [0.7295],
  "points_per_branch": 4,
  "launch_branches_after_each_depletion": false,
  "launch_branches_once_finished": false,
  "launch_branches_sequential": false,
  "branch_number": null,
  "dump_input": true
}

```

#### inputMain.json for KZL6 case – assembly FA3\_3\_G – 1/6 symmetry

```

{
  "reactor": "KZL6",
  "assembly": "FA3_3_G",
  "configurations": ["ARO", "B4C"],
  "geometry_type": "EXTERNAL",
  "calculation_scheme": "SHEMMOC",
  "boundary_conditions": "ROTATION_TRANSLATIONXMAX",
  "leakage_model": "B2ZERO",
  "out_number_of_groups": 2,
  "output_settings": [6, "PBP"],
  "mpo_configurations": ["ARO", "B4C"],
  "usage": "depletion",
}

```

```

"flux_normalization": [42.5, "PowerDensity", ""],
"generate_output": true,
"generate_mpo": true,
"generate_archive": false,
"generate_tripoli": false,
"depleting_configuration": "ARO",
"generate_branches": false,
"burnup_steps": <burnup_list>,
"boron_concentration": [800.0],
"fuel_temperature": [900.0],
"coolant_density": [0.725],
"points_per_branch": 4,
"launch_branches_once_finished": false,
"launch_branches_sequential": false,
"branch_number": null,
"dump_input": true
}

```

#### inputMain.json for KZL6 case – assembly FA4\_4\_F – 1/6 symmetry

```

{
  "reactor": "KZL6",
  "assembly": "FA4_4_F",
  "configurations": ["ARO", "B4C"],
  "geometry_type": "EXTERNAL",
  "calculation_scheme": "SHEMMOC",
  "boundary_conditions": "ROTATION_TRANSLATIONXMAX",
  "leakage_model": "B2ZERO",
  "out_number_of_groups": 2,
  "output_settings": [6, "PBP"],
  "mpo_configurations": ["ARO", "B4C"],
  "usage": "depletion",
  "flux_normalization": [42.5, "PowerDensity", ""],
  "generate_output": true,
  "generate_mpo": true,
  "generate_archive": false,
  "generate_tripoli": false,
  "depleting_configuration": "ARO",
  "generate_branches": false,
  "burnup_steps": <burnup_list>,
  "boron_concentration": [800.0],
  "fuel_temperature": [900.0],
  "coolant_density": [0.725],
  "points_per_branch": 4,
  "launch_branches_once_finished": false,
  "launch_branches_sequential": false,
  "branch_number": null,
  "dump_input": true
}

```

#### inputMain.json for KHM2 case – assembly 13AU – 1/6 symmetry

```

{
  "reactor": "KML2",
  "assembly": "13AU",
  "configurations": ["ARO"],
  "geometry_type": "EXTERNAL",
  "calculation_scheme": "SHEMMOC",
  "boundary_conditions": "ROTATION_TRANSLATIONXMAX",
  "leakage_model": "B2ZERO",
  "out_number_of_groups": 2,
  "output_settings": [6, "PBP"],
  "mpo_configurations": ["ARO"],

```

```

"usage": "depletion",
"flux_normalization": [42.5, "PowerDensity", ""],
"generate_output": true,
"generate_mpo": true,
"generate_archive": false,
"generate_tripoli": false,
"depleting_configuration": "ARO",
"generate_branches": false,
"burnup_steps": <burnup_list>,
"boron_concentration": [600.0],
"fuel_temperature": [900.0],
"coolant_density": [0.7526],
"points_per_branch": 4,
"launch_branches_once_finished": false,
"launch_branches_sequential": false,
"branch_number": null,
"dump_input": true
}

```

#### inputMain.json for KHM2 case – assembly 390GO – 1/6 symmetry

```

{
  "reactor": "KML2",
  "assembly": "390GO",
  "configurations": ["ARO", "DYO"],
  "geometry_type": "EXTERNAL",
  "calculation_scheme": "SHEMMOC",
  "boundary_conditions": "ROTATION_TRANSLATIONXMAX",
  "leakage_model": "B2ZERO",
  "out_number_of_groups": 2,
  "output_settings": [6, "PBP"],
  "mpo_configurations": ["ARO", "DYO"],
  "usage": "depletion",
  "flux_normalization": [42.5, "PowerDensity", ""],
  "generate_output": true,
  "generate_mpo": true,
  "generate_archive": false,
  "generate_tripoli": false,
  "depleting_configuration": "ARO",
  "generate_branches": false,
  "burnup_steps": <burnup_list>,
  "boron_concentration": [600.0],
  "fuel_temperature": [900.0],
  "coolant_density": [0.7526],
  "points_per_branch": 4,
  "launch_branches_once_finished": false,
  "launch_branches_sequential": false,
  "branch_number": null,
  "dump_input": true
}

```

#### inputMain.json for KHM2 case – assembly 30AV5 – 1/3 symmetry

```

{
  "reactor": "KML2",
  "assembly": "30AV5",
  "configurations": ["ARO"],
  "geometry_type": "EXTERNAL",
  "calculation_scheme": "SHEMMOC",
  "boundary_conditions": "ROTATION",
  "leakage_model": "B2ZERO",
  "out_number_of_groups": 2,
  "output_settings": [3, "PBP"],

```

```

"mpo_configurations": ["ARO"],
"usage": "depletion",
"flux_normalization": [42.5, "PowerDensity", ""],
"generate_output": true,
"generate_mpo": true,
"generate_archive": false,
"generate_tripoli": false,
"depleting_configuration": "ARO",
"generate_branches": false,
"burnup_steps": <burnup_list>,
"boron_concentration": [600.0],
"fuel_temperature": [900.0],
"coolant_density": [0.7526],
"points_per_branch": 4,
"launch_branches_once_finished": false,
"launch_branches_sequential": false,
"branch_number": null,
"dump_input": true
}

```

The burnup points used are [MWd/t]:

```

<burnup_list> = [0, 1.00E+01, 2.00E+01, 3.00E+01, 4.00E+01, 5.00E+01,
7.50E+01, 1.00E+02, 1.50E+02, 2.00E+02, 2.50E+02, 3.00E+02, 3.50E+02,
4.00E+02, 4.50E+02, 5.00E+02, 7.50E+02, 1.00E+03, 1.50E+03, 2.00E+03,
2.50E+03, 3.50E+03, 4.00E+03, 4.50E+03, 5.00E+03, 6.00E+03, 7.00E+03,
8.00E+03, 9.00E+03, 1.00E+04, 1.10E+04, 1.20E+04, 1.30E+04, 1.40E+04,
1.50E+04, 1.60E+04, 1.70E+04, 1.80E+04, 1.90E+04, 2.00E+04, 2.10E+04,
2.20E+04, 2.30E+04, 2.40E+04, 2.50E+04, 2.60E+04, 2.70E+04, 2.80E+04,
2.90E+04, 3.00E+04, 3.20E+04, 3.40E+04, 3.60E+04, 3.80E+04, 4.00E+04,
4.20E+04, 4.40E+04, 4.60E+04, 4.80E+04, 5.00E+04, 5.20E+04, 5.40E+04,
5.60E+04, 5.80E+04, 6.00E+04, 6.20E+04, 6.40E+04, 6.60E+04, 6.80E+04,
7.00E+04]

```

## 9. Appendix C – Detailed results

In this appendix, we report the detailed error distribution on the normalized absorption and fission reaction rates for all test cases selected for the first NEMESI V&V campaign. The complete DICE report (including raw data) will be uploaded to an open access platform according to CAMIVVER's dissemination plan.

Results are reported as follows.

### Un-rodded configurations:

- KZL6: FA4\_4\_F in Figure 17, and FA3\_3\_G in Figure 18;
- KHM2: 13AU in Figure 19, 390GO in Figure 20, and 30AV5 in Figure 21;
- KAIST: UOX2 in Figure 22, UOX33 in Figure 23, UGD in Figure 24, MOX\_GD in Figure 25, and MOX in Figure 27;
- Minicore: A37 in Figure 28.

### Rodded configurations:

- KZL6: FA3\_3\_G in Figure 29;
- KHM2: 390GO in Figure 30;
- Minicore: A37 in Figure 31.

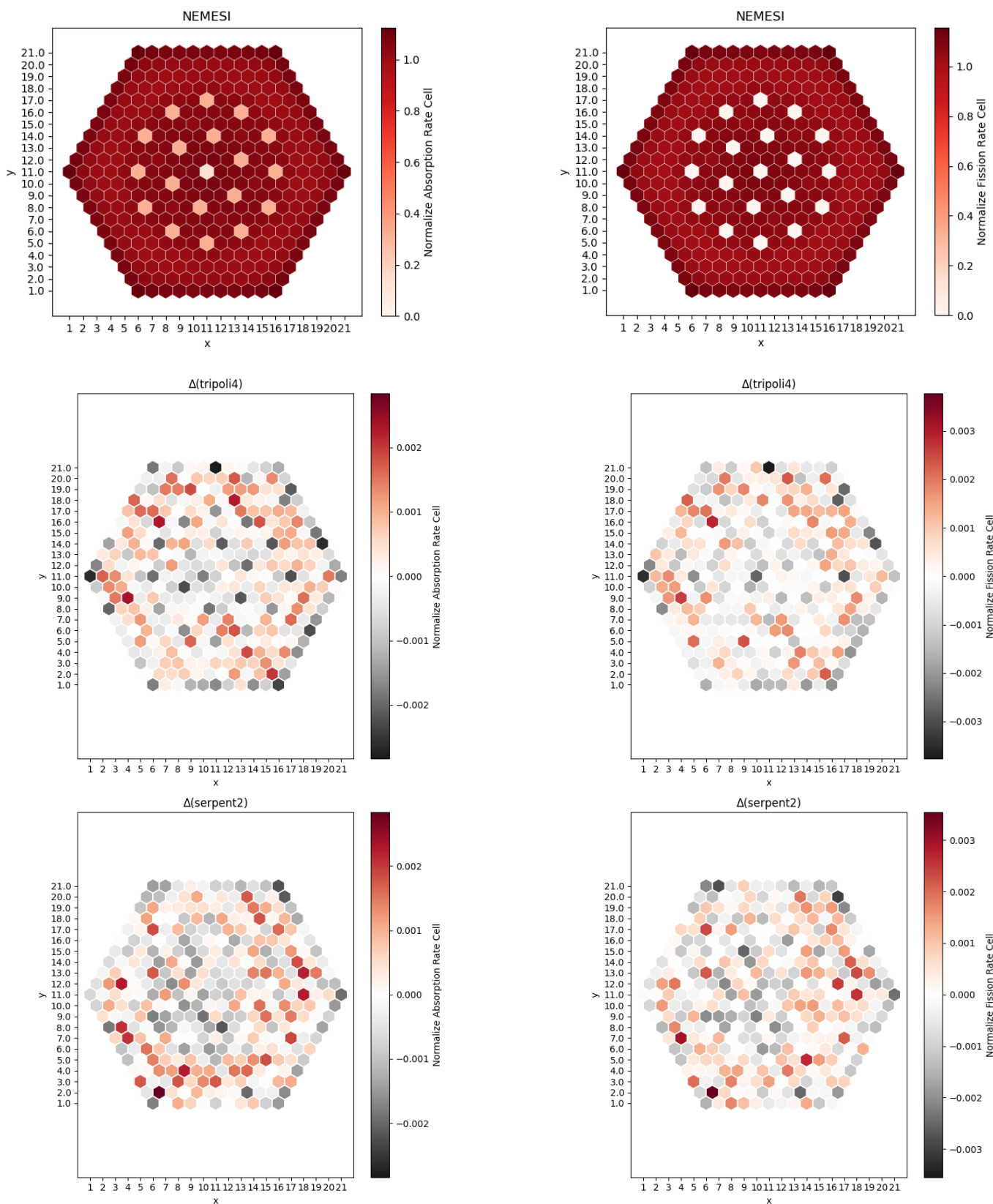


Figure 17 - Normalized absorption and fission rates for KZL6 – FA4\_4\_F obtained with NEMESI and comparisons with TRIPOLI-4® and SERPENT-2.



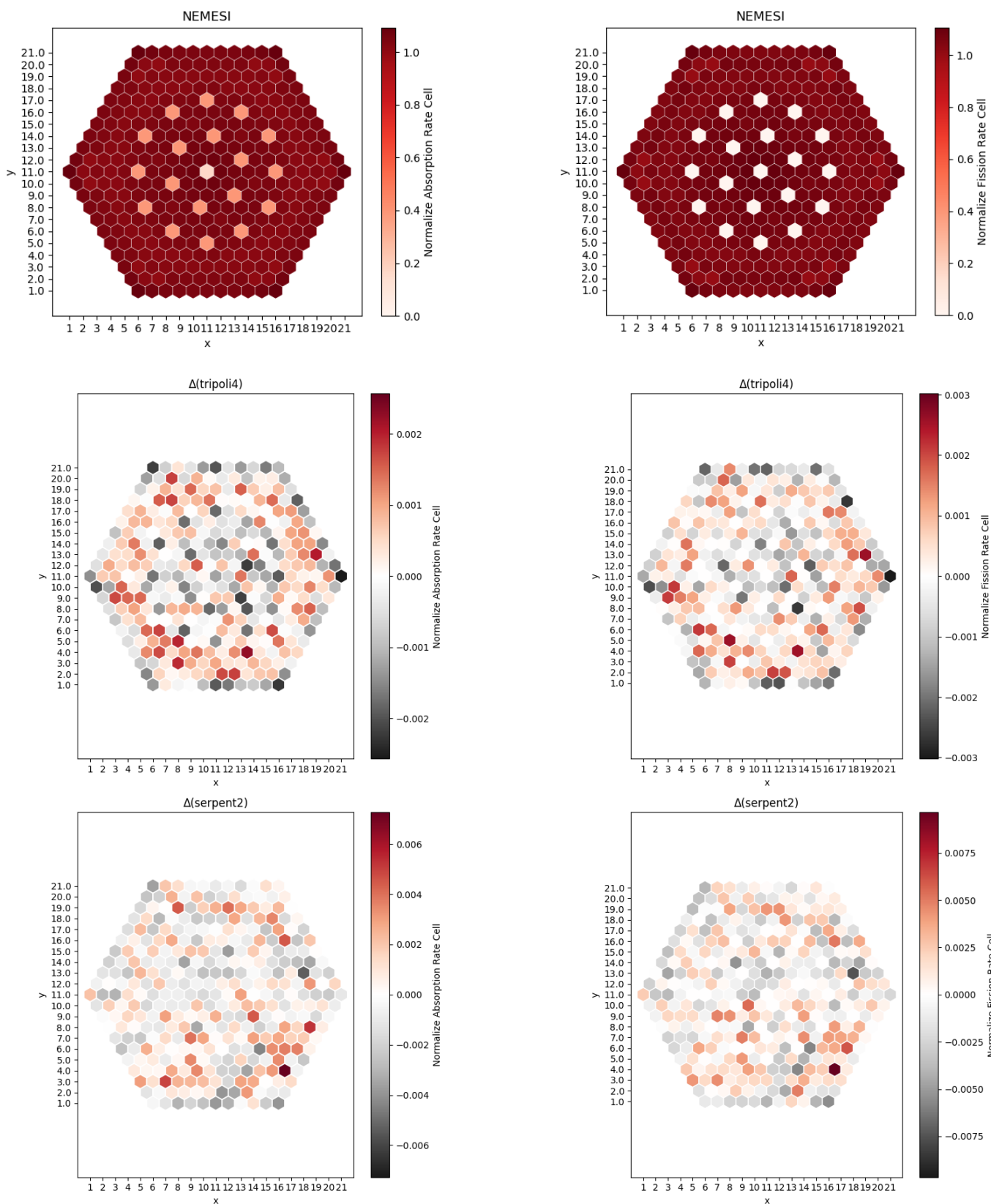


Figure 18 – Normalized absorption and fission rates for KZL6 – FA3\_3\_G obtained with NEMESI and comparisons with TRIPOLI-4® and SERPENT-2.

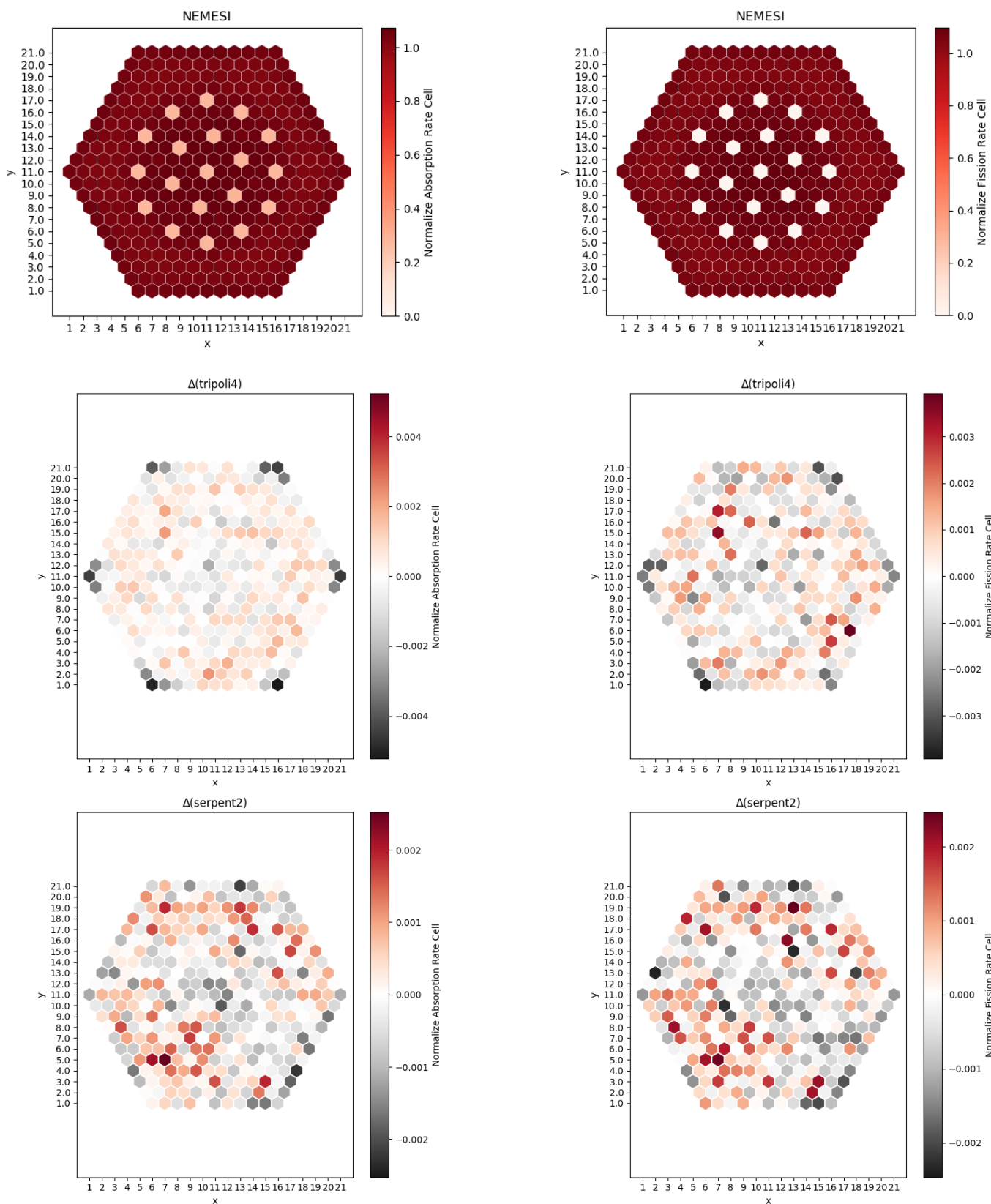


Figure 19 – Normalized absorption and fission rates for KHM2 – 13AU obtained with NEMESI and comparisons with TRIPOLI-4® and SERPENT-2.

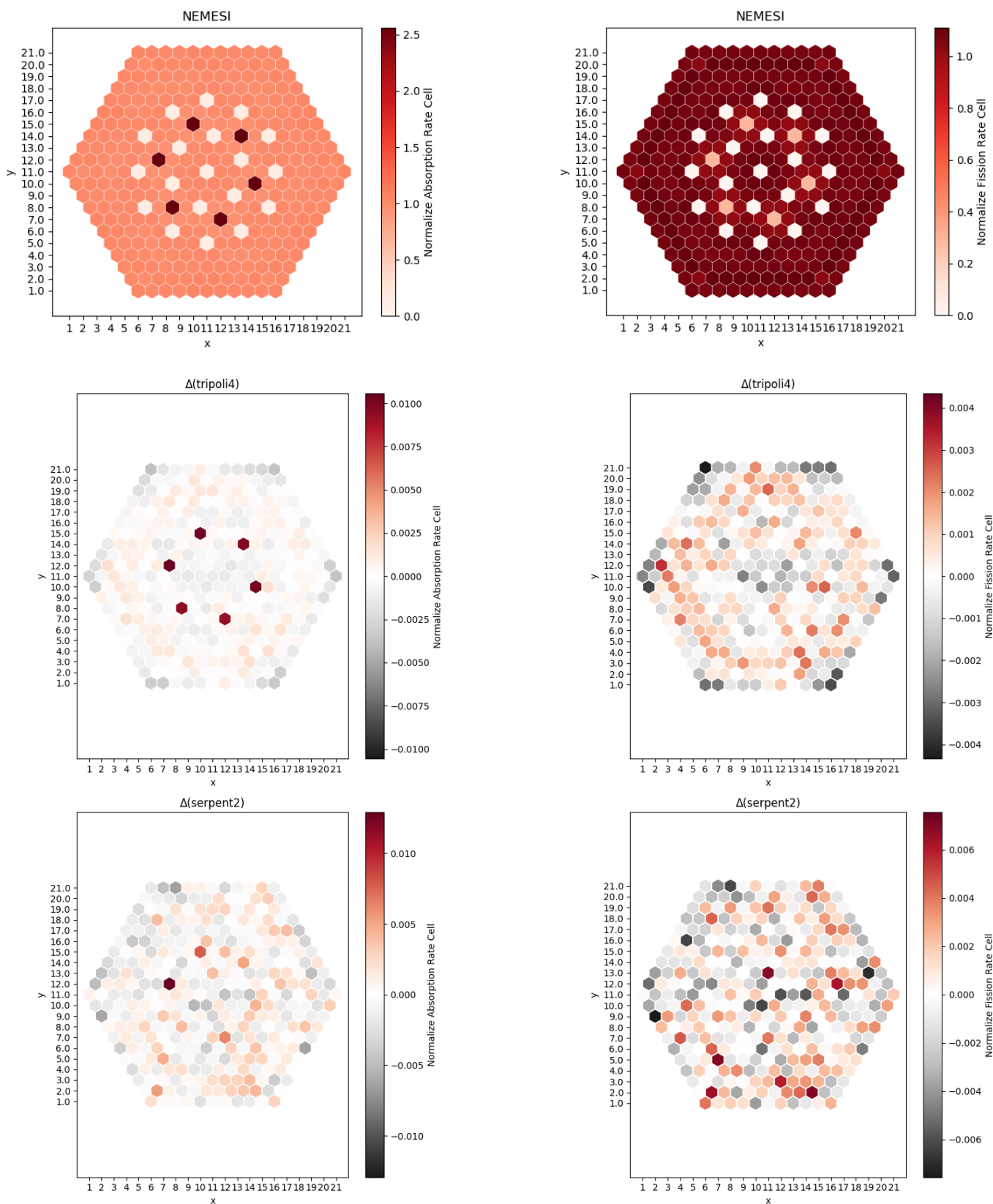


Figure 20 – Normalized absorption and fission rates for KHM2 – 390GO obtained with NEMESI and comparisons with TRIPOLI-4® and SERPENT-2.

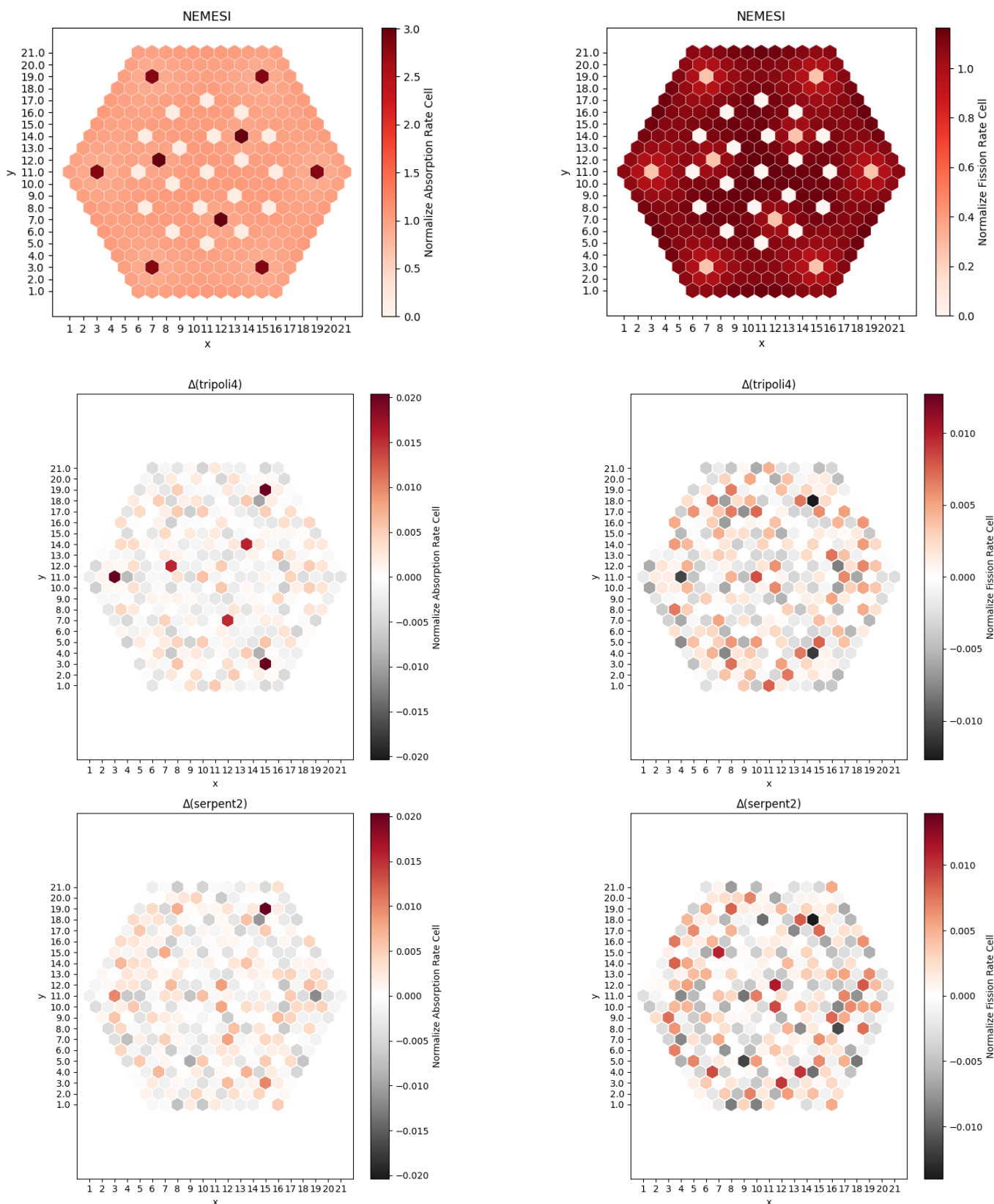


Figure 21 – Normalized absorption and fission rates for KHM2 – 30AV5 obtained with NEMESI and comparisons with TRIPOLI-4® and SERPENT-2.

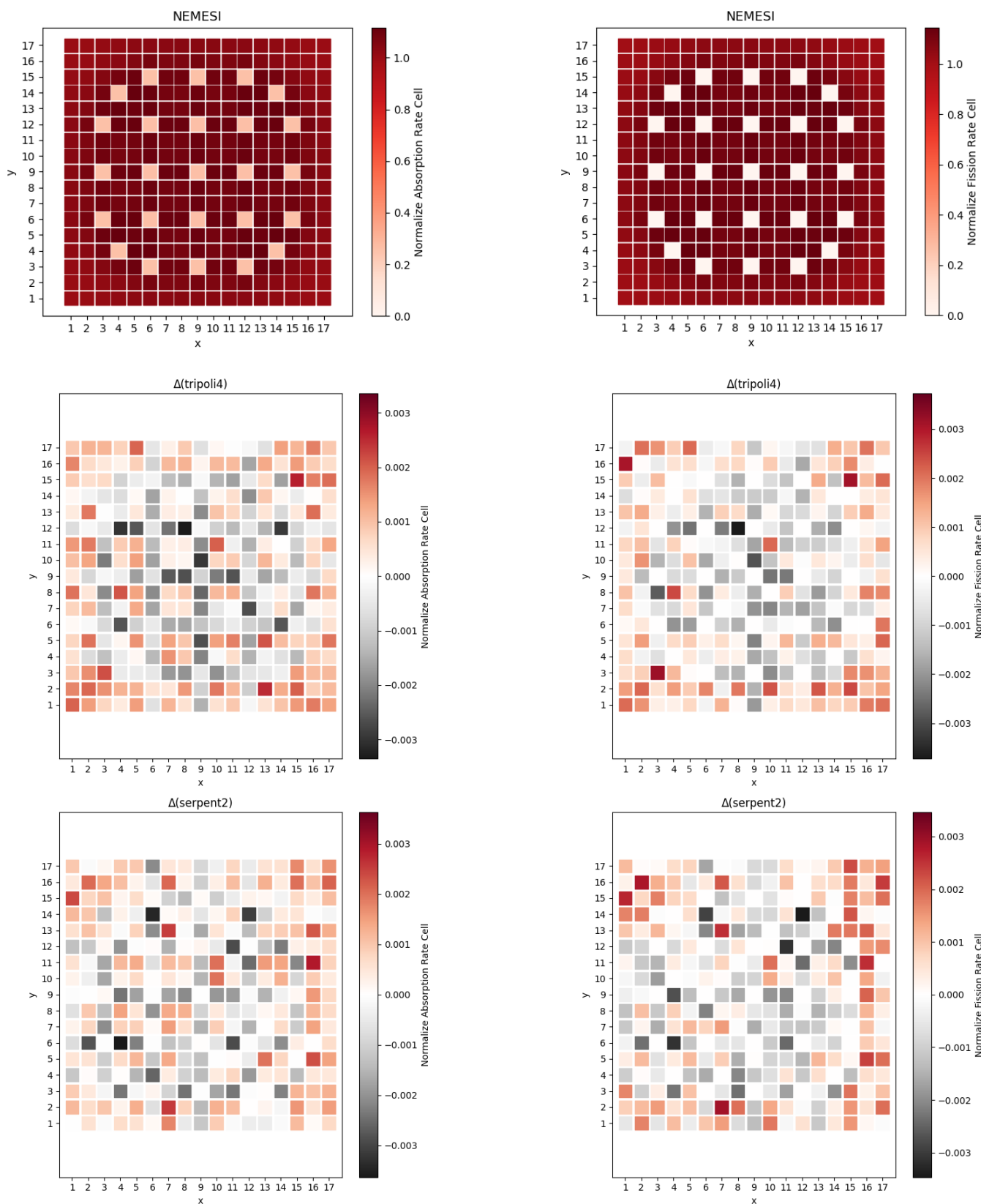


Figure 22 – Normalized absorption and fission rates for KAIST – UOX2 obtained with NEMESI and comparisons with TRIPOLI-4® and SERPENT-2.

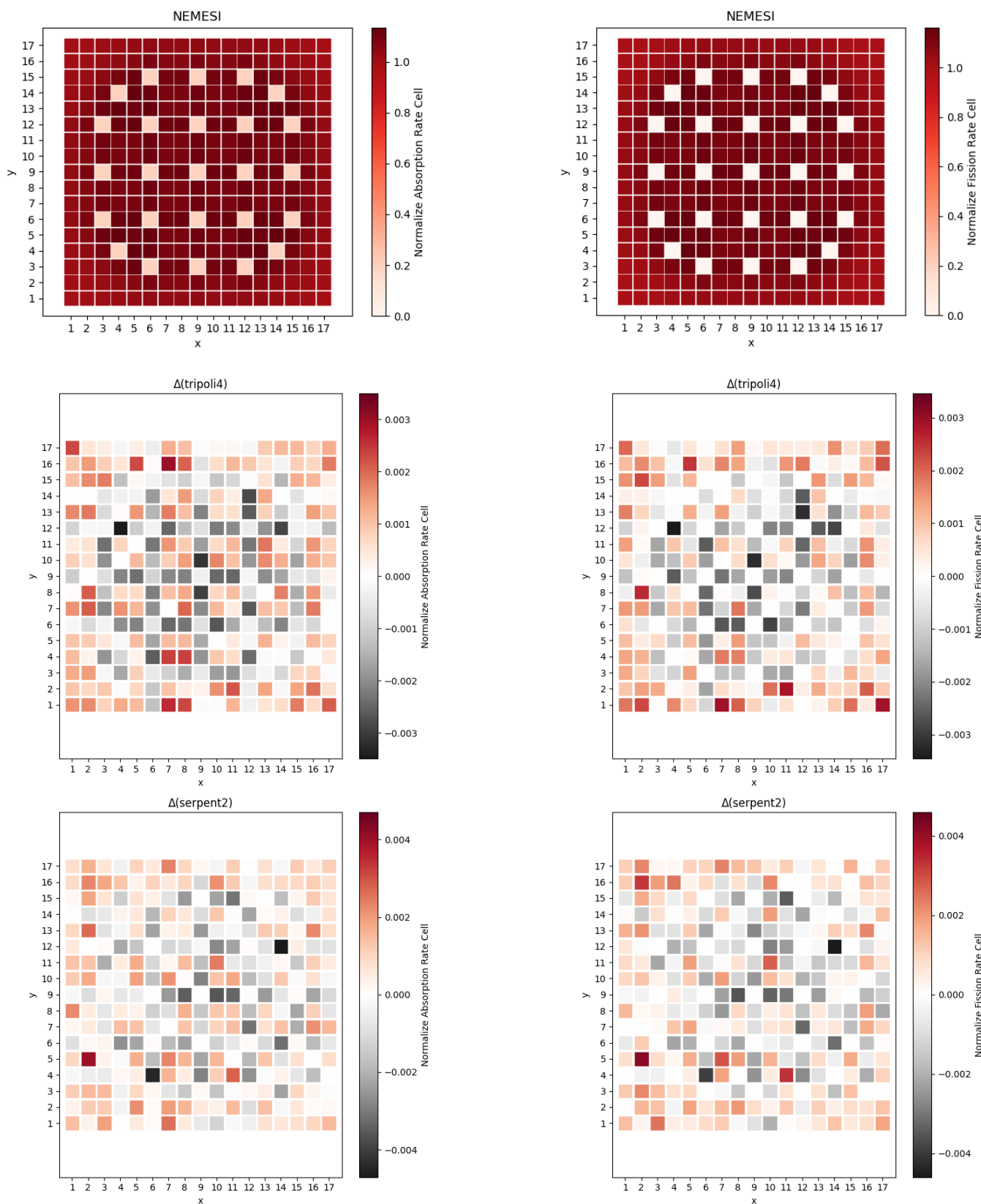
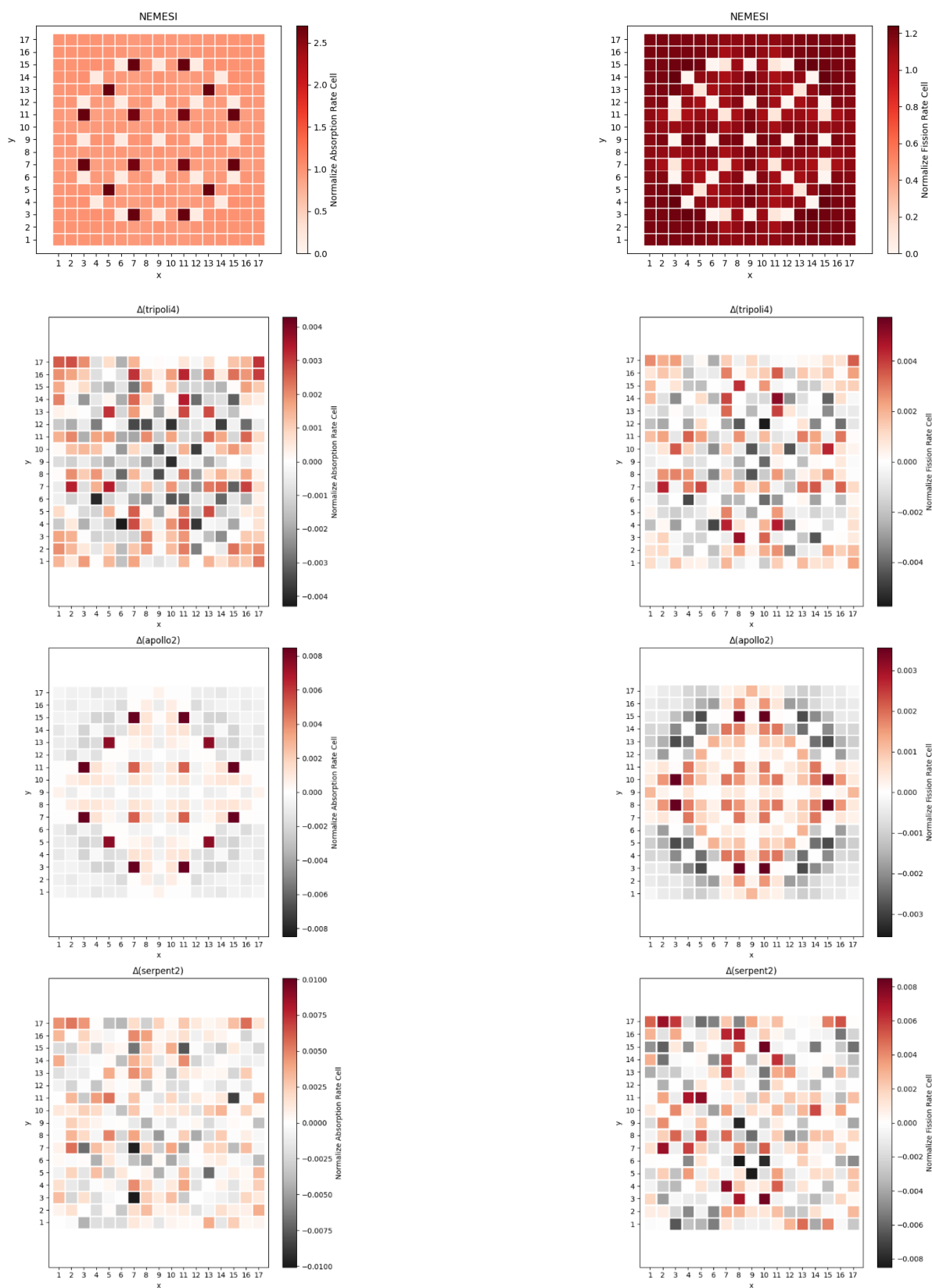


Figure 23 – Normalized absorption and fission rates for KAIST – UOX33 obtained with NEMESI and comparisons with TRIPOLI-4® and SERPENT-2.



**Figure 24 – Normalized absorption and fission rates for KAIST – UGD obtained with NEMESI and comparisons with TRIPOLI-4®, APOLLO2 and SERPENT-2.**

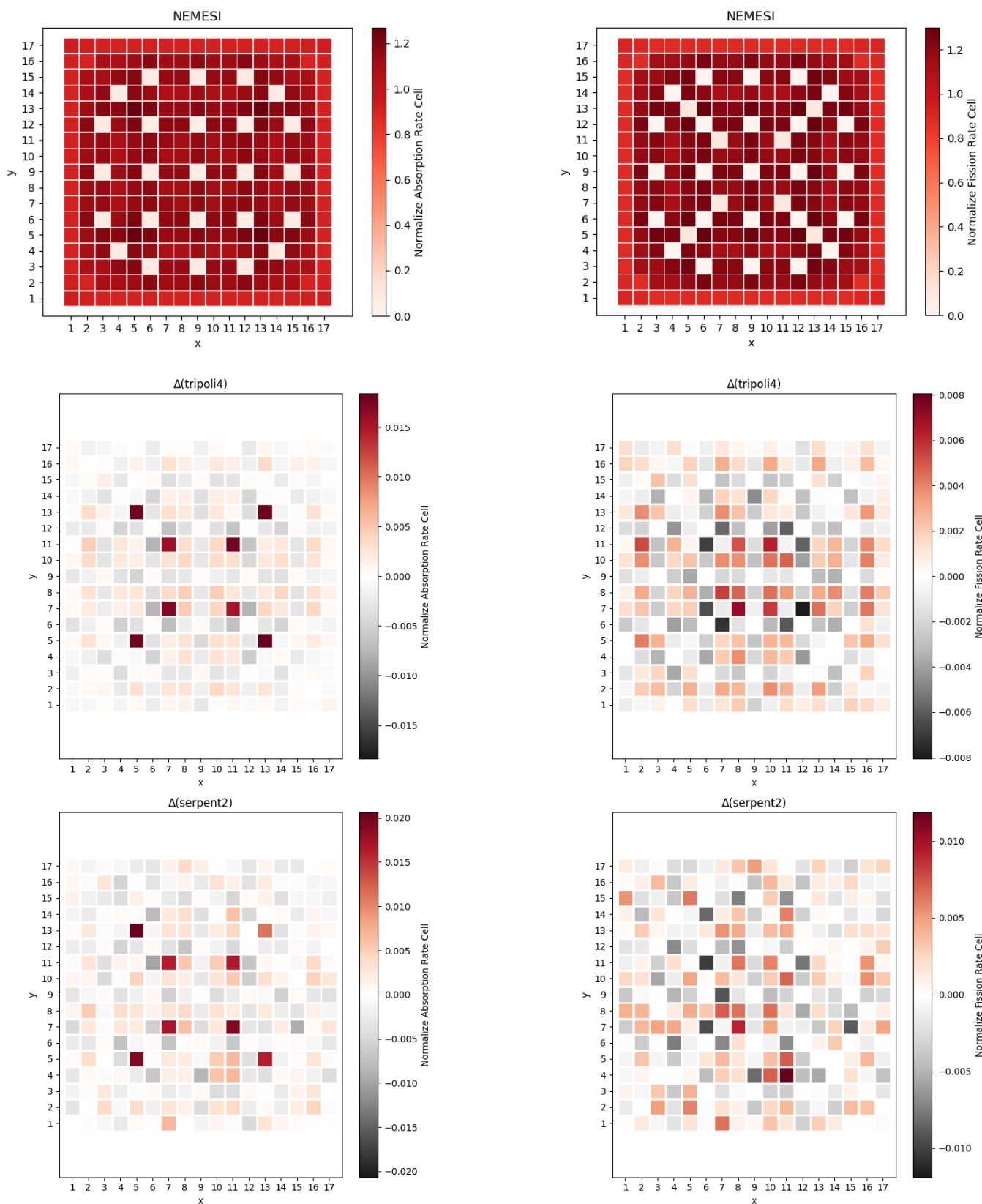


Figure 25 – Normalized absorption and fission rates for KAIST – MOX\_GD obtained with NEMESI and comparisons with TRIPOLI-4® and SERPENT-2.



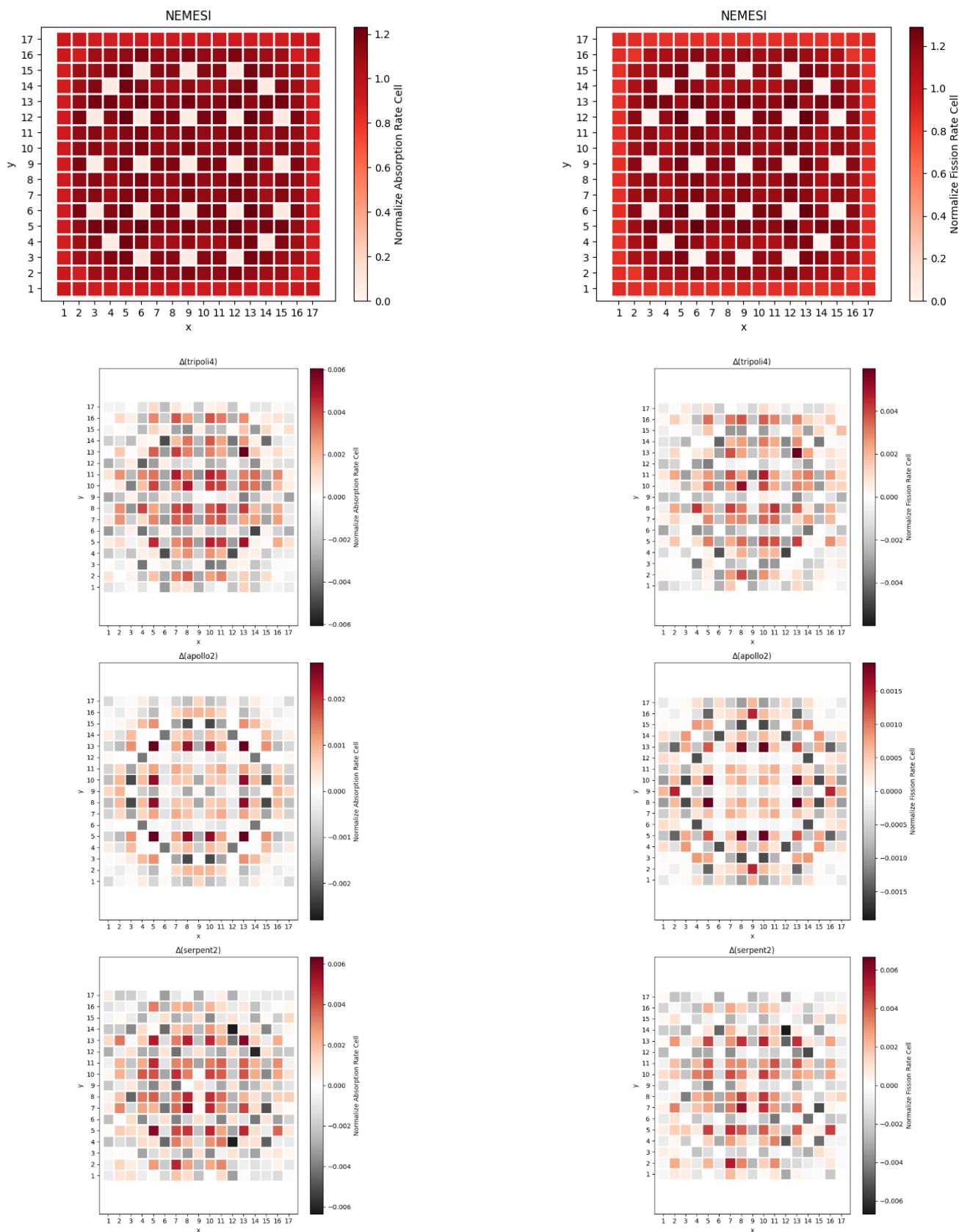


Figure 26 – Normalized absorption and fission rates for KAIST – MOX obtained with NEMESI and comparisons with TRIPOLI-4®, APOLLO2, and SERPENT-2.

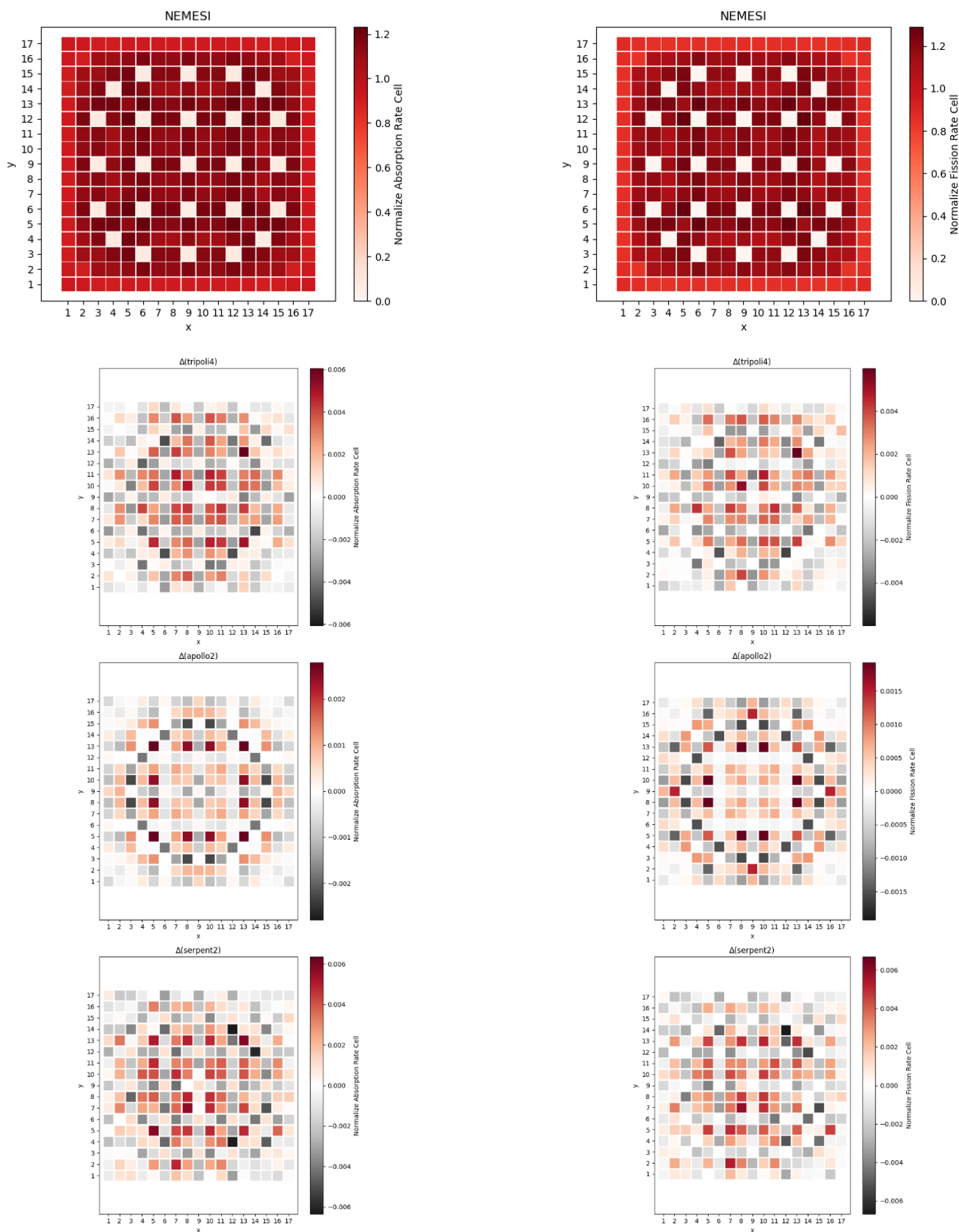


Figure 27 – Normalized absorption and fission rates for KAIST – MOX obtained with NEMESI and comparisons with TRIPOLI-4®, APOLLO2, and SERPENT-2.

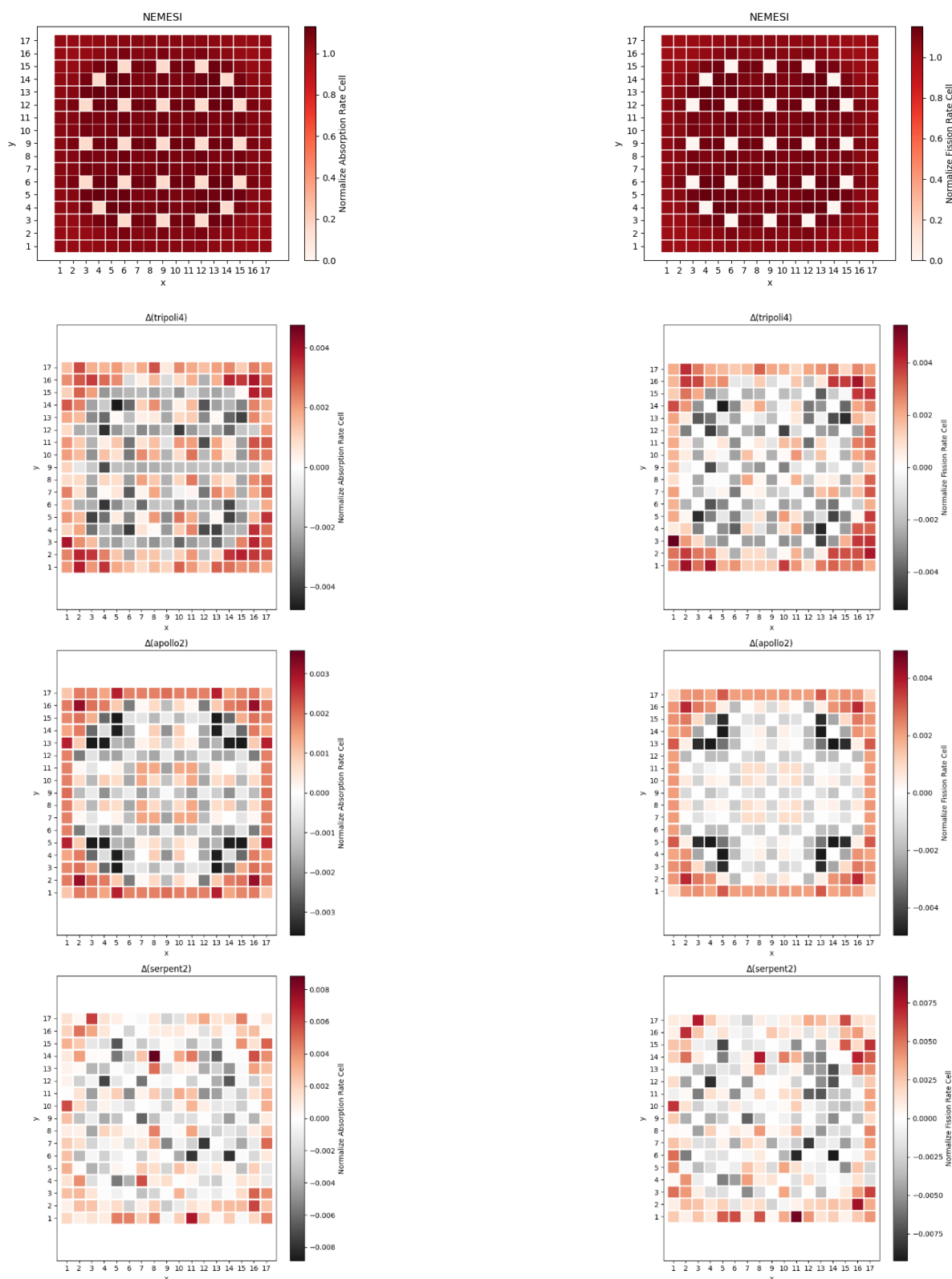


Figure 28 – Normalized absorption and fission rates for Minicore – A37 obtained with NEMESI and comparisons with TRIPOLI-4®, APOLLO2, and SERPENT-2.

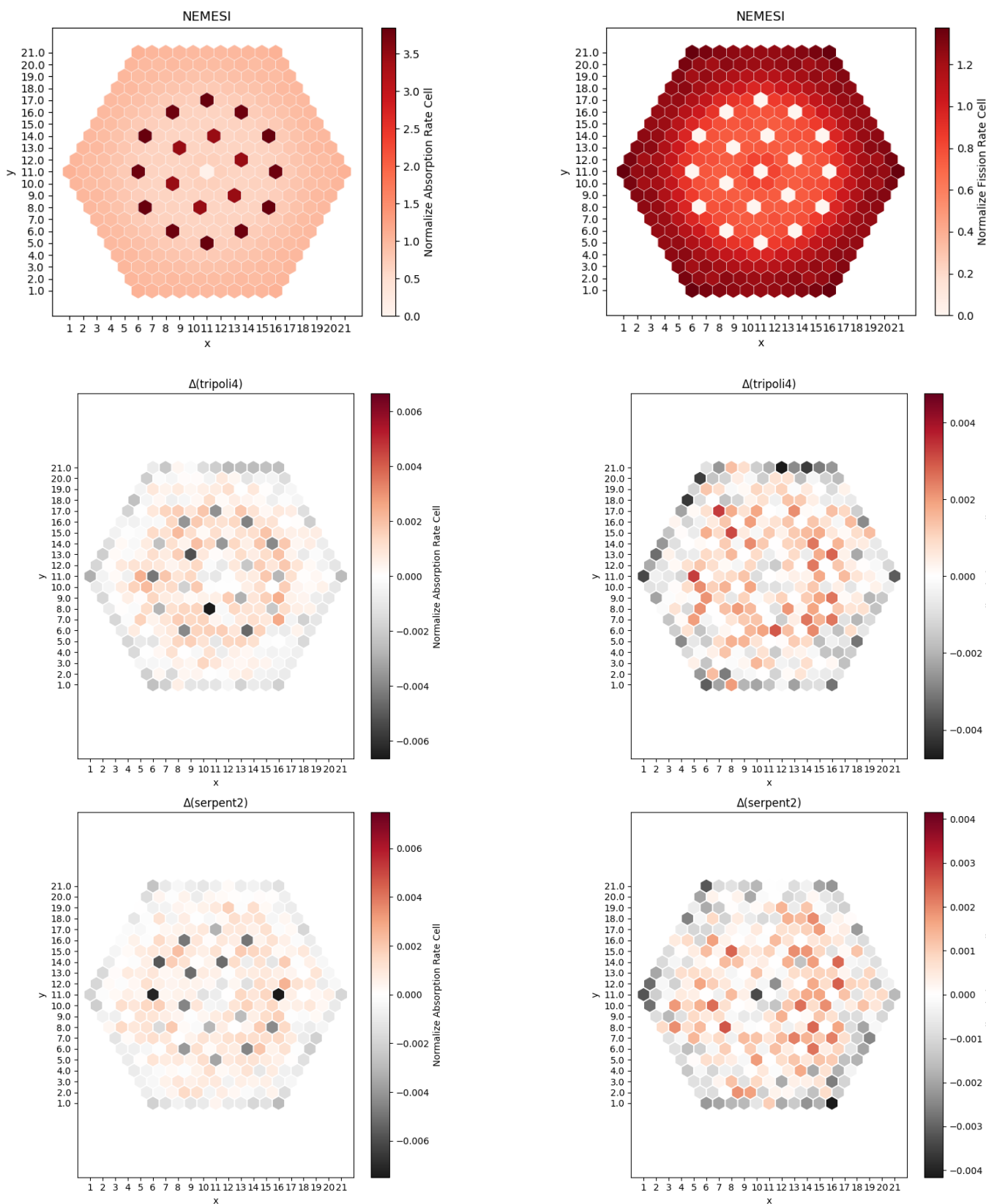
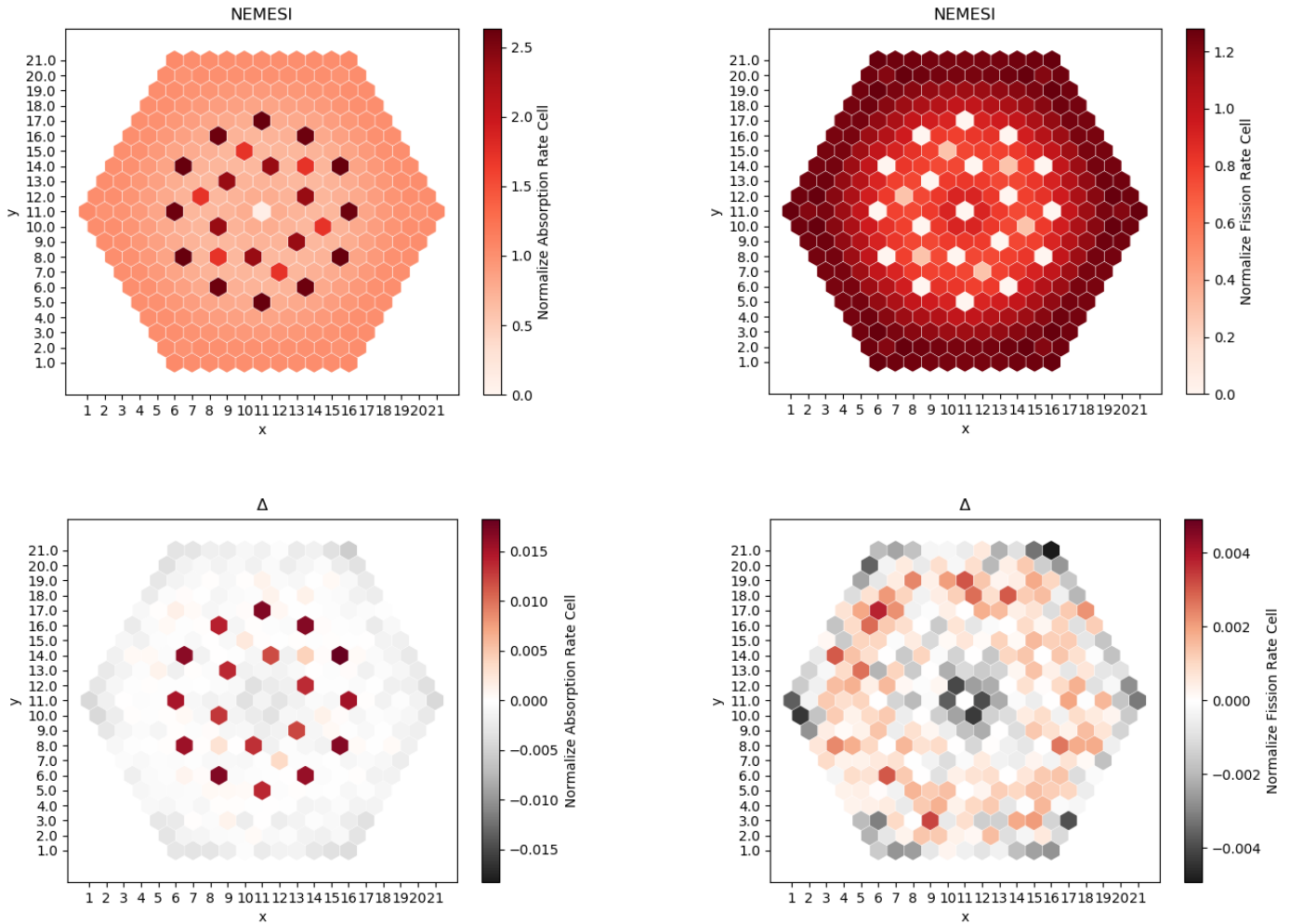


Figure 29 – Normalized absorption and fission rates for KZL6 – FA3\_3\_G, with B<sub>4</sub>C rods inserted, obtained with NEMESI and comparisons with TRIPOLI-4® and APOLLO2.



**Figure 30 – Normalized absorption and fission rates for KHM2 – 390GO, with Dysprosium rods inserted, obtained with NEMESI and comparisons with TRIPOLI-4® and APOLLO2.**

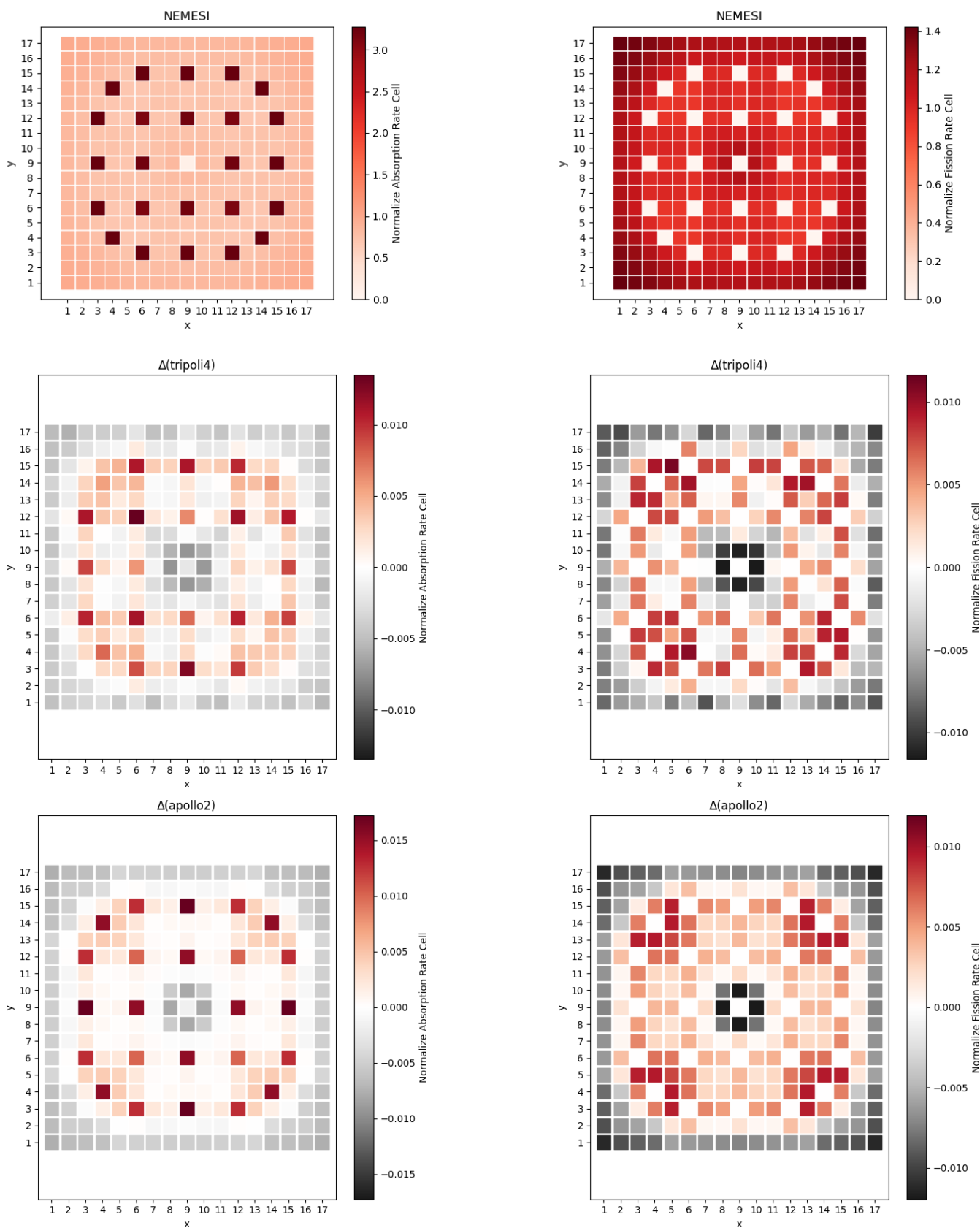


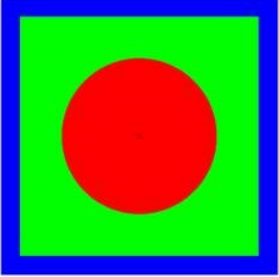
Figure 31 – Normalized absorption and fission rates for Minicore – A37, with AIC rods inserted, obtained with NEMESI and comparisons with TRIPOLI-4® and APOLLO2.

## 10. Appendix D – TRIPOLI-4<sup>®</sup> and SERPENT-2 analysis

### 10.1. Appendix D.1 – A simplified benchmark

A simplified pin cell benchmark was defined to investigate the differences between the two Monte Carlo codes. The benchmark specification is summarized in Table 16. Different variations of this base case were proposed: Removing atoms of U238; not considering scattering laws for hydrogen; activating unresolved resonance; and using fixed thermal scattering cross sections for H at 294K. Results are presented in Table 17. Initially, comparisons between TRIPOLI-4<sup>®</sup> and SERPENT-2 are between 40 and 60 pcm, except for Case B, with 5 pcm difference. Additionally, a second NDL obtained from the IRSN GitHub repository [25] was used, reducing the discrepancy up to less than 25 pcm between the cases. The main difference between the NDLS is the energy grid points observed during SERPENT-2 execution for the involved atoms, the amount of grid points in the IRNS JEFF3.1.1 NDLS is between 2 and 4 times higher, which could explain the differences in the results.

**Table 16 – Pin-cell benchmark description.**

Geometry	Parameter	UOX37 (in red)	Moderator (in green)
	Composition (10 <sup>24</sup> at/cm <sup>3</sup> )	O16: 4.57138E-02 U235: 8.56113E-04 U238: 2.19932E-02	H1: 4.79222E-02 O16: 2.39611E-02
	Temperature	300 K	300 K
	Fuel radius	0.4096 cm	
	Cell pitch	1.26 cm	
	Boundary conditions	Reflective (between green and blue)	

**Table 17 – Pin-cell benchmark results.**

CASE	DESCRIPTION	TRIPOLI-4 <sup>®</sup> (1 $\sigma$ = 9e-5)	SERPENT-2 JEFF311-VTT (1 $\sigma$ = 2e-5)	DIFF. (pcm)	SERPENT-2 JEFF311- IRSN 1 $\sigma$ = 2e-5	DIFF. (pcm)
A	Base	1.43265	1.43177	-43	1.43279	+7
B	Without U238	1.87542	1.87559	+5	1.87627	+24
C	Without scattering law for H	1.43508	1.43386	-59	1.43464	-21
D	With unresolved resonances	1.43286	1.43200	-42	1.43296	+5
E	With scattering law for H @ 294 K	1.43265	1.43185	-39	1.43279	+7

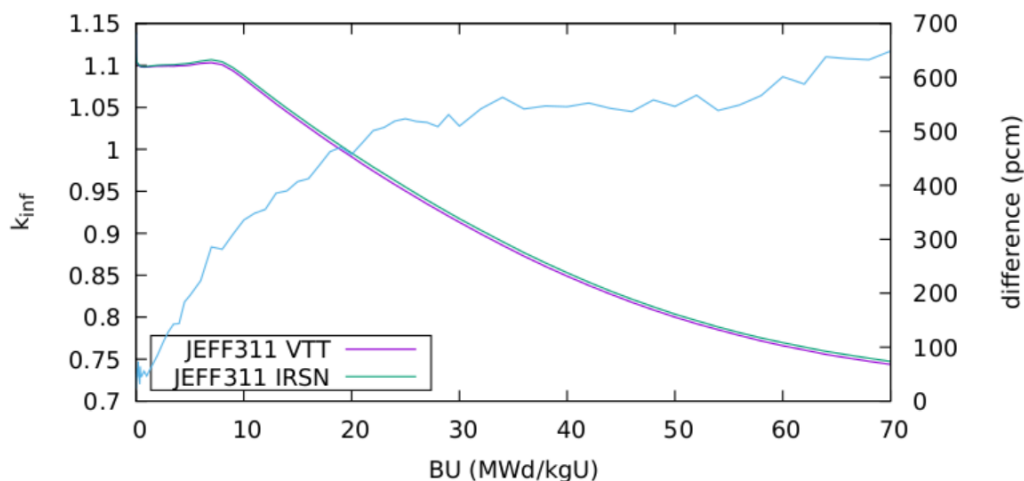
## 10.2. Appendix D.2 – Results comparison with different NDLs

Table 18 shows the comparison of the results obtained with the two NDLs adopted with SERPENT-2 (the default one and the JEFF3.1.1 IRSN) for the different assembly types in the DICE test matrix (at BU=0). The overall discrepancy against TRIPOLI-4® improves very well with less than 30 pcm for most cases, except for the KZL6 FA3\_3\_G case with a 42 pcm difference. It is important to mention that Gd-152 was unavailable in the new NDL, so it was removed from the material composition. An analysis to evaluate the impact of Gd-152 was performed only in the KHM2 390GO case using JEFF3.1.1 VTT NDL, giving differences less than ~10 pcm at fresh composition and ~40 pcm at 70 GWd/t.

**Table 18 – Updated results using the JEFF3.1.1-IRSN NDL. Gd-152 was not available in the NDL and was omitted.**

Assembly	TRIPOLI-4®	SERPENT-2 JEFF311-VTT	DIFF. (pcm)	SERPENT-2 JEFF311-IRSN	DIFF (pcm)
KHM2 13AU	0.96943	0.96853	-96	0.96942	-1
KHM2 30AV5	1.13966	1.13868	-76	1.13933 (*)	-25
KHM2 390GO	1.24895	1.24793	-65	1.24883 (*)	-8
KZL6 FA_3_3_G	1.24060	1.24034	-17	1.24124	42
KZL6 FA_4_4_F	1.31760	1.31623	-79	1.31728	-18
KAIST UOX2	1.10444	1.10342	-84	1.10451	6
KAIST UOX3	1.25350	1.25257	-59	1.25355	3
KAIST UGD	1.04750	1.04662	-80	1.04719 (*)	-28
KAIST MOX_GD	1.12547	1.12470	-61	1.12568 (*)	17
KAIST MOX	1.16349	1.16232	-87	1.16351 (*)	1
MINICORE A37	1.30554	1.30447	-63	1.30557	2

The burnup cases were re-calculated too with the JEFF3.1.1 IRSN NDL. They are presented from Figure 32 to Figure 36. In general, a systematic gain in reactivity during the burnup evolution is observed for all the cases. For the VVER cases (30AV5, 390GO, and FA\_3\_3\_G) and KAIST UGD, a gain of around 600 pcm at 70 GWd/t is obtained. For the minicore A37 case, there is a gain of around 300 pcm. It was investigated that JEFF3.1.1 VTT NDL includes additional isotopes from ENDF7 (loaded during burnup calculation), which are not included officially in the JEFF3.1.1 release. Therefore, differences during burnup are associated mainly with some missing isotopes in JEFF3.1.1 IRSN NDL, but in accordance with the JEFF3.1.1 release.



**Figure 32 – KHM2 30AV5 burnup calculation with SERPENT-2.**



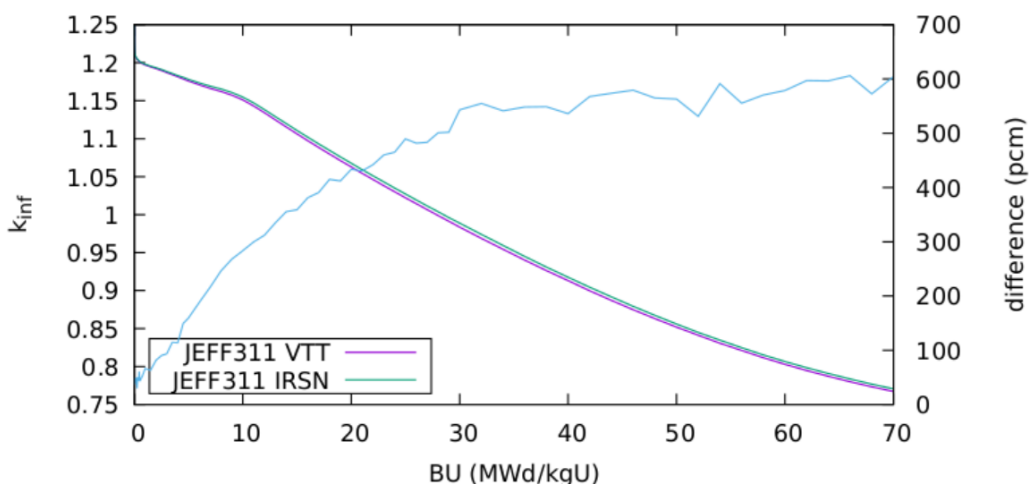


Figure 33 – KHM2 390GO burnup calculation with SERPENT-2.

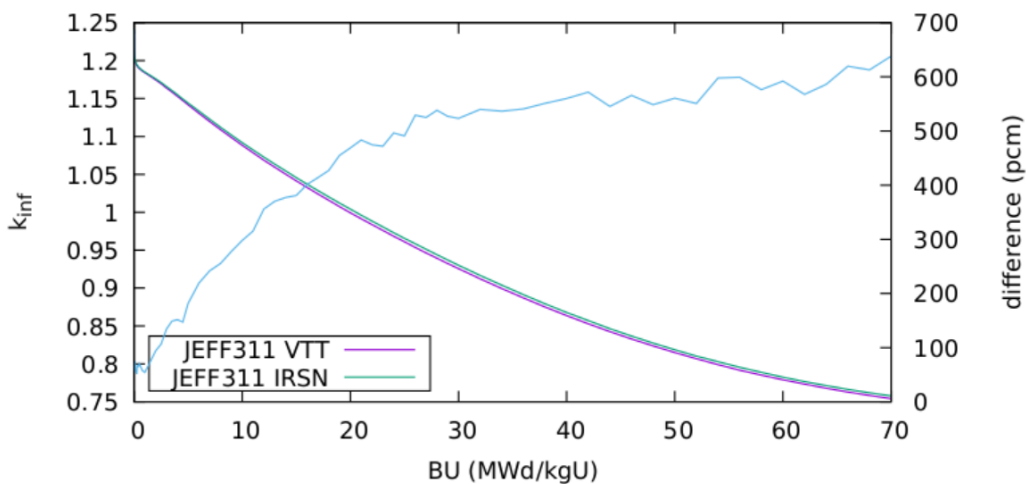


Figure 34 – KZL6 FA\_3\_3\_G burnup calculation with SERPENT-2.

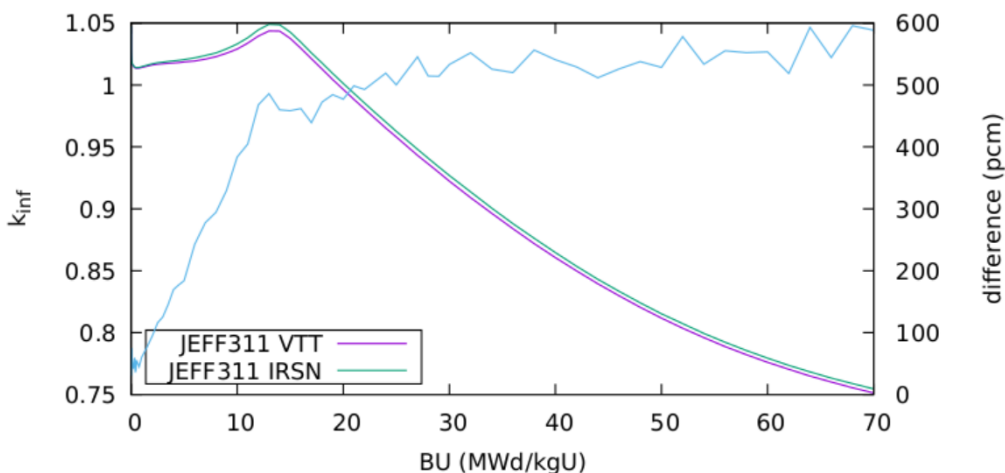


Figure 35 – KAIST UGD burnup calculation with SERPENT-2.

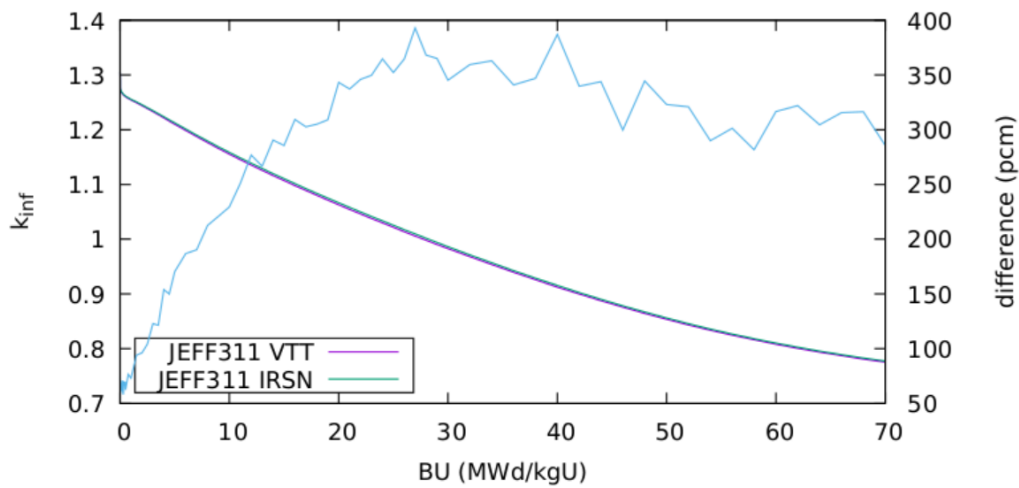


Figure 36 – Minicore A37 burnup calculation with SERPENT-2.

## References

- [1] CAMIVVER – Codes and Methods improvements for VVER comprehensive safety assessment – H2020 Grant Agreement Number 945081
- [2] APOLLO3®: Overview of the new code capabilities for reactor physics analysis, in *Int. Proc. M&C 2023 Conference*, Niagara Falls, Ontario, Canada, August 13-17, 2023, P. Mosca et al.
- [3] D4.2 - Description of the architectural choices and implementation of the multi-parameter library generator prototype and future perspectives. A. Brighenti et al.
- [4] D4.3 - Definitions of tests cases for the verification phases of the multi-parametric library generator. A. Willien, B. Vezzoni.
- [5] IAEA Safety Standards – Deterministic Safety Analysis for NPP, [https://www-pub.iaea.org/MTCD/Publications/PDF/PUB1851\\_web.pdf](https://www-pub.iaea.org/MTCD/Publications/PDF/PUB1851_web.pdf)
- [6] D3.2 – The CAMIVVER Definition report with specification for NPP VVER 1000 reactor with respect to selected transient – A. Stefanova et al.
- [7] X2 VVER-1000 benchmark revision: Fresh HZP core state and the reference Monte Carlo solution. Y. Bilodid et al. [Excel file material\_composition.xlsx (X2 benchmark specification dataset – Y. Bilodid – URL: <http://doi.org/10.14278/rodare.200>]
- [8] Benchmark Problem 1A: MOX Fuel-Loaded Small PWR Core (MOX Fuel with Zoning) – Nam Zin Cho. <http://nurapt.kaist.ac.kr/benchmark>
- [9] Benchmark Problem 1B: MOX Fuel-Loaded Small PWR Core (MOX Fuel without Zoning) – Nam Zin Cho. <http://nurapt.kaist.ac.kr/benchmark>
- [10] The CAMIVVER project: Assembly and reflector description for PWR minicore - Task 5.3 Benchmark - Framatome document D02-DTIPD-F-20-0580 A
- [11] The CAMIVVER project: WP5 task 5.3 – PWR test case to be employed in coupled neutronics and thermal hydraulic analysis - Framatome document D02-DTIPD-F-20-0582 A
- [12] Upgrade of APOLLO3 internal thermohydraulic feedback model with THEDI and application to a control rod ejection accident, *Int. Proc. M&C 2019 Conference* – C. Patricot et al.
- [13] The JEFF-3.1.1 Nuclear Data Library, *JEFF Report 22*, NEA–OECD, A. Santamarina et al.
- [14] Overview of SERMA’s Graphical User Interfaces for Lattice Transport Calculations, *Energies*, vol. 15, no. 4, p. 1414, 2022. D. Tomatis et al.
- [15] AP3-2.2 release version, CEA - DES/ISAS/DM2S/SERMA/LLPR/NT/2021-69277/A, document available to French partners, 2021. P. Mosca
- [16] AP3-2.3 release version, CEA - DES/ISAS/DM2S/SERMA/LLPR/NT/2022-70923/A, document available to French partners, 2022. P. Mosca
- [17] Development of a Multi-Parameter Library Generator Prototype for VVER and PWR Applications Based on APOLLO3®, in *Int. Proc. M&C 2023 Conference*, Niagara Falls, Ontario, Canada, August 13-17, 2023, A. Brighenti et al.
- [18] Determination of the Optimized SLEM Mesh for Neutron Transport Calculations, *Mathematics and Computation, Supercomputing, Reactor Physics and Nuclear and Biological Applications (M&C 2005)*, Avignon, France (2005). N. Hfaiedh and A. Santamarina.
- [19] APOLLO2 year 2010, *Nuclear Engineering and Technology*, 42, 5, 474 (2010), R. Sanchez et al.
- [20] French Calculation Schemes for Light Water Reactor Analysis, *Proc. Int. Conf. on the Physics of Fuel Cycles and Advanced Nuclear Systems (PHYSOR2004)*, Chicago, IL, USA, April 25-29, 2004. A. Santamarina et al.
- [21] TRIPOLI-4®, CEA, EDF and AREVA Reference Monte Carlo Code. *Annals of Nuclear Energy*, 82:151–160, 2015. E. Brun et al.
- [22] ROOT reference documentation, <https://root.cern/doc/v628/>
- [23] The Serpent Monte Carlo code: Status, development and applications in 2013, *Annals of Nuclear Energy*, 82:142–150, 2015. J. Leppänen et al.
- [24] Serpent Manual – set edepmode,

EDF R&D	CAMIVVER - D4.4 - Results of the verification phases on PWR and VVER geometry configurations	6125-1108-2023-02020-EN Version 1.0, CURRENT
---------	--	---

[https://serpent.vtt.fi/mediawiki/index.php/Input\\_syntax\\_manual#set\\_edepmode](https://serpent.vtt.fi/mediawiki/index.php/Input_syntax_manual#set_edepmode)

[25] PyNjoy2016 git repository, <https://github.com/irsn/pynjoy2016>, IRNS

[26] Valjean framework. Documentation, <https://valjean.readthedocs.io/en/latest/index.html> –  
Git repository, <https://github.com/valjean-framework/valjean>

[27] MPOLib. Git repository, <https://codev-tuleap.cea.fr/plugins/git/apollo3-camivver/MPOLib>